ASYMMETRIC SURFACE DIELECTRIC BARRIER DISCHARGE AS A NOVEL METHOD FOR BIOLOGICAL DECONTAMINATION

By

KEDAR KAMLAKANT PAI

Bachelor of Technology in Mechanical Engineering
National Institute of Technology Raipur
Raipur, Chhattisgarh
2010

Master of Science in Mechanical and Aerospace Engineering
Oklahoma State University
Stillwater, Oklahoma
2012

Submitted to the Faculty of the
Graduate College of the
Oklahoma State University
in partial fulfillment of
the requirements for
the Degree of
DOCTOR OF PHILOSOPHY
December, 2015

ASYMMETRIC SURFACE DIELECTRIC BARRIER DISCHARGE AS A NOVEL METHOD FOR BIOLOGICAL DECONTAMINATION

Dissertation Approved:

Dr. Jamey D. Jacob

Dissertation Adviser

Dr. Arvind Santhanakrishnan

Dr. Ronald Delahoussaye

Dr. Sundarajan V. Madihally

Dr. Li Maria Ma

Dissertation Co-Adviser

Acknowledgements

I would like to dedicate this work to my family and friends without whom this journey would not have been as exciting and interesting. Most of all, I would like to thank my parents for their support and patience. They were understanding and supportive during the long distance phone calls that helped cope through some stressful times, and throughout the course of my Ph.D. I also owe a great amount of gratitude to my advisor Dr. Jamey Jacob, for introducing me to the fantastic world of plasmas, and giving me the freedom and support to explore this field. I would like to thank Dr. Li Maria Ma and Dr. Sundarajan V. Madihally for their support and guidance, and letting me be a part of their labs. I also appreciate the long talks with Dr. Madihally, and the lovely food and conversations with Dr. Ma. I would also like to thank Dr. Aravind Santhanakrishnan, and Dr. Ronald Delahoussaye for being a part of my committee and providing valuable advice and guidance. I am deeply appreciative of Dr. Arland 'AJ' Johannes and Dr. Frank C. Chambers, for vastly increasing my knowledge on plasmas and fluid dynamics and also letting me work with some 'cool toys' like the Wind Tunnel.

I appreciate all the intriguing conversations with Dr. Kaan Kalkan, Dr. Saravan Kumar Shanmugvelayudam and Dr. Sudheer Bandla at Panera bread, which were a welcomed respite from regular research. I am grateful to everyone in the Mechanical and Aerospace Engineering department for helping me with our daily logistical and academic issues, especially Dr. Charlotte Fore, Beth Powers, and Diane Compton. I would also like to thank Chris Timmons who has been the other brain of this project. I always enjoyed our discussions on abstract topics other than research during the course of our experiments together.

This acknowledgement wouldn't be complete without saying thank you to my close friends, Pratik Deokar and Roshan Revankar. We came to this university together and have been here for the last five years and become more like brothers. Thank you for all your support and patience, both as roommates as well as friends. I would also like to thank my good friends Vijeta Jambaulikar, Unnati Madhavi, Chetan Borkar, Kumar Singarapu, Girish Malkarnekar and the list goes on. There is a huge roster of people I would like to thank, without whom I wouldn't have made it this far, especially all my teachers from 1st to 12th grade, they are the ones that inspired me. Finally, I am thankful to everyone from the HAL and NIMFFAB lab groups.

Name: KEDAR KAMLAKANT PAI

Date of Degree: DECEMBER, 2015

Title of Study: ASYMMETRIC SURFACE DIELECTRIC BARRIER DISCHARGE AS A NOVEL METHOD FOR BIOLOGICAL DECONTAMINATION

Major Field: MECHANICAL AND AEROSPACE ENGINEERING

Abstract:
Scope and Method of Study:
The current study investigates the characteristics of a Surface Dielectric Barrier Discharge (SDBD) plasma actuator as a viable technology for biological decontamination, specifically asymmetric design in arrangements of electrodes. The aim of this work is to demonstrate biological decontamination and understand the plasma interaction mechanism with the cells. The effect of scaling an array of electrodes on power is analyzed and the range of voltage for optimum operation is identified. The improved effectiveness of the asymmetric SDBD is validated by a comparative analysis with a symmetric SDBD arrangement via inactivation of a 5-strain-mixture of *Listeria monocytogenes*. Variation in performance is analyzed using a variable distance between the actuators and the samples to demonstrate the impact of the asymmetric design. The dose dependence and plasma based effect on different cell types is analyzed using three different mammalian cells, namely, Endothelial cells (HUVECs), Neuroblastoma and Hepatocytes (HepG2). The higher tolerance of mammalian cells to plasma treatment when compared to prokaryotic cells is observed through analysis of viability, functionality and morphology. Finally, the primary mode of plasma interaction with cells was analyzed using different assays to quantify the role of each generated plasma species, such as ions, reactive oxygen/nitrogen species, etc.

Findings and Conclusions:
This study helped demonstrate specific trends in voltage requirements for scaling of linear electrodes. The asymmetric arrangement of electrodes demonstrated a 2.5 Log_{10} greater reduction when compared to symmetric configurations, which persisted until 3 cm away from the sample. This suggests the asymmetric design is capable of producing a larger area of plasma and pushing the species further away from the electrodes. The effective regime for plasma generation between uniform discharge and streamer formation was identified. The dose dependence on plasma was identified in different types of mammalian cells demonstrating a need for a proper matrix while treating different tissue. However, mammalian cells demonstrated higher resilience to plasma treatment with retention of functionality up to a treatment time of 4 minutes. Finally, Reactive Oxygen Species (ROS) were identified as the primary agent for plasma-cell interaction with synergistic effects from ions at close proximity to the sample in a non-aqueous medium. OH radicals (identified from Optical Emission Spectroscopy), Ozone (O_3), and resulting acids such as nitric oxide form acids including nitric (HNO_3) and nitrous acid (HNO_2), and are hypothesized to be responsible for antimicrobial effects.

TABLE OF CONTENTS

LIST OF FIGURES

Chapter 1

Chapter 2

Chapter 3

Chapter 4

Chapter 5

Chapter 6

Chapter 7

Chapter 1

Introduction

"The desire that guides me in all I do is the desire to harness the forces of nature to the service of mankind."

- Nikola Tesla

Sterilization and decontamination are essential for preservation of good health. This is true for both the medical and the food industry. Both these industries deal with materials which are temperature and chemical sensitive such as polymers and fruits, respectively. The currently used sterilization methods suffer from various drawbacks due to certain properties of the sterilizing agent used, the method of sterilization or both. These instruments are cleaned with various methods such as Ethylene Oxide (EtO) gas, which may be expensive as well as time consuming [1]. Formaldehyde, for example, is carcinogenic and irritates the skin and mucous membranes. The use of ionizing radiation, such as γ-rays, requires highly radioactive materials for their production. This is best done in a heavily shielded fixed facility and cannot be easily implemented in the field. Also, this method can prove destructive to sensitive equipment and also may prove lethal to the operator. Application of thermal energy, such as in autoclaves, can also prove to be slow at the temperature limits required to avoid damage to heat sensitive equipment like plastics.

A detailed review on different technologies for sterilization and disinfection can be found elsewhere [1]. Most of these technologies suffer from significant shortcomings. Hence, an easier to use, non-destructive and convenient technology is needed. Sixty-five million Americans live in where are officially deemed primary care shortage areas, and adults throughout the United States face difficulty obtaining prompt access to primary care [2]. Up to one in three patients receiving treatment at remote clinics become infected from unsterilized medical instruments.

The food industry too suffers from similar drawbacks due to the chemicals used, such as chlorine wash, which may be fast but has other effects which may cause damage to the commodity as well as be harmful to the consumer [3, 4]. According to the Center for Disease Control (CDC), 1 in 6 Americans suffers from foodborne illnesses and 128,000 get hospitalized, resulting in 3000 deaths per year [5]. *Salmonella, Listeria monocytogenes* and *Escherichia coli* are some of the major human pathogens responsible for these foodborne illnesses. Use of chemicals, such as chlorinated water wash, to decontaminate commodities contaminated by these pathogens, may degrade the quality or even harm the consumer if the produce and meats are not handled with care. Nonionizing radiation, such as UV, requires line-of-sight application. i.e. can only effect object directly in the path of the radiations and can be quite time consuming [4]. Hence, an urgent shift in paradigm is necessary.

Non-thermal atmospheric plasmas (Cold plasma) have been tested in recent years and are effective, especially in the field of sterilization and decontamination [6-10]. Their low-temperature operation with no detectable damage to the object being decontaminated makes cold plasma ideal for such applications. They produce a cocktail of reactive species which effectively kill pathogens without damaging the object being decontaminated [11, 12]. Recent studies have shown, as will be mentioned in the following chapters, that cold plasmas are very effective against drug resistant

as well as the toughest pathogens to deal with [9]. However, most of the devices developed for such applications are only functional at close proximity [13, 14] or need special gases [15, 16]. These devices may result in desiccation [17] or even burns [18] if working with sensitive tissue. These devices also differ in their effects and interactions with substrates, such as change in pH [19, 20], and the type of species they produce [18, 21].

Hence, to mitigate these issues, we explore the potential of Dielectric Barrier Discharge (DBD), especially a special design of Surface Dielectric Barrier Discharge (SDBD) known as asymmetric SDBD which does not just produce plasma but also induces a flow close to the discharge (downstream). This design has been investigated for flow modification in applications for aerodynamics and flow control [22-25]. However, no major strides have been seen to leverage this technology in the field of decontamination. There has been no substantial analysis of the ability of this design to carry the reactive species generated in the plasma zone to the surface being decontaminated via induced flow. Similarly, there has been no analysis of how the SDBD plasma affects various cells that make up some of the crucial tissues in our body if this technology is to be applied for decontaminations applications in fields such as dermatology.

Ample research has been conducted on how various scaling parameters such as power and frequency influence the plasma characteristics but this technology needs to be studied for trends in scaling with regard to plasma volume and geometric modifications. The advantages of this technology can prove to be an excellent boon to the sterilization/decontamination industry, as it is a non-contact method that is especially beneficial for sensitive materials such as those sensitive to electromagnetic fields. Researchers have observed that atmospheric pressure gas plasma are very effective and contain many active agents which result in decontamination of surfaces [26]. Hence, this mode of plasma generation in a more scalable and flexible form , which is the subject of this

research, can prove to be a great sterilization solution. However, we need to better understand the major components that are responsible for the effects observed with various surfaces. The understanding of the underlying factors that dominate the mechanism of plasma-surface interaction will help better design this technology to cater for various applications. The goal and objectives, as outlined below, are designed to test and validate the performance of the cold plasma generation device being investigated.

Goal and Objectives

In this study, we investigate asymmetric SDBD plasma actuators as a novel method of cold plasma generation for biological decontamination and assess the fundamental mode of interaction between the plasma and the cells. In doing so we demonstrate the effectiveness and ability to utilize the induced flow for decontamination and plasma exposure. Based on this broad goal we have objectives to achieve the same detailed below:

- Identification of scaling effects of electrode dimension on SDBD plasma actuator.
- Biological validation of asymmetric SDBD plasma actuators in inducing flow and effective decontamination.
- Evaluation of the effects of asymmetric SDBD generated plasma on mammalian cell morphology and cell response.
- Identification of the primary components involved in plasma -cell interaction in asymmetric SDBD plasma actuators.

Outline

This dissertation has been organized into seven chapters. The first chapter provides a basic introduction and scope of this work outlining the motivation, goals and objectives. The second

chapter provides a more in depth review of the fundamentals of cold plasma, the current standards of decontamination and sterilization in the medical and food industries, the state of art in the field of plasma based decontamination and benefits of this technology. The rest of the chapters are organized on specific topics (objectives) based on journal articles which have either been published, submitted or in preparation.

Chapter 3 shows electrode dimensions on power requirements for scaling of the actuators into arrays to help design low power, high impact devices. Chapter 4 demonstrates the benefits of asymmetric design of the SDBD actuator over the symmetric for inactivation of *Listeria monocytogenes*, and to demonstrate the benefits of its ability to induce flow. This chapter also demonstrates the effectiveness of the actuator with proximity. Chapter 5 is designed to demonstrate how different types of cells respond to exposure to plasma and their dose dependent response to plasma by analyzing the effects on cell morphology, viability and functionality. This chapter also highlights the major plasma generated reactive species using Optical Emission Spectroscopy (OES). Chapter 6 investigates the various plasma generated species and their respective role in the observed cellular response. The primary plasma generated component is identified responsible for the observed effects using various colorimetric assays and a variable exposure setup. Chapter 7 provides the overall conclusion of this work and the outlook of this dissertation. It also outlines the future work that needs to be completed for this technology to expand the scope of knowledge and develop systems for implementation in the field.

The work in this thesis helps fill the gap in the knowledge with regards to SDBD plasma generation in the field of decontamination and also understanding its primary mode of interaction with various substrates. It also expands the knowledge base for modulating the actuator parameters for effective generation of certain species (tuning) with low power applications.

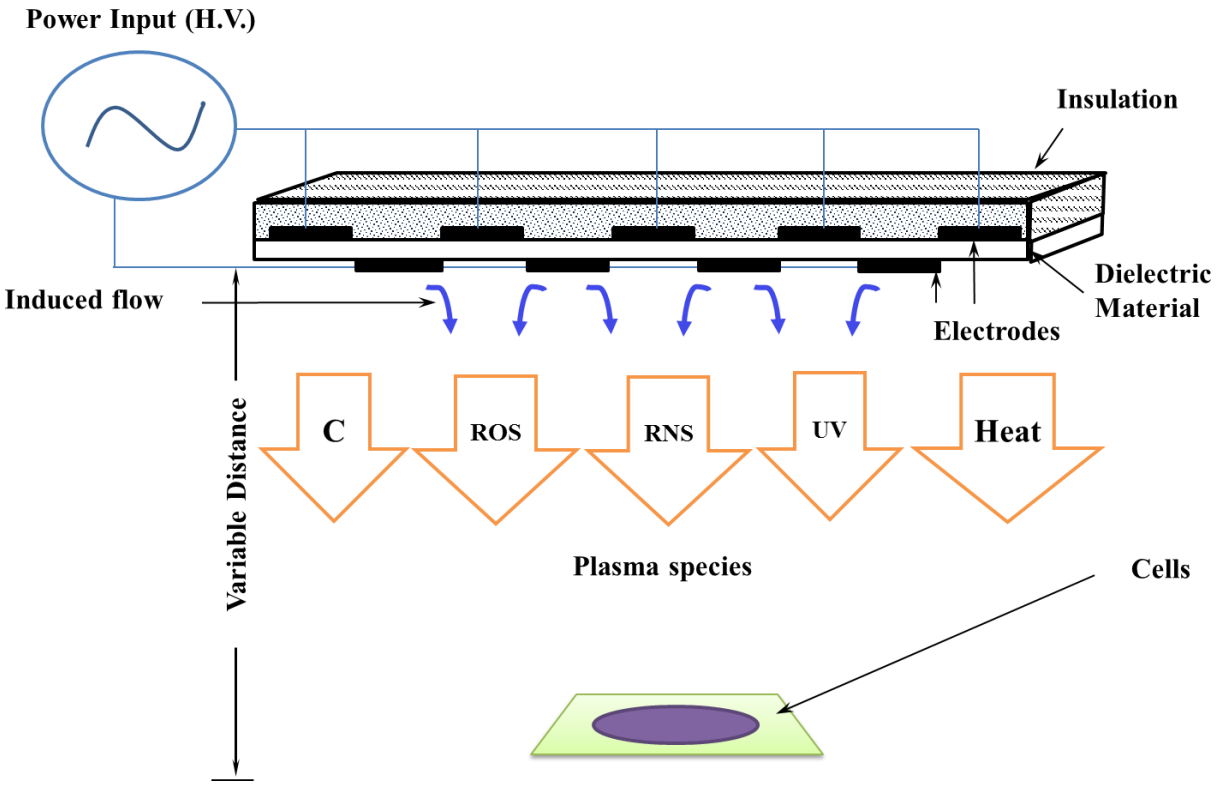

Figure 1 Schematic showing the components /parameters of plasma to be investigated in this study where C= Charged ions; ROS= Reactive Oxygen Species, and RNS= Reactive Nitrogen Species, and UV= Ultraviolet radiation.

Chapter 2

Background

2.1. Fundamentals of Cold Plasmas

In nature we have learnt that there are three states of matter, solid, liquid and gas. But over the past decades a fourth state of matter has been classified as *plasma*. It was Langmuir who saw the similarities between the plasma (the liquid component of blood) and the discharge plasma (ionized gases) based on the analogous characteristics of ionized liquids in biology and ionized gases generated in nature or laboratories [27]. In physics, plasma is an excited, ionized state of matter with either equal or different concentration of opposite charges. It is generally formed by electric discharges in the gas. It can also be produced from solids and liquids through vaporization and ionization [28]. There is a distinction between plasma and gas as the kinetic theory of gases is not completely obeyed in plasma. As plasmas are excited charged mass of ions and electrons, long distance coulomb forces play a critical role in the displacement of the charged particles rather than just the Brownian motion due to collisions as in gases. Electrons and ions are accelerated through an electric field, along the field lines towards the oppositely charged electrodes and in the process transferring their energy elastically or inelastically to other atoms and molecules [29].

In some plasma where the coulomb forces are sufficiently strong over a considerable distance the particles in plasma may even follow a definite path rather than just motion through collisions. Plasma, much like any other fluids, tends to flow from higher to lower potential, but since the particles in this fluid state tend to be charged they flow along the applied electric field lines with respect to the polarity of the prevalent species, that is, charged particles are attracted towards the opposite polarities along electric field lines [28].

In general, plasmas can be classified as a mass of charged and neutral species of atoms and molecules characterized by a collective behavior [28]. This state of matter is also sometimes termed as *quasi neutral* as the total charge density is always equal, that is, the number of ions is equal to number of electrons. The parallel processes of ionization and recombination of the molecules in the plasma maintain this number of ions and electrons the same. Man-made plasmas may be classified based on mode of generation and temperature of operation.

(i) Mode of generation:

In nature plasmas are normally found to exist in stars and comets and may be generated during natural phenomena like lightning during a thunder storm. Plasmas may be generated from liquids and gases through electric discharges at high voltages, and even solids through intense heating by using stimuli such as lasers. The modes of generation also depend on the method of excitation. Plasma can be generated using RF frequencies or even microwaves frequencies of in the order of GHz. Depending on the mode the characteristics of the generated plasma vary. The Industrial, Scientific and Medical (ISM) bands has designated special band widths for frequencies to be used in plasma generation and based on those particular frequencies various radicals and metastable

ions are generated [30, 31]. The frequency dictates the rate of ionization and the time period of existence of particular radicals.

Depending on the type of discharge, the gap between electrodes, the pressure and the feed gas being used the plasma species being generated vary. Higher pressures and higher electrode gaps result in lower ionization rate as the ions combine before reaching the opposite electrode and also lower number of collisions due to higher pressures [28]. Lower pressure and lower gap between electrodes would also result in the electrons not causing a suitable avalanche effect by colliding with ions and thus reducing the volume of plasma being generated. This phenomenon is called the *Paschen's Law* given by the product *Pxd*, where p is the pressure of the feed gas and d is the distance between the electrodes [28].

Based on mode of generation non-thermal plasmas may be classified as follows:

(a) Glow Discharge: This is a low pressure discharge, usually on the order of mbar [32], generated between two flat electrodes. These discharges can typically be generated at low voltages due to low pressure, which allows for longer mean free path of energized electrons. Due to this phenomenon, the electrons typically quickly excite neutral atoms and molecules to provide a characteristic glow for each gas, and hence the name *glow discharge*. These discharges are usually employed in fluorescent tubes. These discharges are typically not preferred at high pressures as they converge into an arc if there is sufficient current. The low pressure on the order of few mTorr or Pascals make them undesirable for industrial applications.

(b) Corona Discharge: This form of plasma discharge is an inhomogeneous (negative corona) or homogenous (positive corona), localized, filamentary glow created near a pointed

electrode or around a wire using a nearby grounded (or electrode of lower potential) or surrounding air. The electrons are accelerated to sufficiently high energy levels by the electric field in the vicinity of the electrode, thus resulting in ionization of the surrounding neutral gas molecules and atoms [33]. Corona discharges can be positive or negative depending on polarity of voltage applied to the electrode. This form of discharge is generated typically at higher potentials, typically on the order of kV, and high pressure (atmospheric or higher). These discharges are typically used in applications such as electrostatic precipitation[28] and surface treatment [34]. However, these discharges are formed at sharp edges or at the edge of pointed electrodes and may not be uniform due to their filamentary nature.

(c) Silent Discharge or Dielectric Barrier Discharge (DBD): This form of discharge combines the benefits of glow discharge and corona discharge i.e. it can be created in large volumes typically at high pressures. This discharge is classified by the presence of a dielectric layer on one or both of the electrodes, hence the name dielectric barrier discharge. The duration of the discharge typically depends on the pressure, dielectric properties and the characteristics of the gas being used [35]. This discharge is characterized by randomly distributed micro-discharges in time and space. The characteristics of this discharge will be discussed in detail in subsequent sections. This form of discharge is typically used in applications such as ozone generation and was first conceived by Siemens in 1857 [36]. The formation of the discharge is based on inter-electrode gap and pressure, and hence, is very much dependent on the Paschen's law.

(d) Radiofrequency Discharge: This form of discharge uses wavelengths on the order of MHz, such as in inductively coupled plasmas (between 2-60 MHz), and are able to produce

homogeneous plasmas as the wavelength is much higher than the vessel dimensions [32]. These plasmas operate at low as well as atmospheric pressures. The electrodes are typically outside the plasma zone thus preventing any erosion effects. These plasmas are typically used for etching applications and find use in the semiconductor industry [32]. Eliasson *et al*.[32] and Grill [28] provides a good description of these types of discharges. However, these discharges incur issues when the reactor is scaled and the dimensions become comparable to the wavelength [28].

(e) Microwave Discharges: This form of plasma discharge is generated in the microwave region (0.3-10 GHz) [32]. These discharges have wavelength of the field typically on the order of dimensions of the vessel they are created in, and as such, can create relatively large volumes of plasma at a wide range of pressures. Most microwave plasmas are generated in waveguides or resonant cavities specifically designed for these applications [32]. A fairly common frequency they are generated at is 2.45 GHz, such as in the microwave oven [32]. These discharges too suffer from similar drawbacks of RF discharges and need specially designed waveguides. They also are not very efficient and sustainable at low pressures (< 1 torr) [28].

(ii) Temperature of plasma components (electrons and molecules):

Based on properties of plasma they are distinguished as *thermal* and *non-thermal* or as *equilibrium* or *non-equilibrium*. Thermal plasmas normally have the same electron and ion temperatures, whereas non-thermal plasmas have electron temperatures several orders above ion temperature ($T_i << T_e$). This may be due to the fact the energy of the electric field used to generate the plasma gets coupled first with the electrons as they are lighter. As a consequence the temperature of the electrons is raised by several thousand degrees. The electrons then transfer this

energy to much heavier ions through collisions and photon emission (photoexcitation). In thermal plasmas due to available high energy the electron collision frequency is higher and result in the ion temperature being approximately equals the electron temperatures ($T_i \approx T_e$). In the case of non-thermal plasma the lower electric field strength results in a lower electron collision frequency. Hence, the electrons remain at temperatures several orders higher than the ions (~ 11600 K), whereas the ions are near to room temperatures. This effect is also coupled with loss of energy to walls surrounding the plasma and thus the energy flux from ions to surrounding dominates over the energy flux from electrons to ions. The terms non-thermal and non-equilibrium are sometimes used synonymously as both represent the inequality in temperatures of electrons and ions in plasma. Thermal plasma generated in a constraint environment will tend to have local thermal equilibrium as at the walls the cooling effect dominates over the electron energy transfer rate [28].

If an electric field is created in plasma the charged particles will try to reduce its effects. The electrons being lighter will move faster to reduce the field. This response of the charged particles to reduce the effects of local electric fields is called *Debye Shielding*. This shielding gives the plasma a characteristic of quasi-neutrality. The quasi-neutrality is a bulk phenomenon between two oppositely charged electrodes as the bulk of the plasma has a net neutral charge. But regions near the electrodes tend to have higher concentration of specific charges in their immediate vicinity, and these charges in turn tend to shield the electrodes from the bulk plasma. Hence the applied potential tends to develop in bulk near the electrode surfaces over a distance of λ_D, called the *Debye length*, as shown in **Figure 1**, defined by:

$$\lambda_D = \frac{\epsilon_o k T_e}{n_e e^2} \qquad \text{---------- Eq 1.1}$$

Where, ϵ_o = the permittivity of free space

e = the charge of the electron

n_e = the number of electrons

λ_D = the Debye length

T_e = the average electron temperature (≈ 11,600 K)

k = Boltzmann's constant

In plasmas the potential is affected by the electron and Ion concentration and its value can be obtained by solving the governing Poisson's equation:

$$\nabla^2 V = -\frac{\rho}{\epsilon_o} \qquad \text{---------- Eq 1.2}$$

Where, ρ = the total charge density

ϵ_o = the permittivity of free space

V = the electric potential

The total charge density, ρ, is given by the equation:

$$\rho = (n_i - n_e) + q\delta(d) \qquad \text{---------- Eq 1.3}$$

Where, ρ = the total charge density

δ = Dirac delta function

n_i = the total number of ions in the plasma

n_e = the total number of electrons in the plasma

q = a point charge introduced in the plasma

In the absence of any external charge, the value of total charge density is equal to zero hence the Poisson's equation has a value of zero thus resulting in the quasi-neutral state of the bulk of the plasma[28].

2.1.1 Surface Dielectric Barrier Discharge (SDBD) plasma actuators

Various methods of cold plasma generation have been developed and implemented over the years for such applications among which Dielectric Barrier Discharge (DBD) has been found to have a high potential for use in the industrial environment [37, 38]. Dielectric barrier discharge (DBD) is a type plasma generation process wherein plasma is created due to the accumulation of charge on one side of a dielectric medium between two electrodes (**Figure 2(c)**). The dielectric medium does not permit the passage of charge that in turn develops to oppose the applied electric field until the field is balanced. This migration of charge and generation of ions in the process continues till the charge stops growing and the discharge extinguishes. This process of charge accumulation in the form of plasma is a very ephemeral process and the discharges last on the order of seconds [22, 37, 39, 40]. There are two types of dielectric barrier discharges, volumetric and surface, shown in Figures 1a and 1b, respectively. Gibalov and Pietsch [37] explained the formation of different discharge patterns in these two arrangements. Over the years volumetric barrier discharge has received a lot of research emphasis. This approach has a gap between the dielectric covered electrode and the cathode, in between which a low pressure gas such as argon is passed. The discharges are random and form a thin region of plasma between the two electrodes. This set-up is used for either direct or indirect treatment of instruments for sterilization [41]. The gas is either passed in the gap with the article to be sterilized placed between the two electrodes, or using the gas flow the species generated that are transported to the site of required microbial

inactivation. This sort of discharge restricts the applications of the technology as it restricts the size of articles that can be placed in between the gap. Also if the indirect mode of activation is employed the charged particles and UV mostly do not aid in the inactivation process. Fridman et al. have shown that direct exposure to plasma is more than an order of magnitude faster than indirect exposure [13].

Surface discharge on the other hand has two electrodes placed asymmetrically with a dielectric between them. **Figure 2(a)** depicts the electrode arrangement for surface dielectric barrier discharge. One of the electrodes (anode) is covered to prevent its contact with the gas while the other (cathode) is left uncovered. Plasma is formed adjacent to the cathode. The form varies from distinct streamers to diffuse discharges with low glow based on the amplitude of AC voltage supplied and the applied frequency [37]. The DBD can sustain a large-volume discharge without the discharge collapsing into a constricted arc at atmospheric pressure. This is because the arrangement is self-limiting [42, 43]. The electrode which is exposed for the negative half cycle of the AC supply is more negative than the dielectric material and the electrode enclosed by it, hence electrons are emitted at a sufficiently high voltage and accumulate on the dielectric surface, thus the name dielectric barrier. As the surface charge builds up it opposes the applied voltage and hence shuts down, and vice versa for the positive cycle, which also helps dissipate energy and control the rise in temperature [22, 42]. The discharge is much more irregular on the positive going half cycle then the negative. The discharge is uniform along the width of the actuator in the voltage negative cycle, but in segregated patches for the positive half [22, 23, 44]. This plays an important role in the momentum coupling between the generated charges and the neighboring but the amount of plasma development is the same for both half cycles.

Interaction of plasma with the applied electric field is responsible for the body force while plasma neutral interaction and momentum coupling is caused by collisions. The mechanical coupling between the air and actuator is caused by plasma, hence it is the intermediary [22]. But the key element is the geometry of electrodes, which effects the direction of flow. The plasma will not expand beyond more than a few mm from the downstream edge of the grounded electrode no matter how high a voltage is applied because the strong electric field is limited to the region between the electrodes. Thus sparking due to excess charge build-up is not a problem. Use of multiple actuators will increase the velocity of induced flow appreciably. For example, two actuators placed strategically will provide twice the velocity as a single actuator at same applied voltage. The thickness of exposed electrode has no effects on the discharge but its thickness affects the efficiency of the actuator – the thinner the electrode the greater the momentum transfer is to the air. **Figure 2(b)** shows plasma being generated in a single SDBD arrangement. The advantages of this technology can prove to be an excellent boon to the sterilization industry. This technology can prove to be an excellent method for sterilization due to its high performance without the need for any moving parts. It is easy to run, uses atmospheric air and can be practically designed into any form factor as it is both flexible and scalable. The electrodes can be positioned such that they can prove conducive to direct the flow of reactive species and ions generated by the energy transfer from the applied electric field into the surrounding air that acts as the active fluid. Researchers have proven that atmospheric pressure gas plasma are very effective and contain many active agents which result in decontamination of surfaces. Hence, this mode of plasma generation in a more scalable and flexible form factor, which is the subject of this research, can prove to be a great sterilization solution.

The SDBD has various benefits over some of the other methods of plasma generation, hence, as mentioned in the preceding sections because of its nature and mode of generation, has found numerous applications in separation flow control in aircrafts [22-24, 45-55]. The plasma actuators based on this principle are fully automatic with no moving parts, have a fast time response for unsteady applications, have a very low mass which is especially important for applications in high g-loads, hence can be applied to surfaces without cavities or holes with an efficient conversion of input power to fluid momentum conversion and easy ability to simulate their effect in numerical flow solvers [22, 54].

In the last decade the ability of surface dielectric barrier discharge for active flow control has been investigated extensively. The asymmetrical placement of the electrodes about the dielectric barrier creates an electric field along which the electrons and ions migrate creating a momentum coupling effect. This effect has proven to generate velocities as high as $8 m\text{-}s^{-1}$ [40]. These velocities can be vectored in the desired direction through adequate geometry and orientation of the electrodes. Similar results have been obtained with corona and coplanar discharges [40]. The flow of the gas is manipulated through the orientation of the electrodes and the actuator profile (by molding the dielectric) to get the neutral gas to flow in the particular direction without adding any extra gas or mechanical parts. This form of adding momentum to stationary gas is known as *zero-net–mass flux* jets [56].

We intend to hence use SDBD, which is a zero-net-mass-flux device generating its own flow and producing plasma using atmospheric air. This technology over the years has proven to be effective against planktonic cells and we feel strongly that it has the potential to do the same with biofilms. This technology has none of the shortcomings of the above mentioned technologies and is easy to use without any harmful byproducts.

2.1.2. Unidirectional flow in Surface Dielectric Barrier Discharge Plasma

The plasma is generated by applying an A.C. voltage across the two electrodes placed asymmetrically on the either side of a dielectric medium. One of the electrodes is exposed to air and the other is covered with a substrate material. This prevents plasma from being generated adjacent to the covered electrode by thwarting its contact with the surrounding air. The plasma is generated by the ionization of the air adjacent to the exposed electrode. The plasma is a mass of ions and electrons along with other neutrals and metastable ions generated by the energy transfer from the electric field to the atoms and molecules in the air. The electric discharge generated once the breakdown of the dielectric medium is achieved. This is mainly due to the accumulation of charge on the surface of the dielectric medium. The whole sandwich serves as a capacitor storing charge which gets dissipated once the threshold electric potential is achieved. Corke *et al.* in his paper on single dielectric barrier discharge plasma explains a model which considers the entire setup to be a series of capacitors and resistances [53]. This model makes it simple to simulate numerically the parameters of the discharge and the power dissipated. But it still does not explain why the coupling of momentum occurs only in one direction. Enloe *et al*. explain that the asymmetry in the discharge, that is, the difference in the discharge characteristics does not control the momentum coupling and hence give a strong indication that the interaction of the applied electric field with the plasma is responsible for the momentum transfer by plasma neutral interaction[22]. During the negative cycle the exposed electrode is more negative compared to the covered electrode and thus electrons are generated in a higher number thus causing a negative charge on the surface of the exposed dielectric. This causes the gas molecules in the immediate vicinity to get ionized as the electrons collide elastically and in-elastically. Elastic collisions may not be enough to ionize the gases but impart momentum instead to the surrounding gas. The

inelastic collisions are responsible for ionization of the gases. Multiple reaction involving the neutral and charged molecules and atoms in the air occur during both the cycles that results in ions and metastable ions being generated and as a consequence U.V. radiation is produced during their de-excitation. These reactions further result in generation of ozone from the nascent oxygen molecules so generated.

The negative ions so generated are then propelled away from the electrode towards the region of low electric potential which lies downstream of the negative electrode away from the plasma sheath of negative charge developed right next to the electrode. For the positive cycle however, the exposed electrode develops a positive charge compared to the covered electrode. The electrons are in turn extracted from the dielectric medium as well as the surrounding gases this results in a positive charge being generated in the gas. These ions in turn combine with the electrons being generated on the more electronegative dielectric during the positive cycle and thus generate the UV radiation as a consequence. The positive ions formed near the exposed electrode are propelled downstream of the electrode again towards the direction of lower electric field concentration or the opposite potential during the negative cycle and vice versa. The reaction of nitrogen and oxygen taking place may be found elsewhere [11, 57, 58]. Some of the positive ions generated, for example, through the reactions of oxygen and nitrogen molecules shown below generated secondary electrons, which provide the negative charge on the dielectric during the negative half cycle.

$N_2 + e \longrightarrow N^+ + 2e^-$ *(near the negative electrode)*

$O_2 + e^- \longrightarrow O_2^+ + 2e^-$ *(Downstream of the positive electrode/ On dielectric medium)*

As more electrons deposit on the dielectric more the electric field is neutralized by the charge developed thus quenching the discharge. The positive ions are pulled towards the more negative dielectric and hence may be a cause of momentum transfer. It is clear from the fact that electron velocities are comparable to the polarity change of the signal of excitation both of which are much higher as compared to the velocity of the induced flow. It is proven that the body force increases linearly with voltage and with decreasing the A.C. frequency [47]. The unidirectional flow may be explained by the fact that more uniform and higher volumes of plasma occur during the negative cycle as compared to the positive cycle [24, 40, 59-61]. As Orlov *et al.*[59] explain in their work, the plasma is more diffuse and uniform during the negative half cycle resembling a glow discharge. Whereas, it is more like a streamer discharge during the positive half cycle. This may be a cause for the difference in momentum transfer in one direction as less secondary electrons are generated during the positive half cycle as compared to the negative half cycle such as in the case of positive and negative corona, respectively [60]. Orlov *et al.* suggest that a more electronegative dielectric during the negative half cycle shields the surface from external electric field thus preventing streamer formation as compared to the positive half cycle. More detailed reactions occurring during the discharge can be found elsewhere [11, 57, 59]. Lagmich *et al.*[60] also suggested that the development of a negative ion cloud over the dielectric results in a downstream force, and hence, an induced flow over the encapsulated electrode downstream of the actuator. This may also be the reason that the force induced during the negative half cycle is larger than the positive half, and due to the larger momentum of ions and neutrals, the net force and flow are downstream of the exposed electrode [52, 61].

This phenomenon explains why the momentum coupling occurs in only one direction of the flow, that is, downstream of the exposed electrode. It also strengthens the inference derived by

Enloe *et al*. that the thinner the exposed electrode, the more is the thrust [23].This phenomenon is attributed to the stronger electric field concentration at sharper edges of the electrodes that results in greater body force. Thinner electrode will also result in comparable dimensions of the Debye length of the plasma sheath that will repel like charges giving rise to the body force. This model proves that the phenomenon associated with the momentum coupling in a Surface Dielectric Barrier Discharge (SDBD) is related not only to the asymmetric geometry but also the chemical reactions taking place in the vicinity of the discharge. Further tests need to be conducted with gases of different molecular masses and a mass balance to help bolster this model and explain the correlation of the body force and molecular mass of the gas, such as those by Font *et al.* [61].

2.1.3. Flexibility in Design of SDBD Plasma Actuators

Keeping in mind all of the factors from the previous sections, we studied different designs of surface discharge. We chose surface discharge due to the numerous shortcomings of volumetric discharge. As we have seen the surface discharge provides what volumetric discharge cannot, and that is a body force which helps manipulate the flow over the actuators. It does not require external flow actuation for short-range applications. For long range an external actuation for flow can be utilized. The actuators can be varied in shapes by manipulation of the geometry of the electrodes and/or the dielectric medium. Looking at these strong points we based our design on surface discharge phenomenon. **Figures 3 (a)** through **3(c)** show plasma being generated using surface discharge in various geometries with both in plasma on and off condition. **Figures 4** and **5** show how the design can be modified to assist flow and even generate uniform effect. This makes highly evident its flexibility. In the past we have seen the ability of various SDBD designs could generate flow that could induce mixing in the bulk fluid [62]. Santhanakrishnan *et al*. [56] and Bolitho *et al.* [63] have shown the ability of SDBD plasma actuators to induce flow with pulsatile flow as

well as vectoring in different directions, which can carry the plasma generated species to the surface being treated.. Hence, SDBD plasma actuators are very versatile and will be a very good candidate for biomedical, non-contact applications.

2.2. Fundamentals of Cold Plasma Decontamination

Everything around us, however clean it may appear to the naked eye, ranging from an instrument used for a surgical procedure to a fresh apple from the market, harbors numerous microorganisms which are invisible to the naked eye. All these objects require sterilization or decontamination to clean then and make them safe for use or consumption. Currently the industries ranging from food to medical instrumentation are facing issues due to contamination by human pathogens.

2.2.1. Medical Sterilization

Sterilization and decontamination of both organic (tissues and wounds) and inorganic (medical instruments) objects is a crucial component of the medical industry. For any device to be considered sterile it has to meet the standard set by the Food and Drug Administration (FDA) and the Centers for Disease Control (CDC) [1, 34]. Currently, due to the incorporation of heat labile materials such as those in implants and probes like endoscopes, sterilization and decontamination technologies like Ethylene Oxide (EtO) gas and gamma irradiation cannot cater to the rising demand for effective and affordable alternatives in all settings[64, 65]. For many patients, surgical implantation of these bioengineered foreign bodies carries risk of infection. Although the risk of infection of these devices is in general only between 1 and 7%, the impact of implant-associated infection is great [66]. Implant-associated infections are associated with considerable morbidity, repeated surgeries, and prolonged antibiotic therapy. For example, mortality of prosthetic valve endocarditis ranges up to 30%, and mortality rates associated with an infected aortic graft approach

40% [66]. The World Health Organization estimates that, per annum in Europe and the USA, approximately 4.5 million and 1.7 million patients, respectively, are affected by Healthcare Associated Infections (HCAIs), accounting for 100,000 and 37,000 deaths per year [67, 68]. HCAIs have a major financial impact, with estimates placing the additional costs at $17-$20 billion each year, much of which is not reimbursed [69-71]. These costs keep rising each year due to a advertent or inadvertent lack in diligence of frequent check on the sources of HCAIs [72-75]. According to the CDC's Hospital Acquired Infections (HAI) report of 2011, even with the current sterilization technologies, there are over 157,000 surgical site infections and nearly 72,000 primary bloodstream infections caused by Methicillin Resistant staphylococcus Aureus (MRSA) and *Clostridium difficile,* and the emergence of unknown superbugs [76]. Approximately 75,000 hospital patients with HAIs have died during their hospitalizations with more than half occurring outside of ICUs. Over 2 billion people suffer from Hospital Acquire Infections (HAI) with over 23, 000 deaths due to the same according to the CDC [77]. Site-of-surgery infections account for approximately 22% of HAIs and need to be handled carefully [76].

While the causes are numerous, a 2013 study reported that about 15% of endoscopes in US hospitals failed to achieve an accepted standard of cleanliness after liquid reprocessing (the prevailing disinfection process used between patient procedures) [78]. Because flexible gastrointestinal endoscopic instruments are heat labile, only high-level sterilization with carcinogenic and cumbersome chemical agents such as EtO gas at low-temperature possible. However, no low-temperature sterilization technology is currently approved by the US Food and Drug Administration (FDA) for gastrointestinal endoscopes such as duodenoscopes [79]. Even though over 10 million gastro intestinal procedures are performed each year in the US alone[79], 400,000 rural healthcare facilities lack a means of sterilization.

2.2.1.1. Different Methods of Medical Sterilization and Disinfection

Steam Sterilization: This is the basic method of sterilization using moisture and heat. High temperatures and pressure are generated using a device known as an autoclave which make the environment inhospitable for pathogens [1]. These devices typically work at 121 ºC and are run for a minimum of 30 minutes [1]. These devices use water and high power to provide these conditions. Autoclaves produce high temperatures and pressure with high moisture content, this may results deleterious effects on some materials including corrosion and combustion of lubricants associated with dental hand pieces [80]. Autoclaves also uses a lot water and are unusable for heat labile instruments [1]. Application of thermal energy can also be quite slow at the temperature limits required to avoid damage to heat sensitive equipment like plastics and typically only evaporates Chemical agents without destroying them, allowing condensation on downstream surfaces.

Ethylene Oxide (EtO): EtO is used for instruments that are heat sensitive [1]. EtO is a colorless gas that is both flammable and explosive. Treatments normally use gas concentration (450 to 1200 mg/l); temperature (37 to 63 ºC); and exposure time (1 to 6 hours), with processing times of over 18 hours [1]. Mechanical aeration for 8 to 12 hours at 50 to 60 ºC allows desorption of the toxic ETO residual contained in exposed absorbent materials. ETO sterilizers need to be designed so as to prevent leakage and corrosion so as to meet OSHA regulations [1]. Chemicals such as EtO (toxic gas), all have long periods of desorption (dispersion or ventilation) and processing times, and this results in high lead times for the instrument to be rapidly available. In addition, they are toxic and irritate the skin and mucous membranes [1].

Hydrogen Peroxide Gas Plasma: These devices use Hydrogen peroxide vapors and produce plasma by ionization, at low pressures (Vacuum) using either RF or microwave frequencies [1]. The hydrogen peroxide vapor diffuses throughout the chamber and initiates the inactivation of microorganisms. Microbicidal free radicals, such as hydroxyl and hydroperoxyl, are responsible for the microbial inactivation. The by-products (e.g., water vapor, oxygen) are not toxic and eliminate the need for aeration. The process operates approximately at room temperature, and has a cycle time of 75 minutes [1]. The excess gas need to be removed and in the final stage (i.e., vent) of the process the sterilization chamber is returned to atmospheric pressure by introduction of high-efficiency filtered air. All of this requires the system to use heavy components like pumps and such. Hydrogen peroxide is also an irritant like EtO and needs to be monitored.

Irradiation: Sterilization by ionizing radiation, using radioactive elements like cobalt 60 gamma rays, or using electron accelerators like Electron Beams (E-beam), are low-temperature sterilization methods that can been used for a number of medical devices. These devices use penetrating radiations that have impact on the cells of contaminants like blood on a molecular level. However, currently there are no FDA-cleared ionizing radiation sterilization processes available for use in healthcare facilities [1]. The use of ionizing radiation, such as γ-rays, requires highly radioactive materials for their production. This is best done in a heavily shielded fixed facility and cannot be easily implemented in the field. Also, this method can prove destructive to sensitive equipment and also may prove lethal to the operator. This method also suffers from issues like high sterilization costs, and high setup cost. Some deleterious effects on patient-care equipment associated with gamma radiation include induced oxidation in polymers [1].

Reference [1] provides a good level of detail on other available methods of sterilization and disinfection, such as Ozone, along with their limitations. Strains of pathogens such as *Bacillus*

anthracis have been shown to be very resilient to heat, pressure, as well as UV treatment [81-84]. Ultrasonic removal of surface contaminants is neither fast nor dry.

Apart from these drawbacks, many underdeveloped countries have remote Primary Health Care (PHC) facilities that cannot afford these technologies since they are bulky, expensive and have a high power requirement. The requirement of short turnaround times along with more effective, less expensive, and mobile sterilization systems is in high demand, and there are over 400,000 PHCs and sub centers in low income regions of the world without adequate sterilization equipment. Combined, these facilities provide care for over 2 billion people. Up to one in three patients receiving treatment at remote clinics become infected from unsterilized medical instruments. This causes over 20 million preventable infections the world. 50% of the world's rural health clinics, serving three billion people annually, operate without electricity. Developments in the field of cold atmospheric plasma for a technology using no chemicals, which is easy-to-use and portable can prove very beneficial to the underserved masses.

2.2.2. Food Safety

According to the Center for Disease Control (CDC), 1 in 6 Americans suffers from foodborne illnesses and 128,000 get hospitalized [5]. 3000 people die each year due to the same. *Salmonella*, *Listeria monocytogenes* and pathogenic *Escherichia coli* are some of the major human pathogens responsible for these foodborne illnesses [5, 85, 86]. The number of cases of foodborne illnesses is bound to increase as the demand for the fresh produce increases [3]. A number of methods have currently been used to address the issue of foodborne pathogens contamination of fresh produce with their unique applications and limitations.

2.2.2.1. Different Food Decontamination Methods

Ozone: Ozone has been used for many years as a disinfecting agent mostly in water based applications. Ozone is a strong oxidant and potent disinfecting agent. It has been found to be effective even at low concentrations of 1-5 ppm [3]. Its antimicrobial ability is stronger than that of chlorine which makes is more suitable than chlorine due to shorter contact times [87, 88]. No negative impacts of ozone treatment have been observed on the nutritional content of vegetables in the range of 1–5 ppm as compared with the traditional chlorine treatment [3]. However, In the processing industry, it is important to keep the ozone levels below a certain threshold, as it is known to increase the corrosion potential of stainless steel above concentrations of 1 ppm [3]. Most materials are compatible with ozone at moderate concentrations [89-91]. However the concentrations need to be monitored and kept to a minimum to prevent adverse effects to both the equipment as well as personnel [3]. Occupational Safety and Health Administration (OSHA) has permissible level of exposure of 0.1ppm for a maximum of 8 hours.

Chlorine: Chlorine is one of the most widely used disinfectant for cleaning fresh produce via washing. This is mainly because it is cheap, easy to use and has rapid antimicrobial action [3].. However, Chlorine works well only in a suitable range of pH and the concentration of the same has to be maintained. It is highly corrosive and is not permitted in certain countries [92]. Apart from these issues, chlorine wash also needs a lot of water that needs to be treated post treatment.

Chlorine dioxide (ClO_2): ClO_2 is an effective oxidant like ozone, and can be produced by various methods such as reacting an acid with sodium chlorite [3]. Unlike chlorine, ClO_2 is effective at a wide range of pH. However, as it is explosive in nature, it needs to be generated on site [3, 92].

The effectiveness of ClO_2 is the same as chlorine and being explosive as well as corrosive in nature needs to be safety monitored.

Ultraviolet (UV) radiation: Bacteria on various surfaces can be destroyed by exposure to UV light [4]. Ultraviolet light can be generated using mercury lamps, and consists of electromagnetic radiation in the wavelength range from 100 to 400 nm [4]. The UV light spectrum is divided into four regions: UV-A (315–400 nm), UV-B (280–315 nm), UV-C (200–280 nm), and vacuum-UV (100–200 nm). UV-C is highly germicidal as it causes photochemical changes to the DNA, which eventually inactivates the pathogen. UV light is a nonionizing, non-chemical, and non-thermal method, which is environmentally friendly, easy to handle, and cost-efficient., A major difficulty with the use of UV light is that the commodities like carcasses have a complex surface topography [4] in addition to shadowing may prevent any treatment of some indented surfaces. Nonionizing radiation, such as UV, requires line-of-sight application. i.e. can only effect object directly in the path of the radiations and can be quite time consuming. But it has been shown that dried spores are resistant to UV [93, 94].

Irradiation: Gamma irradiation and electron beam irradiation is being increasingly used by the food industry. Gamma radiation is produced from radioactive isotopes such as ^{60}Co (Cobalt 60) and is highly penetrating [4, 85]. In electron beam radiation method or E-beam method, unlike gamma irradiation, electrons are produced at a maximum energy of 10 MeV [4], but unlike gamma radiation, it has limited penetration into foodstuffs. Foods irradiated with these technologies are considered safe for consumption. The WHO considers foods irradiated up to 10 kGy to be toxicologically safe. But these technologies have drawbacks as well. Apart from a high cost of installation [4], too high doses of irradiation may cause effects such as discoloration of meat [85].

The rising cases of irradiation resistance much like antimicrobial resistance is also a major issue for the continued application of this technology [4].

Apart from these prominently used technologies, several other technologies and chemicals are available and details on their use, benefits and drawbacks can be found elsewhere [3, 4, 85, 95]. The current start of art makes it imperative that a novel method be developed to tackle problems associated with current technologies.

2.2.3. Benefits of Cold Plasma in Sterilization/decontamination and Current State of Art

In order to address these challenges, we propose the development of an efficient low-temperature decontamination/disinfection technology to tackle these issues. The technology is based on "cold" or non-thermal plasmas, which are gaining interest in different fields ranging from material treatment to medical applications. Cold plasma refers to the plasma generated close to room temperature and receives the term "cold" due to the fact the bulk temperature of the gas is much lower than the electron temperature ($T_g << T_e$) [11, 28, 38]. The low operating temperature creates a scope for application in the field of sterilization, surface modification and coating, and even wound healing and wound sterilization. Cold plasma, if generated with a certain combination of gases, can result in various effects such as etching or oxidation. These mechanisms aid in the removal of impurities on solids as well as in liquids. Cold plasmas have been used extensively for ozone generation in industries to purify water through coagulation and precipitation of impurities like manganese, etc.

Depending on the type of discharge and the energy of the same plasmas is classified as high temperature and thermal plasmas or low temperature or non-thermal plasmas based on the temperature of the generated plasma [11, 29, 38, 96, 97]. Non-thermal atmospheric plasmas, in

general, have been tested in recent years and have found numerous applications such as wound healing [10, 14, 16, 98-104], dental care [7, 10, 105-108], and especially in the field of medical sterilization and decontamination of both instruments as well as biological surfaces, which has a compendium of literature published [10, 26, 34, 99]. A basic prototype for sterilizing dental instruments was tested by Sung *et al.* which shows potential use of cold plasma to replace old technology like autoclaves [6]. The use of non-thermal plasma, due to its beneficial properties, is gaining a lot of attention in the fields of disinfection and sterilization. Different sources for various types of plasma generation methods have been proposed over the years [7, 8, 13, 26, 41, 81, 101, 105, 109-123]. Ehlbeck *et al.*[34] and Kong *et al.*[99] provide a very good review for various types of plasma discharges used for medical applications of non-thermal plasmas. Plasma kinetic procedures are minimally invasive and can offer significant advantages over conventional, invasive surgical intervention regimes making them much more attractive.

Non-thermal plasma prove promising in this regard as they have a multi-component dynamic while interacting with the contaminants on food as well. Various research groups have shown their effectiveness on different foods [10, 110, 124-127]. The ability of plasmas to decontaminate food with little to no sensory effects make them very attractive for such applications. Machala *et al.* [10], Niemira *et al.* [128], and Selcuk *et al.* [129] give a good account of use of plasmas in the food industry, and the book on Microbial decontamination of food by Demirci *et al.* [4] gives a good account of current state of art in the field of food decontamination and how plasmas can help mitigate certain issues.

However current methods of plasma generation have certain disadvantages. The aforementioned methods of plasma especially radiofrequency and DBD are the most used methods of plasma generation but have issues with scaling and power consumption. As some designs of

DBD use the material being decontaminated as an electrode which can cause damage to the substrate such as that seen by Pavlovich *et al.* [18]. The DBD, especially volumetric DBD as used by Ziuzina *et al.* [41, 125] has the issue of high power requirements as the gap between the electrodes increases. The commodities also need to be placed within the plasma region which may cause desiccation. A similar desiccation effect was observed by Kieft *et al.*[17] with mammalian cells. Most of the devices currently designed need to be placed close to the surface being treated [13, 14] or have an issue with scaling such as certain plasma jets using radiofrequency dischages, such as the plasma pencil [44, 130, 131] and the plasma needle[108], which may have issues of uniform treatment at large scale applications.

Hence, we propose a SDBD based cold plasma technology to overcome the short comings of these technologies. Its structure make the circuit complete on the actuator itself so as to mitigate any effects such as burns etc. This design can be scaled and modified fairly easily with an added advantage flow induction [56, 62, 63]. Making this a viable technology for these kinds of applications. With all the benefits of silent discharges, coupled with the induced flow, this device does not need any exotic gases or additional flow such as in the case of other designs [12, 26, 34].

2.3. Different Active Components of Plasma Involved in Decontamination

Use of plasmas for sterilization and other medical applications has gained popularity in recent years due to its rapid effects and flexibility of use. It has been shown that cold atmospheric plasmas are effective against a broad spectrum of gram negative and gram positive bacteria, bacterial spores, yeasts, viruses and biofilms [117, 119, 132]. Recent studies have shown the effectiveness of using low temperature plasma for sterilization and cleaning. Whittaker et al. [7] showed results of treating orthodontic files when exposed for a short-term to low-pressure oxygen–argon plasma,

before being re-examined. In all cases, the amount of organic material was reduced to a level below the detection limit of the instrument as can be seen in **Figure 6**. However, the detailed processes and impact on cell structures are largely unknown. Similar results were observed in case of endotoxins and prion inactivation by Shintani *et al*[111]. Researchers have shown effectiveness of devices like the MicroPlaSter to be effective against antibiotic-resistant strains like Methicillin Resistant Staphylococcus Aureus (MRSA) besides being fungicidal [9, 103, 104, 133-135].

Depending on the type of micro-organism, the medium in which they are cultured and the methods of exposure, i.e. direct or indirect (reactive species come into contact with specimen but not the plasma itself), the survivor curve takes a definite shape. In the course of plasma based inactivation processes of micro-organisms, the key components known to cause cell death are reactive species and charged particles. The effects of heat are negligible as the temperature in the process does not cross the required value at which cellular death occurs. As the ozone generated in DBD discharge has an absorption spectrum which peaks at 250 nm and the lethal band width is below 300 nm for successfully killing the micro-organisms, the role that UV plays in cellular death is still up for debate[39, 136] .The components of plasma based cellular inactivation (**Figure 7**) proposed by various research groups are as given below:

Ultraviolet (UV): UV radiation is known to possess bactericidal properties, and has been implemented for the same for decades. UV causes formation of Thymine dimers in the DNA thus inhibiting cellular replication [137, 138]. However it is not the primary killing agent [139, 140]. This was supported by Laroussi et al., among others [116, 141, 142]. The effects of UV are only substantial in the range of 220-280 nm and high enough doses with a germicidal peak around 254 nm [137, 138]. Most gas mixtures such as air do not result in high enough doses of UV which are lethal. Also the wavelengths generated by DBD are either absorbed by ozone and the remainder

either does not have enough propagation length or penetration depths to cause cellular inactivation. Vacuum Ultraviolet Radiation (VUV) is found to be more effective in killing microorganisms then UV at atmospheric pressure as it has shorter wavelengths, and can be generated specially using argon gas due to argon excimer Ar*. In low-pressure plasmas VUV is considered one of the major sterilizing agent as compared to the radicals of the inert gases [121]. But at atmospheric pressure most of the UV radiation is absorbed by the plasma volume, with little contribution to the efficacy of decontamination [121]. Many researchers have found that UV has little to no contribution in cell inactivation compared to the effects of the actual discharge and exposure to other components [116, 118]. However, some research groups using argon plasmas, such as those generated in the device named MicroPlaSter, produce UV which contributes to decontamination of microbes, even on skin [104, 133].

Reactive Species: Reactive species are generated by the impact between electrons, ions and neutral atoms. This is due to excitation and dissociation of different molecules and atoms, the inelastic and elastic collisions of electrons and ions generated in the plasma with the background gas (in the case of atmospheric pressure plasmas in air). As air has rich concentrations of various gases such as oxygen and nitrogen it is known to generate numerous active species and metastable ions known to be germicidal, for example ozone, which affects cellular respiration. Oxygen in particular is known to produce short lived metastable ions in plasma, Hermann et al. [143] showed the impact of presence and absence of oxygen on the D value (increase with decrease in oxygen concentrations). Kuzmichev et al. [142] concluded that the best bacterial effects are obtained in air with good moisture content and oxygen. The OH radicals formed in presence of moisture are very effective in degrading the cell membrane and atomic oxygen which has a life time of 1 ms and is easily propelled toward the surface to be decontaminated by the body force generated by DBD.

The adversely damaging effects of reactive oxygen species in the form of oxidative stress are well know from previous literature [144-146]. Oxidative stress is experienced by cells when the exposure limit to such species exceeds the tolerance capacity of the cell defense mechanism. Beyond a point of damage a cell is unable to recover from the state and eventually becomes nonviable and dies. The nitrogen in the air helps form NO_x that further strengthens the lethality of the plasma. Other gases known to enhance bactericidal effects of plasma are H_2O_2 [141] and CF_4. NO_x and CO_2 from the air, for instance, are shown to produce acidic pH and directly relate to cell inactivation [147]. Similar involvement of oxygen radicals and metastables such as singlet oxygen were found to be the major components for cellular inactivation in corona discharges by Sysolyatina *et al* [139, 140]. Atmospheric cold plasma discharges differ from low pressure plasmas as the plasma chemistry is dominated by reactive species such as ozone and singlet oxygen rather than ions [148, 149]. Hydroxyl radicals are also known to contribute to a large extent towards the potency of cold plasmas in presence of humidity [114, 150-152]. However, higher water vapor content increases hydroxyl radical concentration at the cost of ozone as the water vapor reduces resistance and increases dielectric capacity, thus reducing the total charge transferred [152].

However, presence of humidified air is hypothesized to contribute to higher bactericidal efficiencies due to OH radicals [121]. Other species include superoxide and peroxide, superoxide being short lived [153-155]. All these species contribute to damage to DNA, RNA, proteins and other biomolecules of the cell. Lipids in particular are most susceptible and damaged during oxidative stress, thus alluding to lipid peroxidation as a possible mechanism of cell damage and eventually death [145, 156].

Along with peroxide and superoxide, ozone is considered as a major disinfecting agent produced by plasmas. It is known to react with many biomolecules such as lipids. Ozone is also

be bactericidal at high enough concentrations on the order of 0.1-0.2 ppm [157]. It may even contribute to the break in single strand DNA through oxidation, which when unrepaired can be lethal to the cells [158, 159]. Ozone also contributes to damage in the cell wall through oxidation of proteins [144, 145]. The bactericidal efficiency of ozone is however effected by the presence of other compounds which may react with it [160].

Charged Particles: Ions have been proven to be biocidal generated both in air as well as nitrogen [161-166]. Charged particles mostly include ions and electrons, but these species only have effect on cellular death in close proximities of a few centimeters. The ion temperature being low and the electrons having temperatures in the range of eV does not really support the theory that they would bombard the cell wall. But instead, in a different observation it has been seen that the charged particles may accumulate on the cell wall and cause a disruption in the electrostatic charge on the cell membrane thus resulting in rupture of cell wall due to generation of an electrostatic force. Mendis *et al.* [167] in his technical note explains how this phenomenon may occur which is further supported by Laroussi *et al*[168]. It is mostly correct with respect to dusty plasmas, and in case of air we can make a close approximation. Although this phenomenon may be mostly correct for the gram-negative bacteria, as they have a more fragile cell wall with lower tensile strength, for gram-positive bacteria it would require higher charge accumulation due to the presence of a stronger cell membrane. Fridman *et al.* reported that high effectiveness of plasma sterilization by direct exposure in DBD is attributed principally to the charged particles and electric field [13]. The authors arrived at this conclusion based on the experiments direct and indirect exposures to DBD plasma. In the first case, cells were deposited in the DBD inter-electrode gap and exposed to all reactive agents; in the second case, cells were located below the meshed metallic electrode and not exposed to the charged species and electric field. Similar results were observed by Machala *et al*

[169]. But researchers and still are in conflict as given times of charge formation around 500 ms, which is much lower than recorded cellular disruption times, and do not give sufficient time for the process to occur [151, 167]. However the mechanism of charge dominated cell wall disruption is refuted by Sysolyatina *et al* [139, 140]. Sysolyatina et al. explained that cells are immersed in a dielectric liquid medium stressed by the pulsed electric field that can provide a transient voltage drop about of 1V across the cell membrane, can enable the perforation of bio-membranes [170].

However, charged particles in gaseous plasma not always can destruct the intracellular components. Kalghatgi *et al.* in their work reported that the charged species and electric field of dielectric barrier discharge (DBD) have no influence on DNA damage which is in contradiction to the work of Fridman *et al* [13]. These results hence refute the models by Mendis *et al.*[167]and Laroussi *et al.*[168] for cell inactivation by DBD as the mechanism of electrostatic disruption proposed by these authors assumes implicitly that cell to be strongly charged levitates in free space or in this case plasma. As strong charging of cell requires too high electric field strength in DBD plasma in order to provide high electric potential of a cell up to 16 V. However, the proposed mechanism is not applicable to a cell deposited on the electrode or the agar as pointed out by Sysolyatina *et al* [140]. The electrical breakdown or electroporation of the cell membrane requires a field of atleast 10^6 V/cm, but literature suggests that only positive coronas may be able to provide electric fields of such magnitudes [171]. But Sysolyatina *et al.* suggests from their observations that the magnitude of the averaged field may be insufficient for electroporation, however, it may be responsible for cell damage working in synergy with other reactive agents [139, 140, 171].

Temperature: Temperature is not considered a major factor in cell inactivation as the temperatures registered with cold atmospheric plasma are near room temperature. But temperature

as high as 50-60°C has been observed on increasing frequencies, and high temperatures denature proteins and change the ambient conditions to inhospitable form favorable[172].

The species generated by plasma depend on the feed gas used. If it is air, which is the case in atmospheric pressure dielectric barrier discharge, there are a wide variety of species generated such as Reactive Nitrogen Species (RNS) and Reactive Oxygen Species (ROS) due to the high nitrogen and oxygen concentrations of air. OH^- (Hydroxyl ion) radicals may be generated due to the vapor content of air while OH- ions help damage the cell wall and DNA by oxidation. Hence, air is a very effective feed gas and the overall effectiveness is very much improved by adding moisture to the air. DBD generates high amount of ozone as well (in the order of 10-100 ppm depending on the power and the array size), which in itself is a very affective oxidizing agent. Ozone along with these species results in a very effective antimicrobial mass of decontaminants [8, 12, 13, 26, 94, 112, 113, 115, 116, 118, 122, 136, 140-142, 147, 151, 173].

The ease of use of this technology and supporting research will help produce high performance, easy to use devices and also provide the medical professionals' incentive to be more diligent during processing and reduce risk of human error, as the mechanism of plasma-cell interaction is primarily physio-chemical and hence does not face the problem of pathogens developing a resistance. Although cold plasma based application of sterilization has been investigated[8, 26, 41, 44, 62, 106, 112-116, 118, 127, 136, 141-143, 151, 174], limited plasma based tools are currently available. The major hurdles that prevent widespread application of the plasma-based devices include the issues below.

i) Cost of device development and implementation

Most of the devices currently under investigation either need extensive power[41, 122] or are too cumbersome to scale to small sizes due to the conservation of inter-electrode gap and sample size that needs to be placed between the plasma generating electrodes. If the inter-electrode gap has any protruding artifacts where the sample is placed the plasma will cease or short to an arc[41]. Such a design also requires artificial gas flow such as that used by Frohling *et al*.[122] for indirect treatment of samples to prevent heating and desiccation. For this reason SDBD is much more efficient and cost effective as it does not depend on the inter-electrode gap and the power requirement is only a function of the thickness of the dielectric, as discussed above.

ii) Limited understanding of the mechanism of plasma- cell and plasma-surface interaction

Even though there have been numerous studies of the mechanisms responsible for plasma cell interaction (inactivation)[12, 17, 140, 175-178], most of them are restricted to either volumetric discharges and corona discharges. SDBDs however are not well investigated as far as the plasma-cell and plasma-surface interaction is concerned. Pai *et al*. have investigated the applications of SDBD in biological decontamination[62] and interaction with mammalian cells,[179] which shows a potential application of the electrohydrodynamic [40, 50, 55, 63] (flow induction) capability of this kind of discharge in plasma based sterilization and decontamination of both organic and inorganic substrates. The major incentive is the induced flow and the ease of scalability with a lower power consumption compared to other methods that are slaved to inter-electrode gaps.

To summarize, non-thermal atmospheric plasmas have been explored in recent years in the field of medical sterilization. Applications ranging from inactivation of bacteria and sterilization [12, 44, 113-115, 118, 136, 141-143, 151, 175] to blood coagulation and wound healing [100, 180, 181] have been investigated intensively. Various methods of cold plasma generation have been developed and implemented for such applications among which DBD is the one found to have the highest potential[37]. Plasma applicators varying from atmospheric pressure plasma jets [44, 98, 114, 143] to DBD plasma devices for close proximity applications [176], and plasma needle using RF excitation [17, 182, 183] have been devised and tested against both prokaryotic as well as eukaryotic cells. All these designs however require a gas flux to propel the plasma generated species to the sight of exposure, or have to be placed in close proximity to the sample being treated as they do not have any ability to induce flow. The cost and power required for scaling the device and area of application is high. The gas flux is also responsible for desiccation or interference with the sample if not regulated. To address these shortcomings, we propose a novel design for plasma based cell and tissue treatment.

As seen in **Figure 2**, the SDBD structure is very simple being composed of two electrodes placed asymmetrically about a dielectric material. Hence, this design helps couple the electric field to the fluid inducing a flow while generating plasma due to the breakdown across the dielectric. This is mainly due to the force generated

$$F=q*E \qquad \text{---------- Eq 1.4}$$

Where, F= Induced electrohydrodynamic force

q= Charge on the particle

E= Electric field strength

The use of AC voltage also gives this design a self-limiting capability that quenches the discharge and prevents arcing. This design has been mostly used for flow control in aerospace applications [25, 46, 48-50, 53-56, 62, 63]. However we have investigated the potential utilization of the flow induction capabilities of this design for biological decontamination [62] and interaction with mammalian cells [179] for potential wound decontamination. The induced flow generated by this design pulls the fluid upstream through the plasma region resulting in the fluid carrying the generated plasma species downstream so it can be used for decontamination. The advantage to such a design is the non-contact and indirect nature that allows for a non-damaging environment for the sensitive samples being treated. We have demonstrated that the design is versatile and can be configured to induce mixing and uniform distribution in the bulk fluid [56, 62, 63], resulting in a better uniform distribution of plasma generated species. The concern that some of the short lived plasma species may be unavailable is found not to be an issue as the reactive species which are much longer lived are mostly responsible for plasma induced cell response[140]. These considerations with the advantage of low power consumption are very conducive for the exploration of SDBD based devices for biological decontamination.

Such devices are not restricted to a particular geometry such as corona discharges, which require needle shaped electrodes, or volumetric discharges, which are restricted to planar configurations with smooth electrodes without any artifacts. This is mainly due to the distribution of the electric field obtained in an SDBD as compared to other designs. The distribution provides for a good flow organization, the authors have analyzed which using Particle Image Velocimetry (PIV) [56]. This will also serve for a better treatment of cells and even patients without the risk of desiccation or damage due to arc formation. Using Pulse Width Modulation (PWM) to reduce total power input while still providing adequate plasma formation can also mitigate the problem of

overheating as incurred by other discharges. The combination of both mechanistic and fluid flow analysis will help develop an effective line of devices based on SDBD for biomedical applications.

The work in this dissertation aims to further investigate the application of SDBD, based on its numerous potential benefits, for sterilization and decontamination of surfaces. In this process we intend to investigate the long and short range effectiveness of SDBD in decontamination of surfaces that emulate potential zones of contamination. The work also aims to demonstrate the differential and dose dependent behavior of prokaryotic versus eukaryotic cells. In the process of the evaluation and demonstration of this technology in decontamination of various surfaces even biological tissue, we intend to develop future understanding of the underlying active agents responsible of the effects observed. In the process we will be able to develop a design that serves as a novel device to cater to many different needs beyond the medical industry, namely, the consumer marketplace since the device uses only air and can be used in many common environments. The induced flow serves as an added advantage over existing UV technology as UV can only sanitize or sterilize objects in its line of sight. But due to the ability of this technology to vector flow, and hence the plasma generated species, in any direction needed, the device gives a much faster and 360 degree cleaning effect since the flexibility makes it easy to fashion the actuators into different contours. As it is also scalable, it can be designed into any shape and size, hence, can be used to sterilize objects such as endoscopes that have crevices difficult to reach.

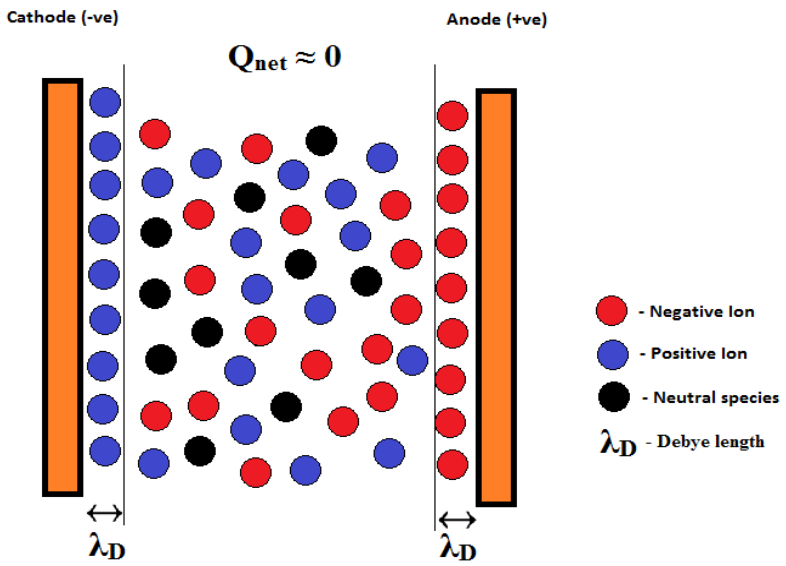

Figure 1 Formation of plasma and phenomenon of Debye shielding.

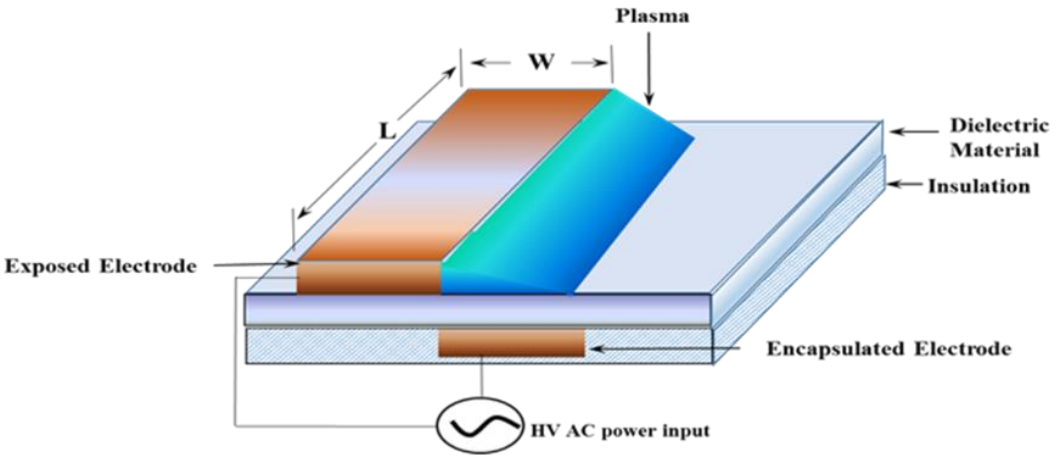

(a)

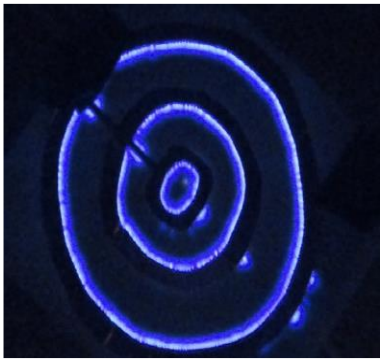

(b)

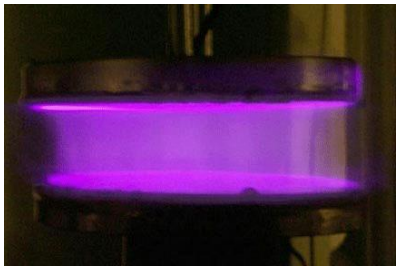

(c)

Figure 2 (a) Schematic of Surface Dielectric Barrier Discharge (SDBD); (b) Plasma discharge for a Surface Dielectric Barrier Discharge; (c) Volumetric DBD plasma generation [184].

(a)

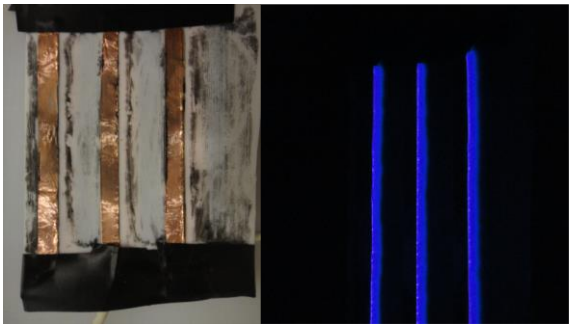

(b)

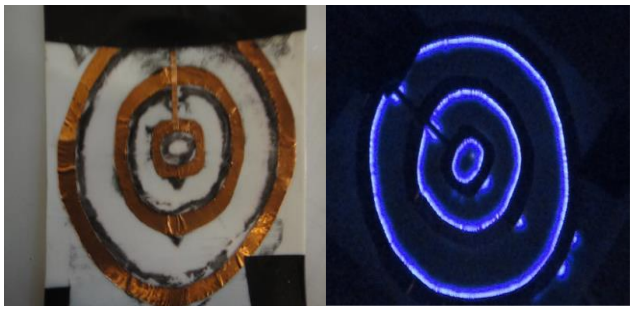

(c)

Figure 3 Different geometries of electrodes for various flow effects: (a) Aztec maze design for complex geometries;(b)Parallel placed electrode array for increased flow velocity;(c) Concentric ring pattern for increased vertical velocity.

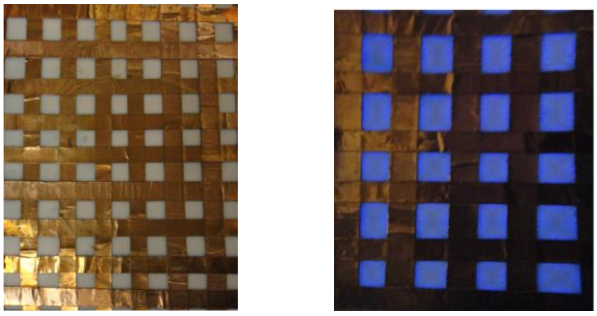

(a) **(b)**

Figure 4 Square mesh design of electrodes: (a) without plasma; (b) with plasma.

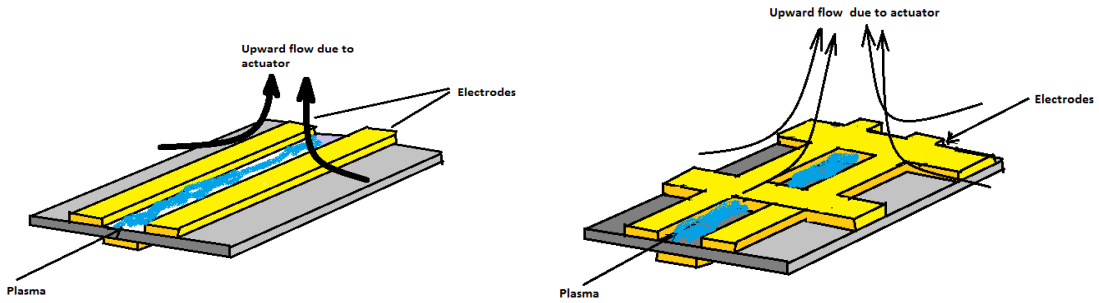

(a) **(b)**

Figure 5 Flow induced by: (a) parallel electrode array; (b) square mesh

(a) **(b)**

Figure 6 Scanning electron microscope images of an orthodontic file: (a) before plasma exposure; (b) following exposure to oxygen–argon plasma[7].

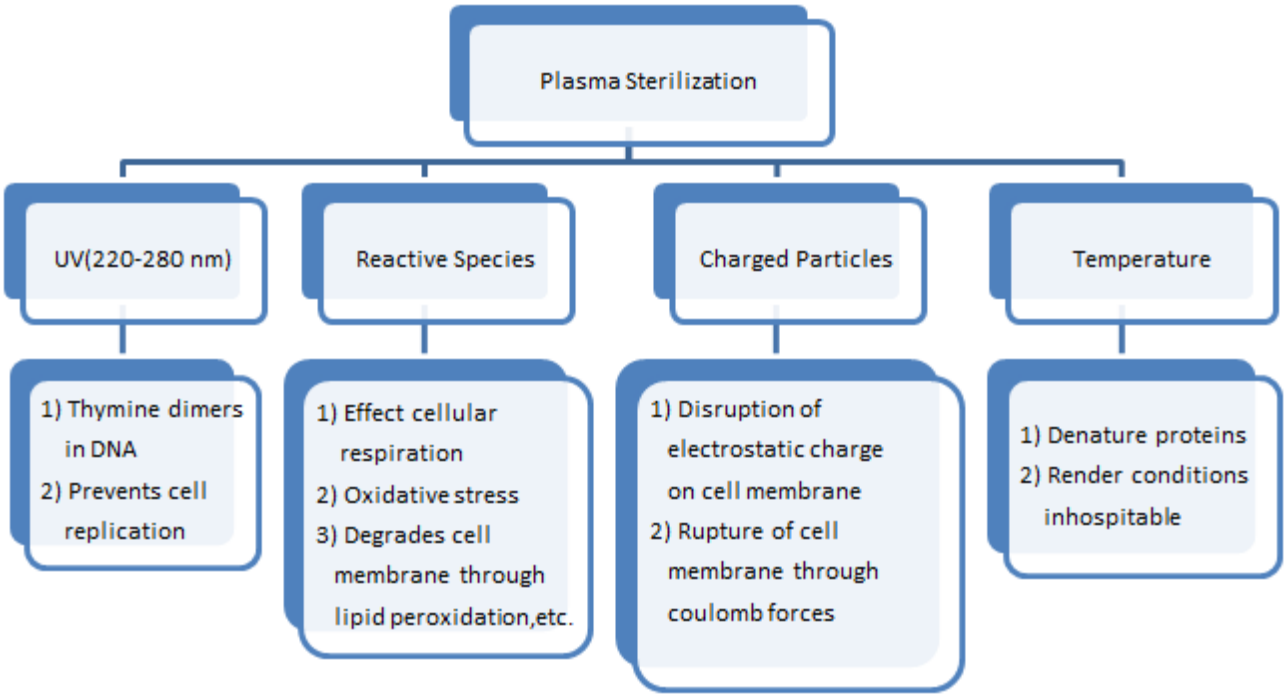

Figure 7 Factors responsible for sterilization in plasma based sterilization process and their roles.

Chapter 3

Scaling of Plasma Actuators

3.1. Introduction

Plasma actuators have been extensively studied for their ability to generate thrust by inducing flow, and have been applied in flow control by numerous researchers across the globe [22, 23, 25, 46-51, 53-56, 63, 185-189]. A simple plasma actuator is based on the principles of DBD, specifically, Surface DBD or SDBD. In such design, two electrodes are placed on either side of a dielectric material and plasma is generated from a development charge on either side of the dielectric when high enough voltage is applied. Plasma actuators for flow control mainly use an asymmetric arrangement of electrodes, as this design has a unique ability to induce flow apart from the plasma generation site. Most of these applications have focused on separation of flow on the surface of the wings of an aircraft or manipulation of flow generated for penetration into the boundary layer. The optical, electrical[22, 51, 54, 188, 189] and thrust[23, 25, 48-51, 186] characteristics have been investigated in the past, but no attention has been paid to the effects on power required when scaling an actuator. If cold plasma actuators based on Surface Dielectric Barrier Discharge (SDBD) are to be used for various biomedical applications in large scale sterilization and decontamination (or even in aerodynamic applications in aircrafts), the cost in

terms of power should be understood for scaling up or down for ease of manufacturing prototypes. In this study, we look at the effects of change in the dimensions and number of electrodes on voltage required to power a plasma actuator. Understanding this trend in input power will help better predict and design for a system using SDBD plasma actuators. The optimization of the actuator will help reduce formation of streamers and loss of energy in the form of heat. Better construction and correlation of the dimensions of the plasma actuator with power will also help prevent deterioration due to fast burn through and edge effect losses.

3.2. Materials and Methods

3.2.1. Construction of Plasma Actuators

Plasma actuators were constructed using Teflon sheets 5 mil thick (McMaster-Carr Supply Company, USA) as a dielectric medium. SDBD actuators were constructed using copper tape (McMaster-Carr Supply Company, USA) and sticking it asymmetrically on either side of the dielectric as shown in Figure 1. The length of the electrodes was varied from 1 cm to 5 cm (increment of 1 cm) and 2.5 cm to 15 cm (increment of 2.5 cm, constant width of 0.5 cm) to get trend in power requirement based on change in length. The width of the electrodes was also varied from 0.5 cm to 3 cm (increments of 0.5 cm, constant length of 2.5 cm) using copper tape of different widths to study the effects on power required to ignite plasma. The grounded electrodes on the side opposite the one facing the sample were insulated to prevent plasma ignition. This structure with one electrode each on either side of the dielectric is called single SDBD arrangement.

The effect in number of electrodes in a parallel electrode configuration was also investigated by increasing the number of electrodes on either side of the actuator, creating a parallel electrode setup known as a multiple electrode or multi-electrode arrangement. Electrodes with lengths of

2.5, 5 and 7 cm (0.5 cm in width) were investigated in this case ranging from 1 to 5 parallel electrodes.

3.2.2. Power Supply and Transformer Setup

A high voltage transformer (MINIMAX7, Information Unlimited, NH) was used to step up the input voltage supplied to the actuator. A 24 V, 1 A power supply was constructed by combining two wall AC to DC adapters with a range of 3-12V each, and a resolution of 1.5V (Enercell, Radioshack, USA). The voltage was varied from 3 to 24 volts with increments of 1.5 V while keeping the current constant at 1 A. The input and output voltages to and from the transformer were monitored using a digital multimeter (Fluke Corporation, WA, USA) and an oscilloscope (Tektronix, Inc., OR, USA). The random error was identified and the corresponding output Voltage for a given input was tracked.

A PVM -11, high voltage (North Star High Voltage, AZ, USA) probe with a step down transformation ratio of 1000:1 was used to measure the voltage output of the transformer. The voltage probe was connected to the output of the transformer and the voltage (peak to peak) was monitored using an oscilloscope. The plasma actuator was connected during the entire calibration done to measure the output voltages over the entire range of the corresponding input voltages. The corresponding output voltage for given input voltage is shown in **Figure 2**.

3.2.3. Limiting Conditions

The readings for input voltage to ignite the plasma were measured at two points, namely, the voltage where uniform discharge was achieved, and the point where complete streamers were formed. These two conditions were selected, and uniform velocity and plasma generation without losses occurs between these two points of operation. After the onset of streamers, there is no

increase in thrust, velocity, or plasma volume. The supplied power gets converted to heat and may damage the actuator, especially actuators possessing a thinner dielectric.

3.3. Results and Discussion

3.3.1. Effect of Changing Different Parameter on Input Voltage

(a) Width of Electrode

The first parameter we manipulated was the width of the electrode. This was done by using copper tape of different widths as described in the previous section (**Figure 3**). The length was kept the same (2.5 cm) for all the samples. It was observed that increasing the width of the actuators (one or both) did not change the voltage required to ignite the plasma for both uniform discharge as well as for onset of streamers. **Figure 4** shows the variation of voltage in kilovolts with the change in width of both the electrodes. These results are in accord with the findings of Thomas el al.[47] and Enloe *et al*.[23] who mentioned that with increase in width the only effect observed is better spread of plasma over the encapsulated electrode and an increase in thrust produced. Although the effect on thrust has been studied extensively, effect of increase in width of the electrodes on quality of plasma has not been researched. Hoskinson *et al*. studied the effect of exposed electrode dimensions and thickness[190-193] The authors in this case found that increasing the width of the exposed electrode did not affect the required voltage or the quality of plasma generated. The encapsulated electrode, however, helped better spreading of plasma with applied voltage, as can be seen in **Figure 3**. Inferring from literature, this might prove beneficial for plasma induced thrust, as well as for more plasma induced reactive species generation. However, the chord-wise spread of plasma was found to have a limit, and did not extent beyond a certain distance once streamers were formed (irrespective of width of the encapsulated electrode).

Thus, increasing the width of the encapsulate electrode can be considered to be limited by maximum spreading of plasma. However, increasing the width does not affect the voltage required.

(b) Length of Electrode

Increasing the length of the electrode while keeping the width constant was used to assess the effect of length of the electrode on input voltage. The electrode length was increased 2.5 cm at a time to see the trend in the input voltage per unit increase in length of electrodes (**Figure 5**). The results of this can be seen in **Figure 6.** We increased electrode lengths in increments of 2.5 cm at a time. It was observed that for every 2.5 cm increase in length, there was a linear increase in voltage required, producing a trend similar to an arithmetic progression. This trend was observed over the range 2.5 to 15 cm of electrode length.

To get a better idea of the effects of the change in length, another set of experiments were conducted wherein the resolution was increased to 1 cm increments (**Figure 7**). It was observed that the voltage remains almost constant between 1 and 2 cm of electrode length, following which an increase in voltage from 2 to 3 cm occurs. This was followed by a constant voltage input up to 5 cm of electrode length, suggesting a step function for power input in case of a single SDBD plasma actuator design. This trend was persistent in both uniform glow as well as streamer discharge phases.

This trend observed in the two scenarios demonstrates two possibilities, either the voltage requirement is a step function with a change in input voltage requirement at every 2.5 cm increase in length, or the voltage requirement increases gradually but the trend is not visible due to the resolution of the current setup. Further investigation is required with a setup of higher resolution.

(c) Number of Electrodes

In applications such as sterilization, a more uniform multi-electrode array would be required. Therefore, the voltage requirement for such a setup would need to be designed based on electrode length and number of electrodes. In this part of the investigation two separate experiments were performed. One with the length of electrodes remaining constant, and the other with change in the length of the electrodes. **Figure 8** shows the electrode arrangements in the experiment in which the number of electrodes was increased while maintaining a constant electrode length.

When the number of exposed electrodes '*n*' was increased while keeping the length of the electrodes constant (2.5 cm), the number of grounded electrodes was increased at a rate '*n-1*'. The trend in the increase in voltage requirement is shown in **Figure 9**. It can be seen that the increase in voltage requirement, both for the uniform glow as well as for streamer discharge, is similar to that seen when increasing the length of the electrodes by 2.5 cm. This shows that the voltage input for plasma generation by these actuators has a linear dependency on the total added length of the electrodes (sum of all exposed or grounded electrodes). A slight discrepancy is observed when considering longer electrodes in the case of single SDBD actuators. Some of the longer electrodes do not match with their multiple electrode array counterparts, which may be attributed to a slightly lower total length of grounded electrode. This trend becomes prominent as the difference in total lengths of the grounded electrodes between single SDBD and multiple electrode array type actuators increases. An example of this can be understood by comparing 7.5 cm and 10 cm length single SDBD with three and four electrode arrays of 2.5 cm long electrodes respectively, where the input voltages for both uniform glow and streamer discharge is the same. When we compare 10 cm and 15 cm single SDBD actuator to multiple electrode arrays of two electrodes each of 5

cm and 7.5 cm (**Figure 10**) respectively, we observe that there is a decrease in input voltage requirement of approximately 0.5 kV for both uniform glow as well as for streamer discharge. Thus a difference of more than 2.5 cm in the total length of grounded electrode shows an effect of decreased voltage requirement.

The second experiment was conducted to see the effects of change in electrode length in multiple electrode array when increasing the electrode length by 2.5 cm. The results are as shown in **Figure 10.** It can be observed that a linear trend in input voltage is observed here as well. It should be noted that the voltage plotted here is input voltage for uniform glow alone. The trend seen here is that for total length of grounded electrode less than or equal to 2.5 cm, the input voltage required for actuators with the same total length of exposed electrodes is the same. This is in accord with the trend described earlier. Hence, input voltage has a direct dependence on total length of grounded electrode, and can be reduced by reducing the number of grounded electrodes.

It was also observed that an increase in the width of electrodes did not have any impact on input voltages (results not shown). The voltages remained unchained from that seen with earlier tests for both uniform glow and streamer discharge.

3.4. Conclusion

An analysis for scaling a SDBD plasma actuator was conducted using a minmax7 transformer. The transformer output was measured and calibrated for given input voltage. The effect of change in width, length, and number of electrodes was investigated on voltage requirement for constant power input of 1 A. The boundary conditions chosen were onset of uniform glow discharge and streamer formation so as to consider optimum conditions of plasma generation without loss of power or non-uniform distribution of plasma along the length of the

electrode. It was observed that changing the width of the electrode (both exposed and encapsulated), for a given length of electrode, did not have any impact on input voltage. However, a linear trend in the form of an almost arithmetic progression was observed when the length of the electrodes was increased by a factor of 2.5 cm. Lower changes in length (increments of 1 cm) showed a trend similar to step function. The authors hypothesize that a higher resolution in the mechanism of voltage input of less than 0.5 kV is necessary to ascertain the actual trend. However, for large scale actuators, the linear trend would work well and be easier to implement. The regime between the formation of uniform discharge and the onset of streamers shows a uniform width and is the zone of optimum operation for effective use of applied power

The authors also investigated the impact of increase in the number of electrodes of the same length on input voltage. A linear trend was also observed when the number of electrodes were increased. It was also observed that the input voltage was a function of total length of the electrodes, i.e. the sum of all the exposed or encapsulated electrodes. The voltage requirement dropped however, when the total length of the encapsulated electrode was lower than the single SDBD counterpart of the multiple electrode array. This was seen to be a difference of greater than 2.5 cm. This also showed that the change in requirement for input voltage for minor changes in length of electrode may be low and can be proven with a higher resolution input setup for voltage.

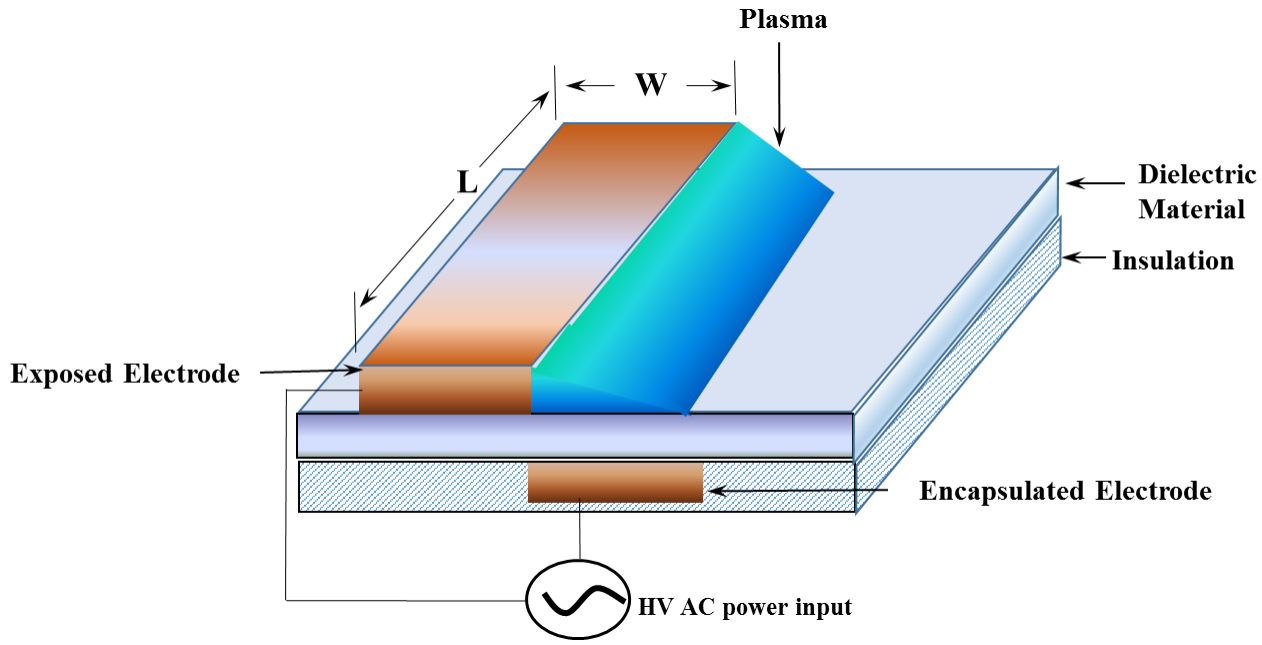

Figure 1 Schematic of a single SDBD plasma actuator of electrode length 'L' and electrode width 'W'

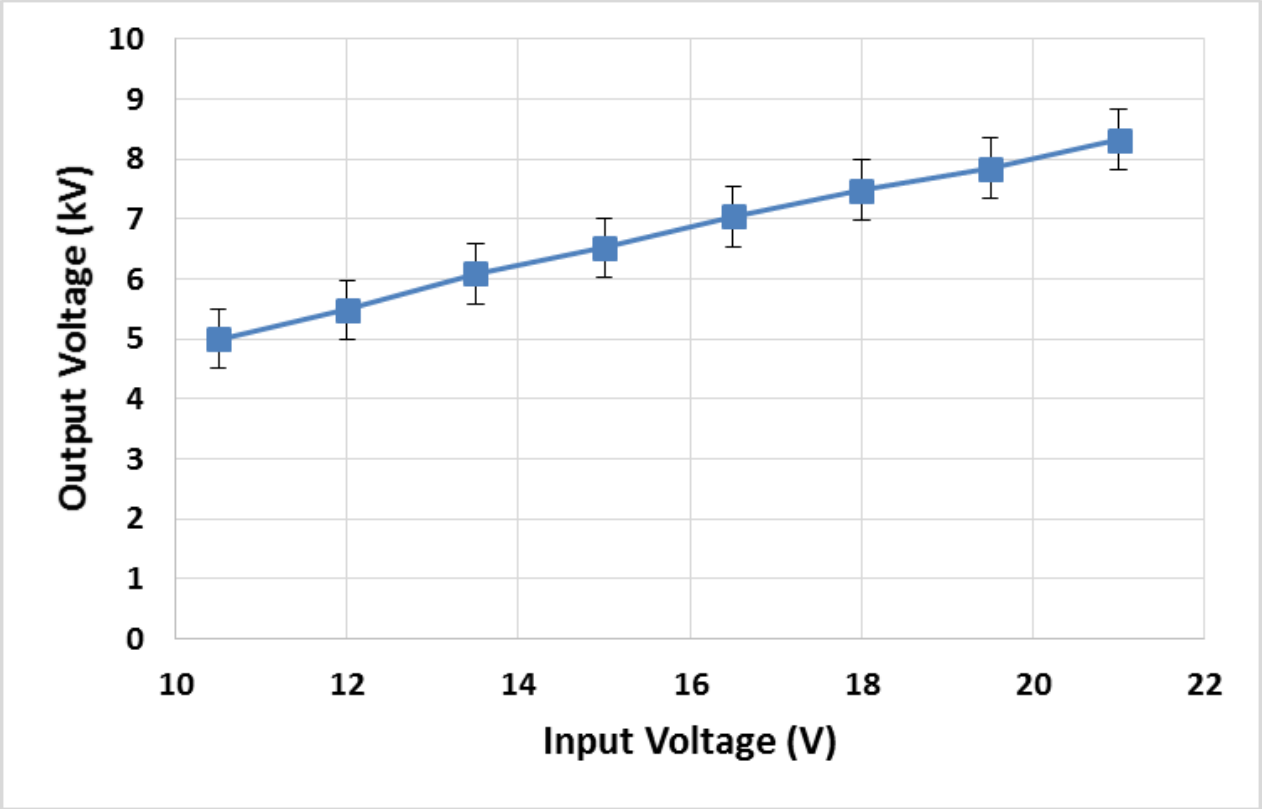

Figure 2 Voltage calibration curve showing input voltage and output voltage (transformer output) for the minimax7 setup

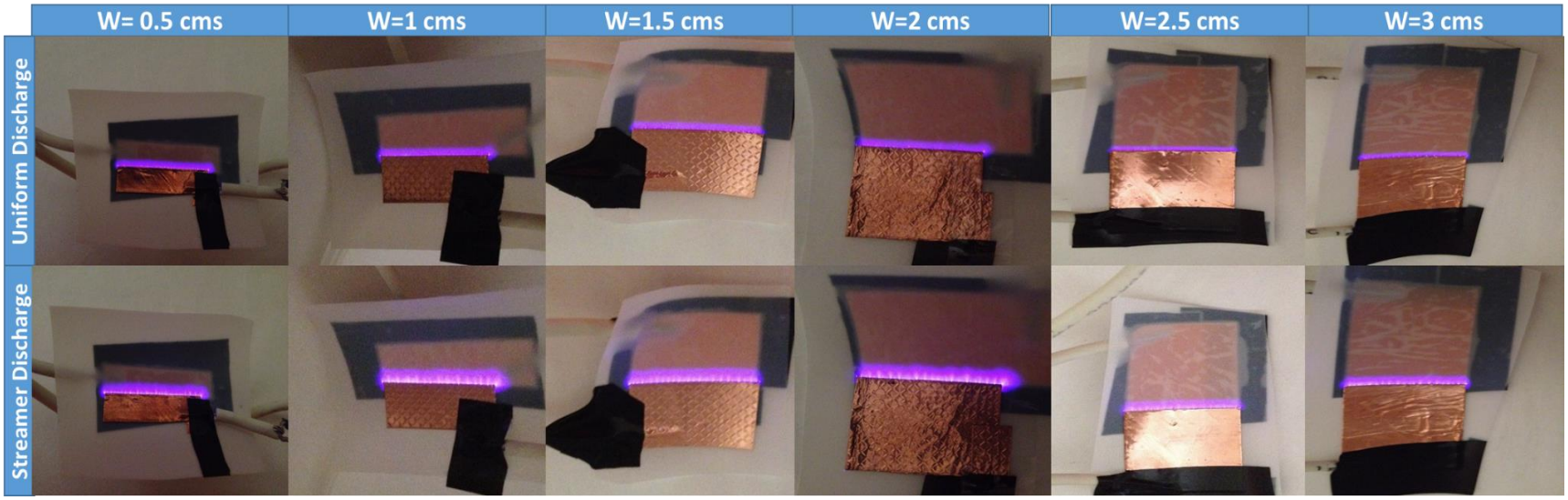

Figure 3 Unifom glow discharge and streamer formation with corresponding change width (W) of electrode (0.5 cm increments in width)

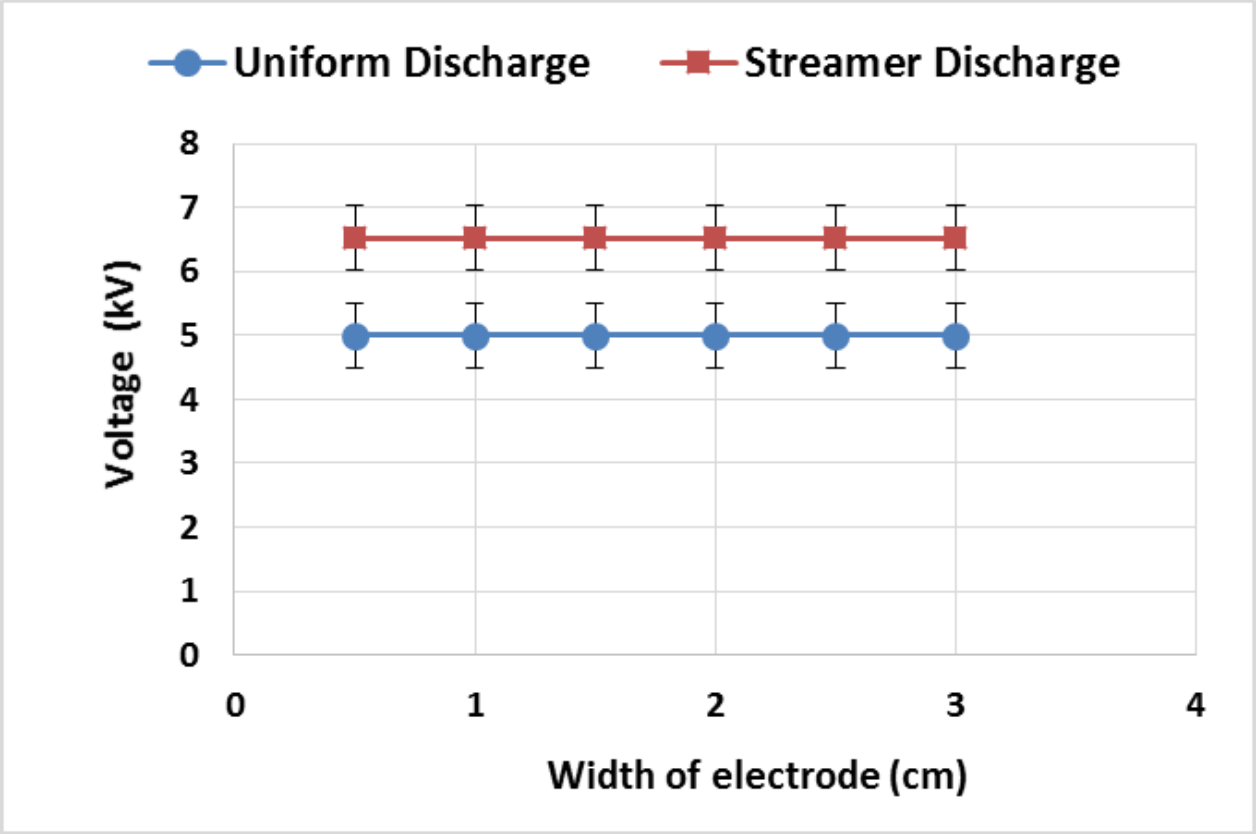

Figure 4 Plot for change in input voltage (V) with corresponding change width (W) of electrode (0.5 cm increments in width)

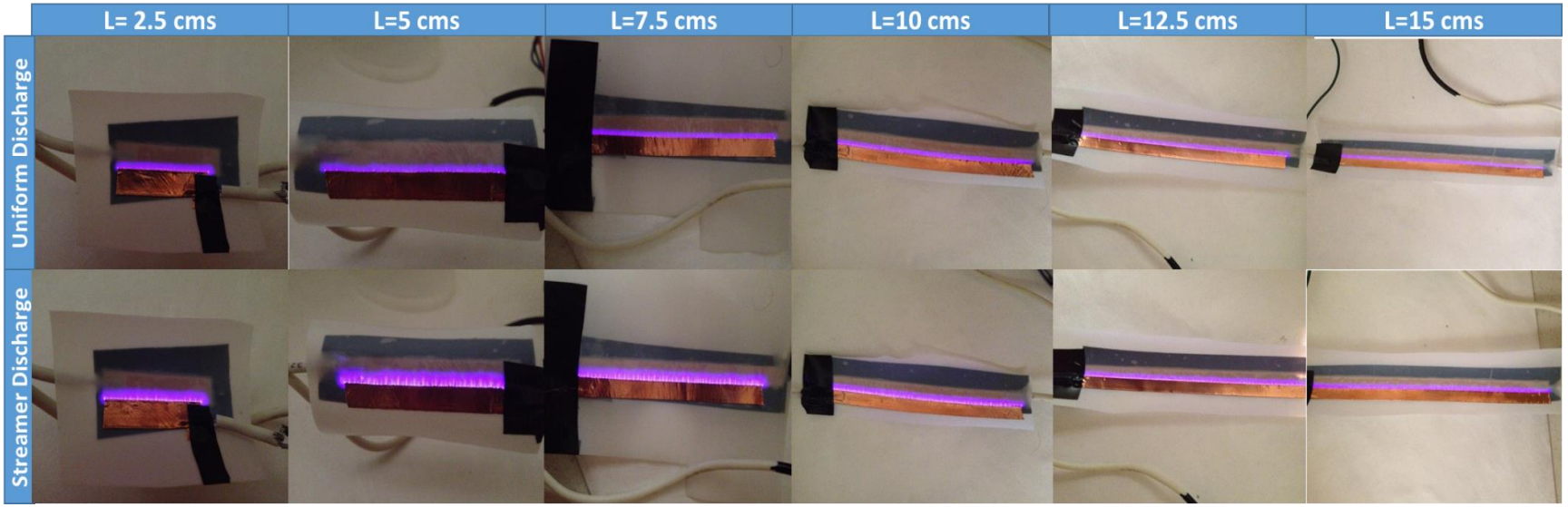

Figure 5 Unifom glow discharge and streamer formation with corresponding change length (L) of electrode (2.5 cm increments in length)

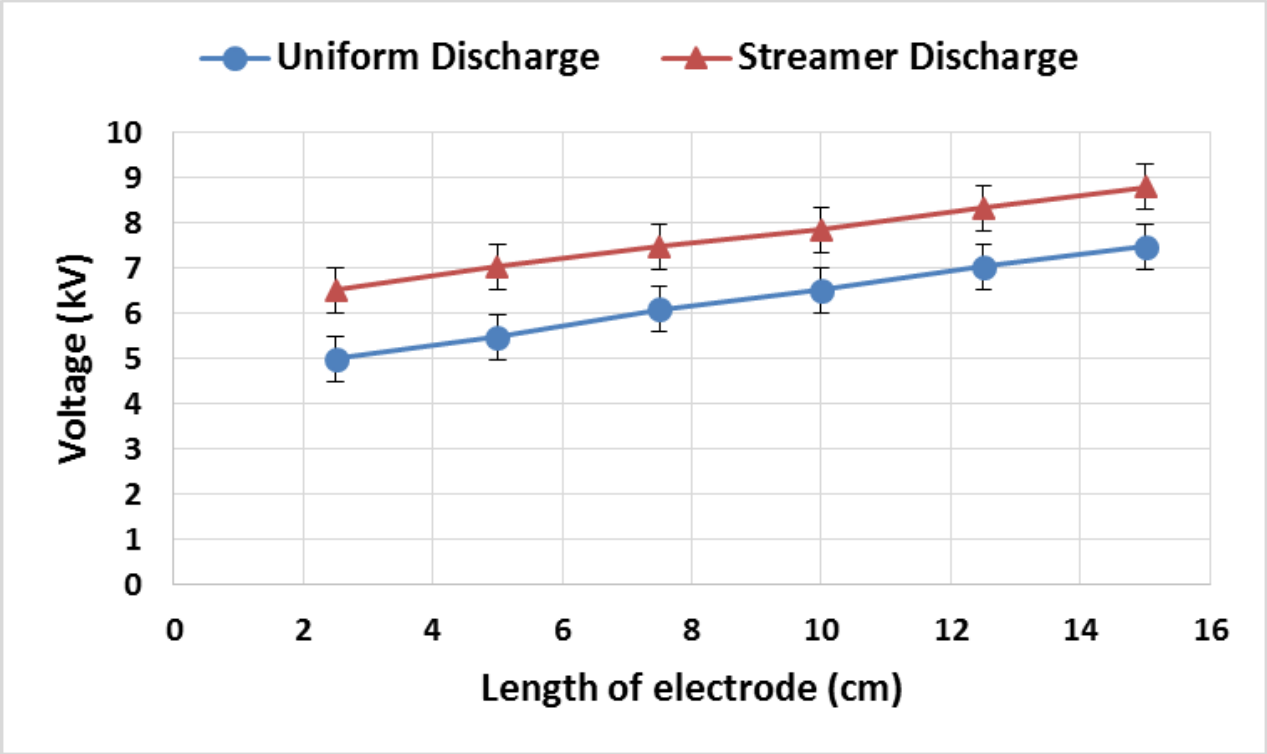

Figure 6 Plot for change in input voltage (V) with corresponding change in length of electrode (L) (2.5 cm increments in length)

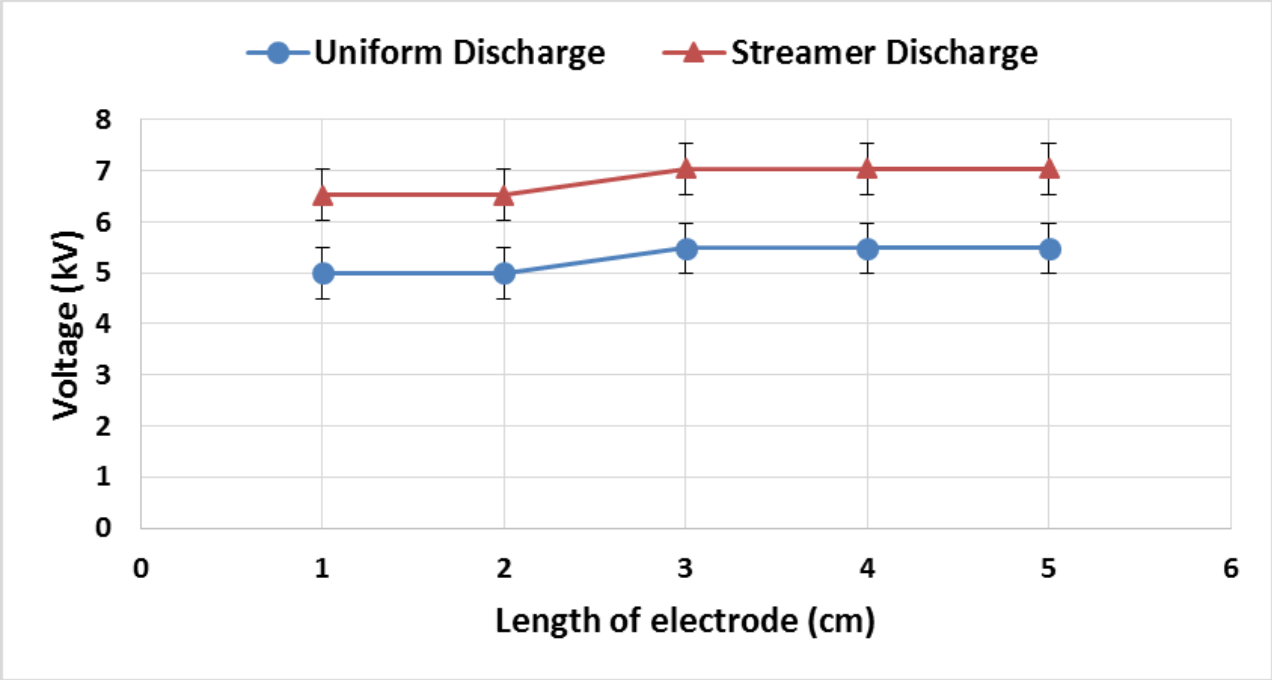

Figure 7 Plot for change in input voltage (V) with corresponding change in length of electrode (L) (1 cm increments in length)

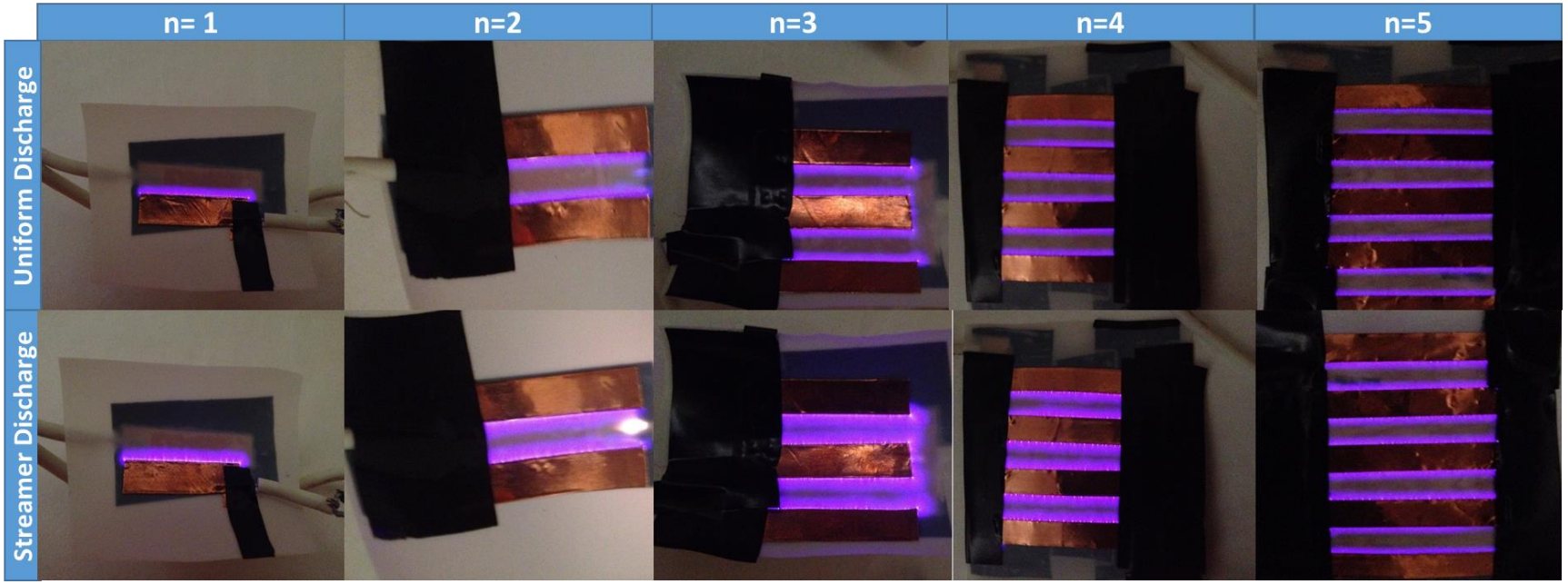

Figure 8 Unifom glow discharge and streamer formation with corresponding change number (n) of electrodes (2.5 cm increments in length)

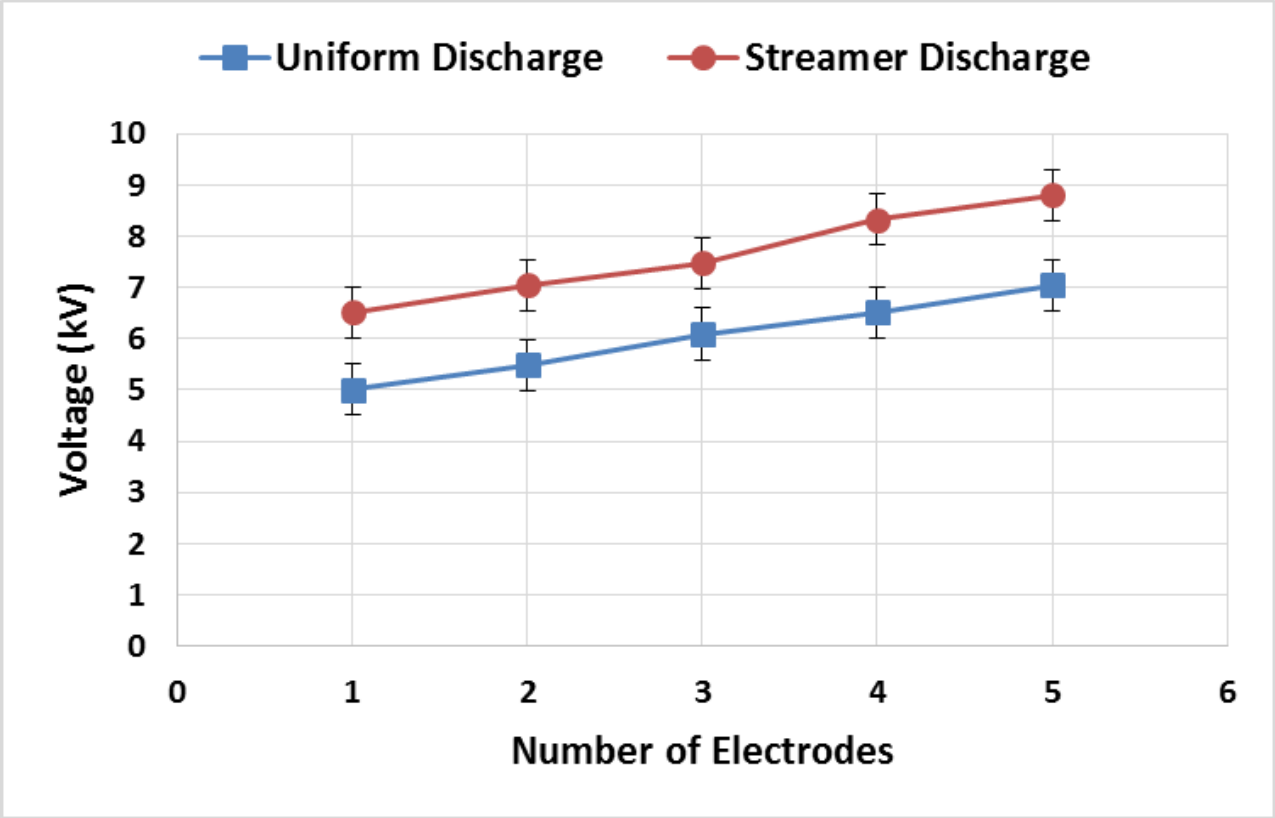

Figure 9 Plot for change in input voltage (V) with corresponding change number (n) of electrodes (2.5 cm in length)

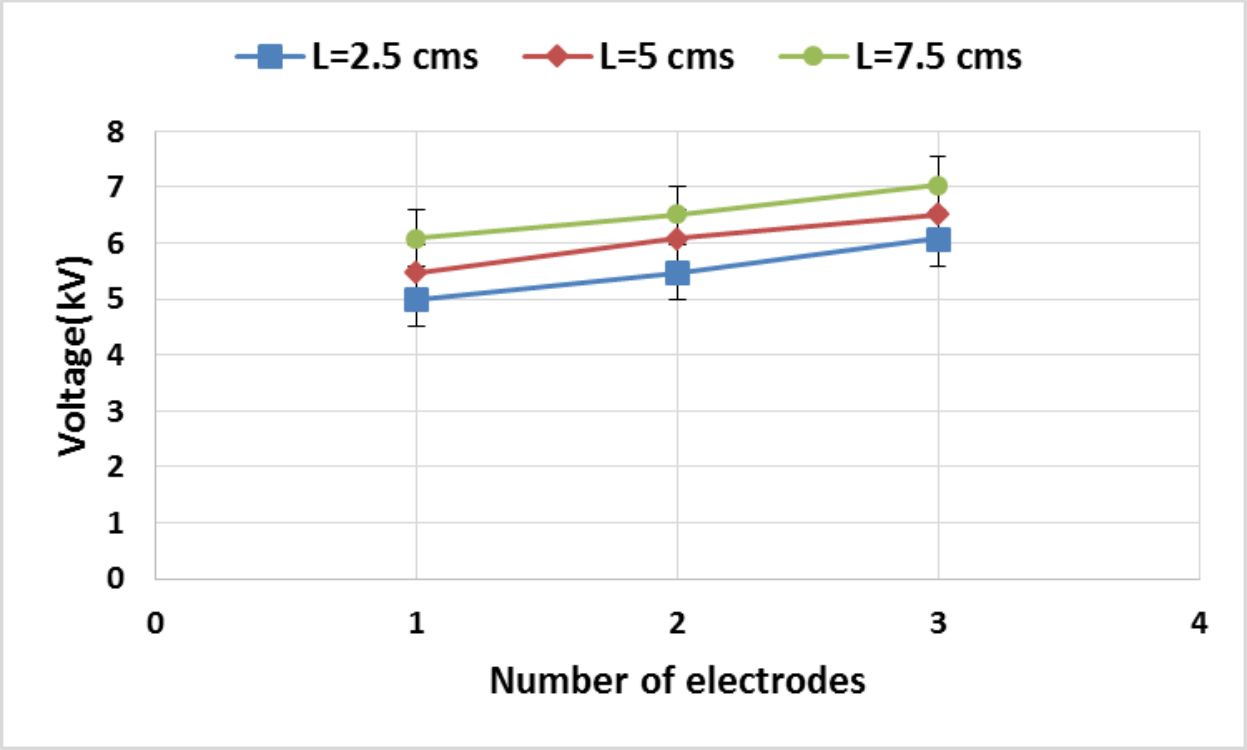

Figure 10 Plot for change in input voltage (V) with corresponding change number (n) and length (L) of electrodes (2.5 cm increments in length)

Chapter 4

Comparative Analysis of Asymmetric and Symmetric SDBD Plasma Actuators

4.1. Introduction

Applications of non-thermal atmospheric plasma, or cold plasma, have gained increased interest in recent years as potential pathogen control measures in the food processing and medical industries. When generated with certain gas combinations, cold plasma can result in etching or oxidation [26] and has been used extensively to generate ozone in the water purification industry [39]. Recent cold plasma applications range from bacterial inactivation [12, 44, 113-115, 118, 136, 141-143, 151, 175], to blood coagulation and improved wound healing [100, 180, 181]. The low operating temperatures and low power inputs of cold plasma generation are major advantages for surface sterilization of food processing and medical equipment, disinfection of water, and decontamination of food products.

Various cold plasma application designs have been devised and tested with prokaryotic and eukaryotic cells, and include atmospheric pressure plasma jets [44, 98, 114, 143], dielectric barrier discharge (DBD) devices [176], and plasma needles using radio frequency excitation [17, 106, 194]. Many of these designs require additional gas flow to propel the newly generated plasma species to the site of exposure[122], or have small plasma generation areas, thus restricting sample size [8, 127]. Many current designs also consume a large amount of power [41, 109, 122], and in the case of plasma jets, may also result in desiccation of the sample. Common DBD arrangements [41] can only be run with a constant gap between the electrodes, thus resulting in a limited zone of plasma treatment area. If the treatment area is increased by changing the inter electrode gap, increased power input is required to keep the discharge generated. As a result of these shortcomings, an improved cold plasma generation design is urgently needed for practical, cost-effective applications of cold plasma technology at the industrial scale. DBD designs are the most widely investigated and show the most potential in overcoming these shortcomings [37].

The two common types of DBD configuration are surface dielectric barrier discharge (SDBD) and volumetric dielectric barrier discharge (VDBD) [37]. The VDBD arrangement has one or both electrodes covered by a dielectric material and a defined gas gap where the plasma is generated. This is inconvenient for large samples, since a limited treatment area is available and an artificial gas flow is required to transport the generated plasma species to the site of application when using indirect treatments. In a SDBD arrangement, plasma is generated between two electrodes where at least one electrode is covered by a dielectric material with no gas gap between the electrodes, and the electrodes may be arranged symmetrically or asymmetrically on either side of the dielectric. The asymmetric design of SDBD possesses the corona discharge ability of flow

induction not common to volumetric methods of plasma generation. The induced flow in the surrounding gas generated by this design is a result of coupling the electric field (Lorentz force) with gas particles, thus imparting momentum to the entrained gas[22, 40]. Therefore, this design does not require an artificial gas flow, as compared to other technologies that have been implemented in the past. In the last decade, the use of SDBD for active flow control has been investigated extensively [22, 40, 56, 62], particularly in aeronautical applications, but there has been little investigation into utilizing its unique capabilities for biological applications. The ability to successfully kill bacterial cells, such as *Escherichia coli*, using SDBD actuators has been demonstrated by Pai *et al.*[62]

In this study, inactivation of *Listeria monocytogenes* was used to demonstrate, and the superior performance of asymmetric SDBD plasma actuators over symmetric SDBD with respect to their abilities to induce flow was investigated using Particle Image Velocimetry (PIV), and to demonstrate its applicability for surface decontamination. *L. monocytogenes* is a major foodborne pathogen that may result in listeriosis in humans and is one of the leading causes of foodborne illnesses, hospitalizations, and deaths[195]. *L. monocytogenes* is commonly associated with processed and ready to eat foods, such as raw milk, processed meats, and deli meat, where the processing equipment is difficult to sterilize using conventional methods. [127, 195, 196] *L. monocytogenes* can be very persistent[196], and is more resistant to plasma treatment than other tested bacterial pathogens[109, 110]. It was therefore chosen to evaluate the performance of symmetrical versus asymmetrical SDBD actuators. Since *L. monocytogenes* is a notorious food surface contaminate [197], a low temperature plasma based decontamination solution would have broad applicability.

4.2. Materials and Methods

4.2.1. Inoculum and Sample Preparation

Five strains of *Listeria monocytogenes* (F6854, 12433, G3982, J0161, and Scott A) were grown in tryptic soy broth (TSB, Difco, MO, USA) for 24 h at 37°C. One mL of each liquid culture was centrifuged at 12,000 rpm for 3 minutes and re-suspended in 1 mL of 0.1% (w/v) sterile peptone (Difco, MO, USA).

Sample inoculum was prepared by combining the 5 strains of *L. monocytogenes* and diluting the 5-strain cocktail in 0.1% (w/v) sterile peptone to a concentration of 10^7 CFU/mL. One hundred µL of the inoculum was uniformly distributed in 15 to 20 droplets over the entire surface of single sterile standard glass coverslips (22 mm). Inoculated coverslips were allowed to dry for 30 minutes at room temperature in a biological safety cabinet prior to cold plasma treatment.

4.2.2. Plasma Actuator Arrangement and Plasma Exposure Method

Plasma actuators were constructed using Teflon sheets 0.127 mm (0.005") thick (McMaster-Carr Supply Company, GA, USA) as a dielectric medium. Two designs of electrode arrangements, namely, symmetric (Figure 1a) and asymmetric (Figure 1b) SDBD actuators were constructed. The asymmetric design has the electrodes placed asymmetrically placed on either side of the dielectric material. Whereas, the symmetric design has both the electrodes placed symmetrically about the dielectric such that they are located on exactly the opposite side of the dielectric above each other. Copper electrodes of 0.5 mm width (McMaster-Carr Supply Company, GA, USA) were placed parallel on the sheets to develop 5×5 cm^2 actuators with 3.6×0.5 cm^2 electrode dimensions on either side of the dielectric. The grounded electrodes on the side opposite the one facing the sample were insulated to prevent plasma ignition.

The inoculated samples were exposed in duplicate to plasma generated by each actuator design for both 2 and 4 min from a distance of 1, 3, 5 and 7 cm from the surface of the coverslip, using a cylindrical enclosure as shown in Figure 2. Two samples used as controls were not treated with cold plasma. All experiments were carried out with identical actuators operating at 13.5 W input power and 50% duty cycle using a high voltage transformer (Information Unlimited, NH). Pulse width modulation (PWM) was used, allowing the actuator to be on for 800 ms and off for 300 ms. PWM was implemented using an Arduino Uno microcontroller setup (Arduino LLC, Italy). All samples were exposed to plasma for 4 minutes. All experimental readings were taken at room temperature, and the plasma was generated in air.

4.2.3. Particle Image Velocimetry (PIV) and Analysis

PIV was used to determine the flow of the bulk fluid induced by the SDBD actuators as previously described [62]. In this setup, a 100 mW, 532 nm EVO laser (Wicked Lasers, Hong Kong, China) was used to generate a sheet of light with the necessary optics to generate the sheet incorporated. A MotionPro X3 high speed CCD camera (IDT, FL, USA) was used to capture images at 100 frames per second using the software MotionStudio (IDT, FL, USA). The images were analyzed using ISSIPIV software (Innovative Scientific Solutions Inc., OH, USA). Composite images were created by superimposing images taken at two different points in time to track the particle motion. Smoke particles with a particle size of approximately 1 μm were used as seed particle for tracking of induced fluid motion. Image analysis was carried out by comparing the procured images and generating composite images to show the motion of bulk fluid for 240 ms. This was done by comparing the relative motion of the particles.

4.2.4. Microbiological Analysis

Following plasma treatment, the coverslips were washed with 10 mL of 0.1% sterile peptone in a 50 mL Falcon tube (Corning Inc., USA) by vortexing for 15 s. The wash fluid, containing surviving bacterial cells, and 2 10-fold serial dilutions were plated in duplicate on TSA and incubated at 37 °C for 24 h. The effectiveness of the 2 SDBD designs were evaluated by comparing the number of *L. monocytogenes* colonies. A uniform layer of cells was obtained by spot inoculation, wherein 100 µl of inoculum was spread uniformly by evenly distributing small droplets over the coverslip. This provided an uniform distribution and reduced effects of shadowing due to clumping of cells, which caused non uniform plasma exposure and yielded variation in results.

4.2.5. Statistical Analysis

All the experiments were conducted in duplicate, and a total of 2 independent experiments were conducted (n = 4). Values were represented as mean ± SD. Significant difference between two groups was analyzed using a paired sample t-test and one-way analysis of variance (ANOVA) with 95% confidence interval. Differences in the results were considered statistically significant when $p < 0.05$.

4.3. Results and Discussion

4.3.1. Microbial Inactivation

The symmetrical SDBD and asymmetric SDBD designs both reduced *L. moncytogenes* populations on the inoculated coverslips following treatment for 4 minutes. It was observed that the asymmetric arrangement produced a greater log reduction of 4.8 Log CFU/ml (**Figure 3**), as compared to the 2.3 Log CFU/mL in the symmetric arrangement, when the samples were placed

at 1 cm from the actuators. A decrease in the performance of both the designs was observed as the distance of the actuator from the sample was increased to 3 cm, with the asymmetric arrangement producing 3.5 Log CFU/mL reduction and the symmetric arrangement producing 1.1 Log CFU/mL reduction. When the distance between the actuator and the sample were further increased, the Log CFU/ml reduction with both designs was approximately the same, with the asymmetric arrangement displaying a slightly better performance. The reason for this difference in performance may be attributed to the arrangement of electrodes. When the electrodes are symmetric, the electric field distribution is not ideal to generate a directional flow or electromotive force [40, 47, 56, 62, 63], whereas in the asymmetric arrangement of electrodes, the electric field is skewed towards the grounded or insulated electrode. The resultant electromotive force couples the electric field into the momentum of air molecules originating upstream of the exposed electrode, directed downstream over the surface of the encapsulated electrode (plasma region).[40] Thus, placing the encapsulated electrode asymmetrically results in a much stronger plasma and a much higher induced velocity.

4.3.2. Flow Analysis using PIV

To evaluate the differences in the flow generated by the two different designs, PIV was used to track the flow of the bulk fluid. It was observed that the asymmetric arrangement resulted in much higher velocities with a much more turbulent flow (**Figure 4 and Figure 5**). The bulk fluid was pulled in from the sides of the actuator and pushed towards the sample in a direction perpendicular to the actuator. The turbulent flow and the generation of vortices as seen in **Figure 4** also results in better mixing of generated plasma species. The flow is pulled through the plasma

region and pushed towards the sample, thus creating a piggy back system which results in the bulk fluid acting as a carrier fluid for the generated plasma species. This effect also results in decontamination of the air passing through the plasma region. In the case of the symmetric arrangement, however, the fluid motion was slower and much more streamline. **Figure 5** shows the flow direction with vectors (arrows) showing the direction and magnitude of flow of air. The length of each arrow represents the magnitude by which the fluid has moved in 240 milliseconds. Hence, it is clearly visible that the velocities induced by the symmetric actuator are at least 3 to 4 orders of magnitude lower than that for asymmetric actuators, if not more. The plasma generation was also weak and not well distributed even though the same amount of power as that used for the asymmetric arrangement was supplied. The slower mixing and the slower induced speeds may be a reason for the reduced ability of the symmetrical arrangement to inactivate bacterial cells. The generated plasma species are short lived and may need to be delivered to the sample at a faster rate, or the concentration generated by this mode may not be enough for a large Log reduction in CFU to be observed. To test whether the plasma generated by the symmetric arrangement was weak due to low power supplied, a test was carried out with fewer electrodes (three). No change in the flow was observed with this arrangement either, thus ruling out lack of proper power supply as a cause for lower velocities (data not shown). Thus, the induction of strong flow and a much more uniform and spread out plasma region is a trait specific to the asymmetric arrangement of electrodes. A higher plasma generation in the case of the asymmetric arrangement was also observed, which may be attributed to the spreading of the plasma over the encapsulated electrode as shown in Figure 1. This is not the case in the symmetric arrangement and may result in a lower concentration of generated plasma species.

A composite image (**Figure 4 (a) and (c)**) was obtained to demonstrate the motion of the bulk fluid and the velocity of flow induced in each arrangement. The asymmetric arrangement demonstrated higher flow rates and better mixing capabilities, as mentioned above. The images selected were taken 240 milliseconds apart so as to obtain a clear distinction between the initial (blue) and the final (green) location of the bulk fluid as seen in **Figure 4** and **Figure 5**. T=0 is the initial image and T=0.24 is the consequent image taken after 240 milliseconds. The actuators were turned on 10 seconds before initiating frame capture to prevent any stray flow and allow the induced flow patterns to stabilize. A clear distinction in the ability of the asymmetric actuator to induce a stronger flow with added mixing capabilities due to a translating vortex (**Figure 5**) along the flow as compared the symmetric design was observed. Thomas *et al*.[47] give a good account of the effects of changing the parameters, such as thickness of dielectric, type of dielectric, and separation or asymmetry between the two electrodes. Work by Santhanakrishnan *et al*.[56], Pai *et al*.[62], and Bolitho *et al*.[63] give a good background on flow induced by asymmetric arrangement SDBD plasma actuators used in different two-dimensional as well as three-dimensional designs.

Similar to the results by Thomas *et al*.[47], it was observed that the power required to excite the plasma decreases with a decrease in the thickness of the dielectric, hence, thin layers of dielectric can be used for plasma treatment effectively. Using strategically placed arrays of electrodes with an asymmetric arrangement to accelerate the fluid can also help accelerate the flow and push the generated plasma species further downstream for decontamination. The design, however, can be optimized to save power and material by choosing different combinations of thickness of dielectric material and electrode arrangements, as it was observed that higher velocities are possible with thicker dielectrics. One must also account for the dwell time of air in

the plasma region for suitable quantities of plasma species to be generated and transported. A higher velocity may result in lower concentration of generated plasma species, and likewise a slower velocity may result in lower concentration of species due to recombination of the short lived charged particles and other generated plasma species.

4.3.3. Benefits of Asymmetric Arrangement SDBD Design

Yong *et al*. [109] used a similar design but with a continuous grounded electrode on the non-plasma generating side, with a power input of 250 W and 15 kHz, and observed a steady decline in the *L .monocytogenes* pathogen concentration with treatment time. This shows that for higher loads of pathogen concentration and higher distances between the ample and the actuator, an optimization of power vs height is required. The results in this paper showed that a 4.8 Log CFU/ml reduction in CFU/ml at 1 cm between the actuator and the sample could be achieved after 4 min of treatment in the asymmetric arrangement of electrodes with an input of 6.75 W, as compared to approximately 4.75 Log CFU/ml in case of Yong *et al*.[109] with their input of 250 W. Their design also used a thicker dielectric layer, as well. Schwabedisson *et al*. were able to produce a 4 log reduction in CFU of *Bacillus subtillis* in a duration of 10 min with their *PlasmaLabel*[112] , which is a similar design. They also ascertain that the design of the actuator influences the inactivation rate and plasma species generation. [8, 112] Designs such as the one used by Leipold *et al*.[8], even though it is a closed design with volumetric plasma generation, produced a 5 Log CFU/ml reduction in 5 min.

Other designs for plasma generation, such as those found in the literature using volumetric DBD and atmospheric pressure plasma jets, have proven to show faster decontamination, but do incur the disadvantages of higher power requirement, more moving parts, and higher setup andcosts of scaling for industrial applications. Leipold *et al*. [8], Frohling *et al*.[122], Ziuzina *et*

al.[41] and Song *et al*.[110] for example, used three different designs for plasma generation. Their designs were effective, but were expensive with respect to the cost of plasma generation and treatment. They either needed high quantities of inert gases or external cooling of electrodes[8, 127], or had too small a treatment gap [110], making it either too expensive or too bulky and inconvenient for larger samples. The authors noticed that in our design, the issues of the actuator heating up could be considerably reduced by pulsing the power. This also improved the actuator life considerably.

The ability of an asymmetric arrangement of electrodes in a SDBD actuator to induce flow and transfer the plasma species to the surface being treated, makes it an ideal candidate for industrial applications, especially in the case of *L. monocytogenes*, where surface decontamination is of the highest priority. The two designs evaluated in this study also showed that mere plasma generation is not enough. With proper arrangement of electrodes and design of actuator, the generated plasma species can be optimized without incurring excess power or material inputs. The authors also point out that the change in design to better help in utilization of short lived generated plasma species is possible by utilization of asymmetric SDBD arrangements which might not be true for other methods of plasma generation.

4.4. Conclusion

Two designs of SDBD plasma actuator with asymmetric and symmetric arrangement of electrodes were evaluated for their effectiveness in killing bacteria. The results indicated that an asymmetric arrangement of electrodes was around 2.5 orders of magnitude more effective in inactivation of *L. monocytogenes*, and seemed promising for application in the industrial environment. The authors also pointed out that the design of the actuator and the electrode arrangement is a key factor in low cost plasma based decontamination. The flexibility in design,

which means it does not have to be planar as demonstrated by Pai *et al*.[62], and the ability to induce flow along with mixing, due to moving vortices in the flow (**Figure 5**), gives the asymmetric arrangement an advantage over other methods of plasma based decontamination. The effectiveness of the plasma actuator in inactivating bacteria correlated the effective log reduction of CFU/ml with the distance from the sample at a given time of exposure (4 min), and demonstrated that the potency of SDBD related reduction of bacterial load reduces with distance from the actuator. Hence, further investigation is required to determine the factors responsible for plasma based decontamination by SDBD and to design an optimized actuator for a more penetrative design for large distance (from sample) applications. A proper matrix describing the relation between bacterial load, power, distance from sample, and time is required to optimize this design for large scale applications.

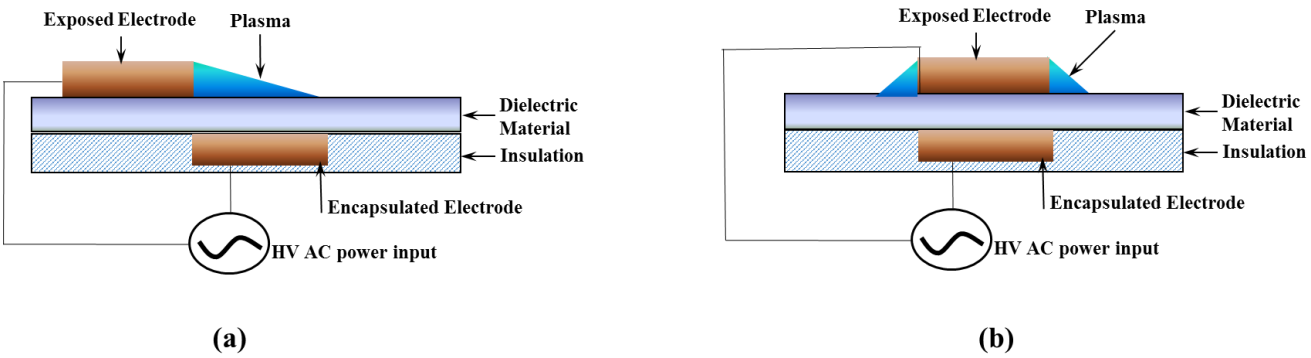

Figure 1 Surface dielectric barrier discharge (SDBD) plasma actuator: (a) Asymmetric arrangement of electrodes; (b) Symmetric arrangement of electrodes.

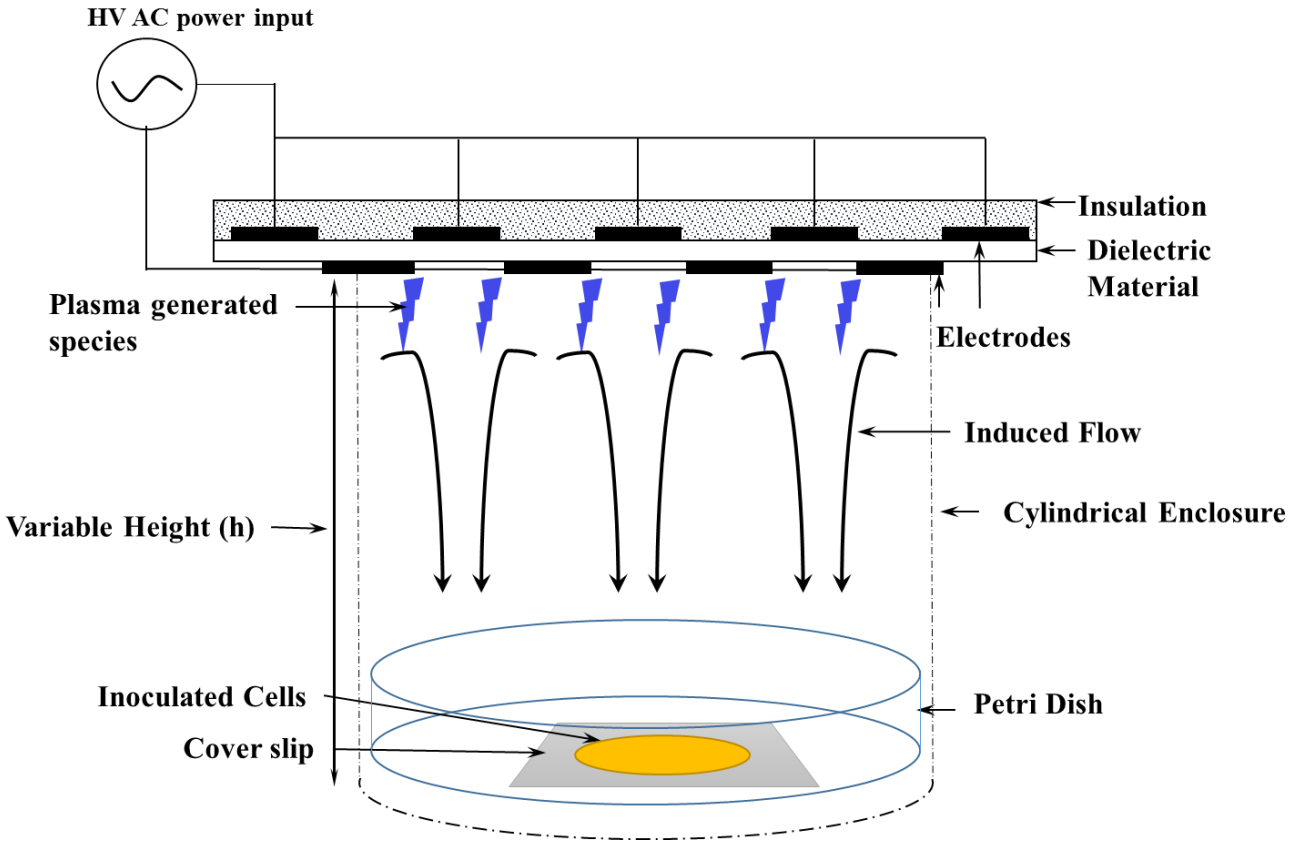

Figure 2 Schematic arrangement of plasma actuator for sample exposure at variable heights.

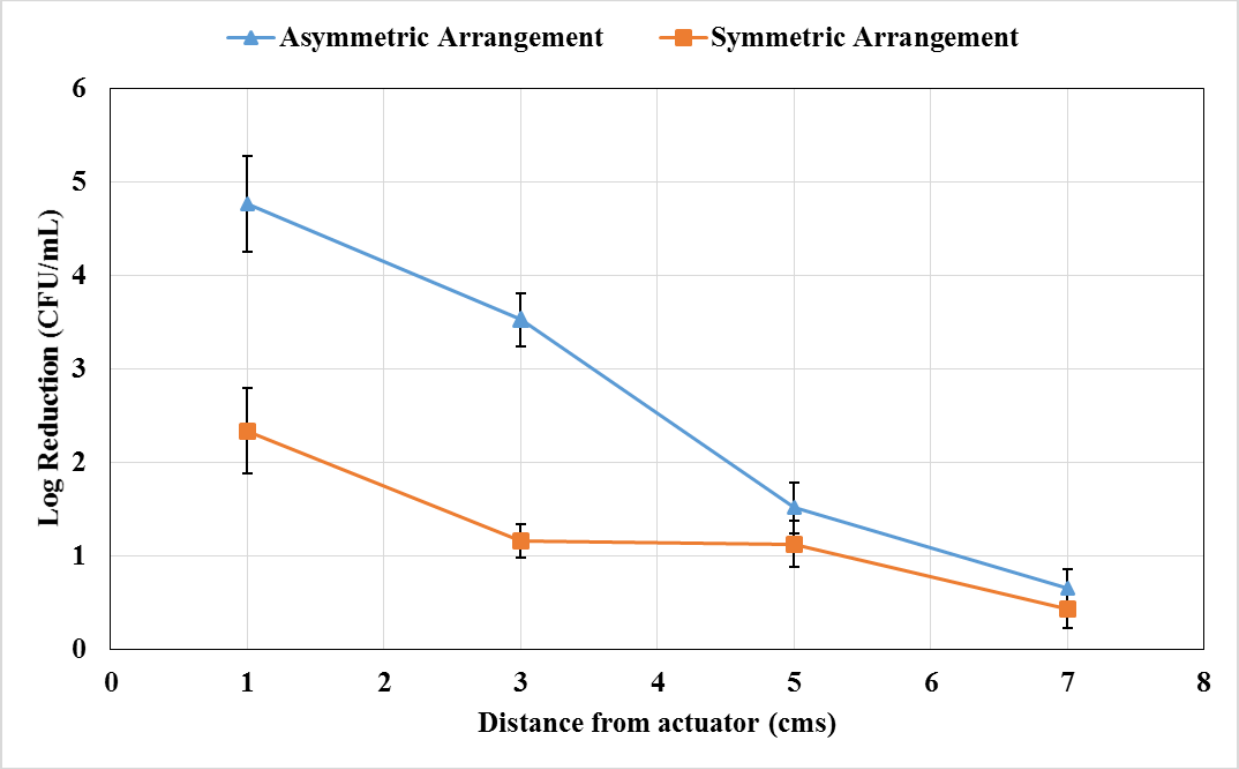

Figure 3 Comparison of inactivation of 5 strain cocktail of Listeria monocytogenes pathogen on glass coverslips using asymmetric and symmetric electrode arrangement SDBD actuators by placing the actuator at various heights.

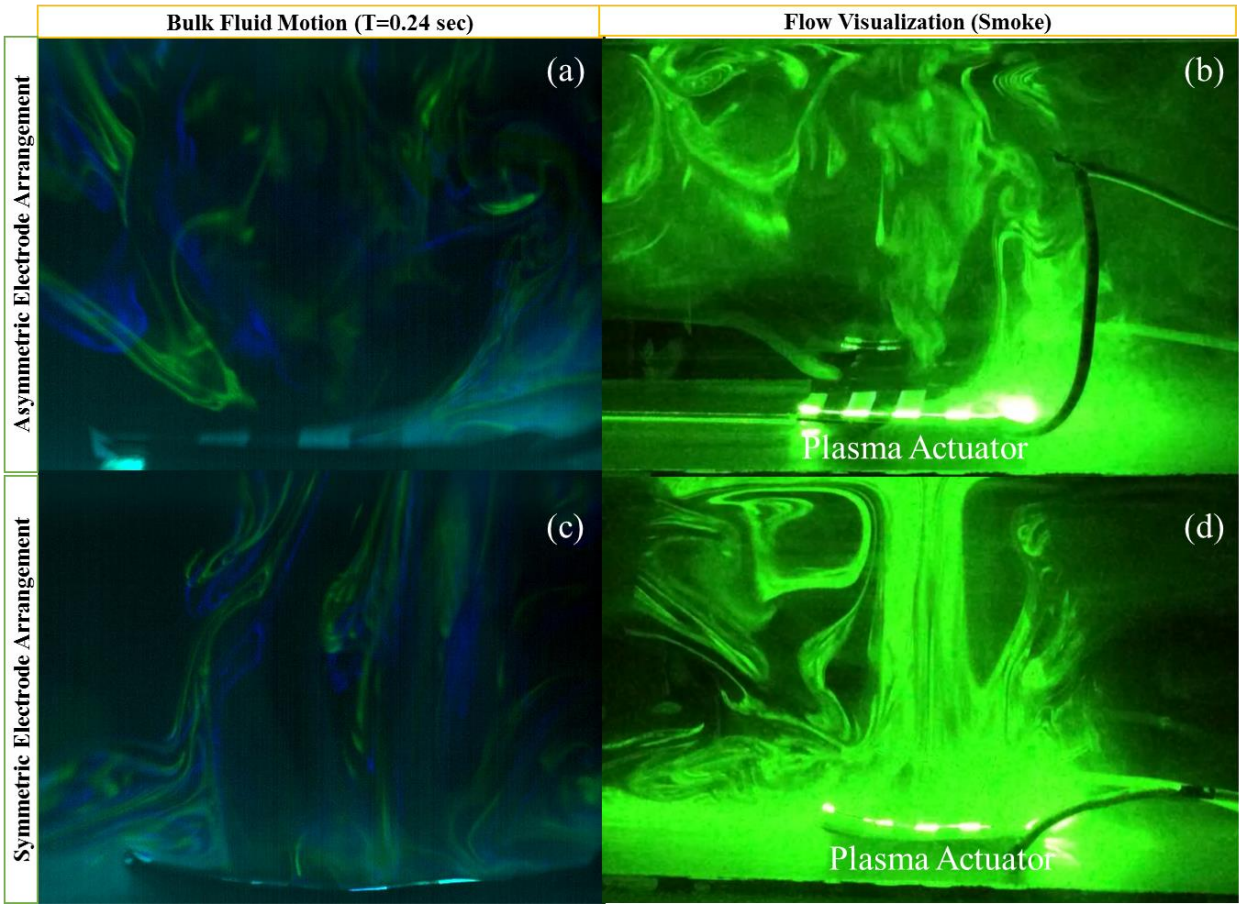

Figure 4 Comparison bulk fluid motion induced by asymmetric and symmetric SDBD plasma actuators: (Left) fluid (smoke) at time T=0 (blue) and fluid at T=0.24s (green); (Right) Bulk fluid motion and flow patterns induced by the actuators.

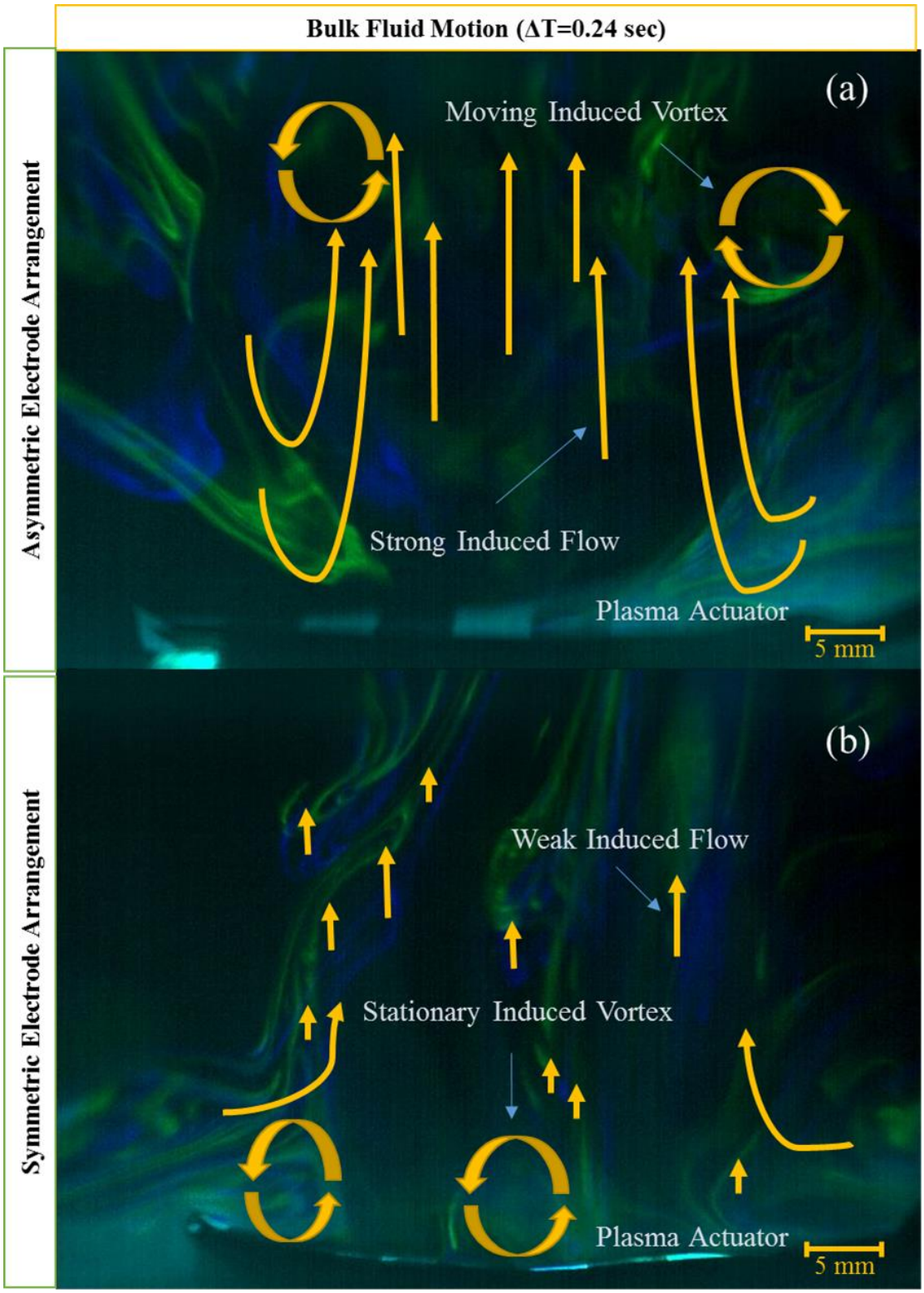

Figure 5 Vectors depicting magnitude (length of arrow) and direction of flow induced by (a) asymmetric arrangement and (b) symmetric arrangement of SDBD.

Chapter 5

Dose Dependent of Response of Different Mammalian Cells SDBD Cold Plasma

5.1. Introduction

"Cold plasma" is generally the term used to define non-thermal plasma generated close to room temperature. The term "cold" is used due to the fact the bulk temperature of the gas is much lower than the electron temperature (Tg<<Te). The low operating temperatures create an opportunity to utilize cold plasma in sterilization applications, surface modifications and coatings. Cold plasma, when generated with certain combinations of gases, can result in various effects such as etching or oxidation. These mechanisms aid in the removal of impurities on solid as well as in liquids. Cold plasmas have been used extensively for ozone generation in industries to purify water through coagulation and precipitation of impurities [39].

Much research has been conducted over the last few decades generating a compendium of cold plasma based decontamination related data [12, 44, 113-116, 118, 136, 141-143, 151, 167, 175]. Applications ranging from inactivation of bacteria and sterilization [12, 44, 113-115, 118, 136, 141-143, 151, 175], to blood coagulation and wound healing [100, 180, 181] have been recently investigated extensively. Various methods of cold plasma generation have been developed

and implemented for such applications and Dielectric Barrier Discharge (DBD) has been found to have potential in the industrial environment [37].

In the past, plasma applicators of varying designs have been devised and tested against both prokaryotic as well as eukaryotic cells; these include atmospheric pressure plasma jets [44, 98, 114, 143], DBD plasma devices for close proximity applications [176], and plasma needle using RF excitation [17, 182, 183]. These designs require a gas flux to propel the plasma generated species to the sight of exposure or have to be placed in close proximity to the sample being treated since they do not have any ability to induce flow. These designs may also induce a necrotic response at shorter exposure levels. Along with these shortcomings, the cost and power required for scaling the device and area of application are high. The gas flux is also responsible for desiccation or interference with the sample if not properly regulated. Thus, an improved method of plasma based cell and tissue treatment is required.

There are two common types of DBD configurations, namely, surface dielectric barrier discharge (SDBD) and volumetric dielectric barrier discharge (VDBD) [37]. The VDBD arrangement has one or both the electrodes covered by a dielectric material and a definite gas gap where the plasma is ignited. This is inconvenient for large samples, and an artificial gas flow is required to transport the plasma generated species to the site of application if indirect exposure is to be used. In a SDBD arrangement, plasma is initiated between two electrodes where at least one electrode is covered by a dielectric material, with no gas gap between the electrodes (**Figure 1**). SDBD possesses the corona discharge ability of flow induction not common to volumetric methods of plasma generation. An example of a SDBD actuator is shown in **Figure 1b**. The flow field

(**Figure 1c)** generated in the vertical direction is due to induced flow and gives this design an additional benefit over existing technologies that have been implemented in the past. In the last decade, the use of SDBD for active flow control has been investigated extensively [22, 40, 56, 62], particularly in aeronautical applications. But no particular strides have been made in the direction of using its capabilities for biological applications. Previously the ability to kill bacterial cells such as *Escherichia Coli* has been studied by Pai *et al* [62]. Three strains of bacteria, namely *Bacillus Cereus, Bacillus Subtillis* and *Escherichia Coli* were tested to determine the effectiveness of SDBD as being both bacteriostatic as well as bactericidal. Their work showed that within a time period of 90 seconds a 3-4 log reduction in cells could be observed. However, it has not been tested on mammalian cells.

In this study, we investigated the impact of SDBD a plasma actuator on three different types of mammalian cells, namely, HUVEC (Human Umbilical and Venous Endothelial Cells), Neuroblastoma and HepG2 (Hepatocytes). These cells were treated through indirect plasma exposure. The species generated in the plasma were analyzed to identify the type of molecules involved in plasma-cell interaction. The changes in morphology and the viability of the cells were analyzed with changes in duration of plasma exposure. The cell mobility and functionality were also assessed post plasma exposure using cell migration analysis. The findings reveal that a number of nitrogen and oxygen based species were generated and may be responsible for the observed cell response. As these oxygen and nitrogen species may result in a change in media composition and have an indirect impact on cells; the pH of the media was also monitored to determine its impact on cell damage. Effects of indirect exposure by SDBD are studied to demonstrate the retention of viability after long durations of plasma exposure. This study shows

the overall impact on the response of mammalian cells to plasma exposure at different durations of exposure and discusses the effects of SDBD as a plasma treatment device.

5.2. Materials and Methodology

5.2.1. Sources for Materials

Human Umbilical Vein Endothelial Cells (HUVEC-2) derived from single donors were purchased from BD Biosciences (San Jose, CA). Medium 200 phenol red free (PRF), low serum growth supplement (LSGS containing 2% v/v fetal bovine serum, 1 µg/mL hydrocortisone, 10 ng/mL human epidermal growth factor, 3 ng/mL basic fibroblast growth factor, and 10 µg/mL heparin), trypsin/EDTA, trypsin neutralizer solution, carboxyfluorescein diacetate succinimidyl ester (CFDA-SE), DAPI (4',6-Diamidino-2-Phenylindole, Dihydrochloride), fetal bovine serum (FBS), and a live/dead cell viability assay kit were purchased from Invitrogen Corp. (Carlsbad, CA). HepG2 (HB-8065), IMR-32 neuroblastoma, trypsin-EDTA solution, and Eagle's Minimum Essential Medium (EMEM*)* were purchased from American Type Culture Collection (ATCC, Manassas, VA). 10 mil thick copper clad Teflon sheets were obtained from TACONIC (Advanced Dielectric Division, NY). Cell Culture-Insert, µ-dish, 35mm, low, were procured from ibidi, LLC, (Verona, WI).

5.2.2. Plasma Actuator Arrangement

Plasma actuators were constructed using copper clad Teflon sheets 10 mil thick (TACONIC, Advanced Dielectric Division, USA). Parallel electrodes were etched on the sheets to develop 5×5 cm^2 actuators with 3.6×0.5 cm^2 dimensions on the side exposed to the sample being treated. A common ground electrode in the form of a square of 3.6×3.6 cm^2 was etched on the opposing side (Figure 2). The ground electrode was covered to prevent plasma ignition of the

side. An asymmetric electrode arrangement was hence developed to be used as the plasma actuator. The actuator was placed 1.15 cm from the surface of the monolayer formed by the three different cell types. All experiments were carried out with identical actuators operating at 13.5 W and 50% duty cycle.

5.2.3. Optical Emission Spectroscopic Analysis

Optical emission spectroscopy (OES) was conducted to observe the species generated by the SDBD actuator. A StellarNet EPP2000CS UV-VIS spectrophotometer was utilized for this task. The range of this device is from 190- 900 nm. Using the Spectrawiz software, the signal from the plasma actuator was collected for an integration time of 350 milliseconds. Two hundred scans were made to average the data so as to get a smooth data plot with less noise. The total acquisition time was 70 seconds. The actuator was a single dielectric barrier discharge (SDBD) design. It was placed under the optical fiber so that the plasma region was aligned along the line of sight of the same. The signal collected from the fiber was sent to the computer via the spectrophotometer. Once the data were collected and processed the emission spectra of the plasma was displayed. The data were then compared and analyzed to get the pertinent atomic and molecular species generated.

5.2.4. Cell Culture

HUVEC

HUVEC-2 was cultured in Medium 200PRF supplemented with LSGS following the vendor's protocols. The final concentrations of the components in the supplemented medium were: fetal bovine serum (FBS) 2% v/v, hydrocortisone 1 µg/mL, human epidermal growth factor 10 ng/ml, basic fibroblast growth factor (bFGF) 3 ng/mL, and heparin 10 µg/mL. HUVECs were

maintained at 37°C, 5% CO_2/95% air, in a humidified cell culture incubator and fed with fresh medium every 36 hours. When confluent, cells were dissociated with 0.025% trypsin and 0.01% EDTA in PBS and neutralized with trypsin neutralizer solution (phosphate-buffered saline (PBS) containing calf serum as a trypsin inhibitor), centrifuged at 125×g for 5 minutes and resuspended in growth medium.

Neuroblastoma Cells

Neuroblastoma cells were cultured with media containing EMEM following vendor's protocol. In brief, Neuroblastoma were maintained in EMEM containing 10% FBS at 37°C, 5% CO_2/95% air, humidified cell culture incubator and fresh media was supplemented every two days. When confluent, cells were detached from TCP using trypsin and neutralized with growth media, centrifuged at 125×g for 5 minutes and resuspended in growth medium.

HepG2 Cells

The HepG2 cells were maintained in EMEM following the vendor's protocol. In brief, EMEM supplemented with 10% FBS was used as the culture medium. Cells were maintained at 37°C, 5% CO2/95% air, humidified cell culture incubator, and fed with fresh medium every 36 hours. When confluent, cells were detached using trypsin and neutralized with growth media, centrifuged at 125×g for 5 minutes and resuspended in growth medium. All viable cells were counted using trypan blue dye exclusion assay.

5.2.5. Analyzing Cell Viability after Plasma Exposure

The cells were seeded in a 6-well plate at a cell density of 50,000 cells/well in 2ml media.

After 24 hours, the cells were treated with the plasma actuator as described in the previous section for 1, 4, and 8 minutes respectively. A volume of 200 µl of media was added to each well before plasma treatment to prevent sample drying. A volume of 200 µl of media was chosen so as to prevent desiccation of the cells while permitting plasma species to penetrate and reach the cells being treated. The researchers observed that with higher volumes of media, there were no observable changes in the cells (data not shown). Hence, a volume of media that produced a thinner layer had to be used similar to the work reported by others [17, 98, 176]. The actuator was placed on each well for the treatment as shown in **Figure 2**. All plasma applications were conducted at room temperature in a biological safety cabinet.

In some experiments, cells were pre-stained with CFDA-SE (2 µM) by incubating at 37°C for 20 minutes, followed by washing the excess stain with growth medium [198]. Images of CFDA-SE stained cells were analyzed using an inverted microscope (Nikon Eclipse TE 2000-U, Melville, NY). Digital micrographs were captured at random locations using the attached CCD camera.

In some experiments, unstained cells of all cell types were used. After 48 h of incubation, percentages of late apoptotic and necrotic cells (low level green-stained with SYTOX green) and metabolically active/live (red-stained with C12-resazurin red) cells were assessed using a live/dead cell viability assay kit. This assay provides a simple, two-color fluorescence assay that distinguishes metabolically active cells from injured cells and dead cells. In this assay C_{12}-resazurin is reduced to red-fluorescent C_{12}-resorufin in metabolically active cells and the uptake of the cell-impermeant, green-fluorescent nucleic acid stain, SYTOX Green dye, in cells with a

compromised plasma membrane (late apoptotic or necrotic cells). Dead cells are found to emit mostly green fluorescence whereas the healthy, metabolically active cells are seen to emit mostly red fluorescence. The injured cells show lower metabolic activity and, consequently, reduced red fluorescence emission; because they possess intact membranes, however, injured cells accumulate little SYTOX Green dye and, therefore, emit very little green fluorescence. Based on these characteristics a dot plot is produced via the flow cytometer and data is interpreted based on manufacturer's protocol.

Samples were processed according to the manufacturer's recommendations. Briefly, plasma exposed cells were cultured for 2 days and were detached from TCP using trypsin. Cells were centrifuged at 125×g for 5 min and dispersed in 100 µL PBS. One µL of 50 µM C12-resazurin red stain and 1 µL of 1 µM SYTOX green stain were added to 100 µL of cell suspension. Cells were incubated at 37°C in an atmosphere of 5% CO_2 for 15 minutes, diluted to 500 µL using PBS by mixing gently, and analyzed according to the vendor's protocol using FACSCalibur (Becton Dickinson, San Jose, CA) flow cytometer.

5.2.6. Cell Migration Assay

Cell Culture-Inserts were used to demonstrate effects of plasma exposure on cell migration and confluence rate. Samples using HUVEC were prepared as per the manufacturer's instructions with a cell density of 3-7×10^5 cells/mL to get a confluent layer within 24 hours. 70 µl of cell solution containing media was added in each of the two chambers in the µ-dish created by the Culture-Insert. The samples were incubated at 37°C and 5% CO_2 for 24 hours to obtain a confluent layer of cells. The plasma exposure was carried out as described in the previous section (1, 4, and 8 minute exposure times) after which the Culture-Insert was gently removed using sterile tweezers

and the samples were incubated. The removal of the Culture-Insert created a gap or scratch in which the cells could migrate to form a monolayer [199]. Images were taken at regular intervals (0, 12, 24, and 36 hours) using a microscope to collect data pertaining to migration and confluence of cells in the gap created by the insert.

5.2.7. Statistical Analysis

All the experiments were conducted in triplicates ($n = 3$) or for $n > 3$. Reported values were represented as mean ± SD. Significant difference between two groups was analyzed using a paired sample t-test with 95% confidence interval. Differences in the results were considered statistically significant when $p < 0.05$.

5.3. Results and Discussion

5.3.1. Plasma Actuator Design and Characteristics

An SDBD arrangement with asymmetrical placement of the electrodes about the dielectric was used in this study. The surface dielectric barrier discharge with such an arrangement created an electric field along which the electrons and ions migrate creating a momentum coupling effect with the surrounding gas. This discharge was generated using AC voltage and frequencies of in the order of 20 kHz. This effect has proven to generate velocities as high as $8 m\text{-}s^{-1}$ [40]. The resulting synthetic jet can be vectored in the desired direction through adequate geometry and orientation of the electrodes [63]. An annular actuator with concentric rings, shown in **Figure 1b** is an example of the same. It can generate a maximum vertical velocity as high as $0.9 m\text{-}s^{-1}$ at 18 kV by forming concentric arrays of electrodes. **Figure 1c** depicts the particle image velocimetry (PIV) results of the flow field generated for the concentric ring arrangement of electrodes shown

in **Figure 1b**. Similar results have been obtained with corona and coplanar discharges [40]. The flow of the gas is manipulated through the orientation of the electrodes and the actuator profile (by molding the dielectric) to get the neutral gas to flow in the particular direction without adding any extra gas or mechanical parts. This form of momentum addition to a stationary gas is known as *zero-net–mass flux* jets [56]. The SDBD eliminated the requirement of artificial gas flux and the velocity of the flow induced can be controlled through the applied voltage and the thickness of dielectric. Any effects of desiccation or heating are also eliminated by a low flow rate and indirect treatment.

5.3.2. Identification of Plasma Generated Species

Optical emission spectroscopy was conducted to establish the type of species generated by the SDBD plasma source. As seen in the spectral data in **Figure 3**, UVC cannot be considered to play a considerable role as we did not observe any wavelengths in the UVC region (200-290nm). Similar results were obtained with dielectrics other than Teflon as well [62]. The peaks from the spectral data were analyzed and showed the presence of N_2 (Second Positive System), N_2^+ (First Negative System), O_2 (Schumann-Runge System), O_2^+ (Second Negative System), NO_2 and NO (NO_β radiation due to β system to ground state transition) [62, 200]. Apart from these reactive species, O_3 and OH^- molecules also are considered to be involved in the mix to act on the cells being treated.

These results suggest a multi-species system being involved in the plasma-cell interaction process and may have an impact on the media composition as well. Oxidative species like ozone and NO have been known to induce cell damage and oxidative stress and may be involved in the

plasma-cell interaction process. The effects of these species and plasma in general, on mammalian cells are explained in the sections that follow.

5.3.3. Impact of Plasma Exposure on Cell Morphology

Three different mammalian cell lines were treated with plasma and observed under an inverted microscope. A thin layer of media was maintained on top of the cells to prevent dehydration. As the depth of penetration of reactive species is low (~ 1mm) [17, 98, 173, 182, 183], increased depth of growth media had negligible effects on cell morphology and viability (data not shown). **Figure 4** shows micrographs recovered using the inverted light microscope after 2 days of incubation post exposure. The untreated cells on tissue culture plastic (referred as control) appeared to have typical spindle or elongated shape (**Figure 4 (a-c)**). All cells adhered to the surface. After 1 minute of exposure all three cell types did not show any morphological differences compared to the respective controls (**Figure 4 (d-f)**). At 4 minutes of plasma exposure, few cells detached; this was more prominent in HepG2. Whereas, HUVEC were much more resilient to the plasma exposure, showing less number of detached cells. All cell types showed a trend of change in morphology from elongated/spindle to spheroidal shape, which is more pronounced in the case of HepG2 cells. This behavior may be due to an increase in stress conditions encountered by the cells as a result of plasma exposure. Neuroblastoma cells showed intermediate response when compared to HUVEC and HepG2 cells. At 8 minutes of exposure, a significant increase in the number of detached cells was observed (**Figure 4 j-l**). All cell types showed formation of granular structures along with cell transparency and visibility of nucleus. This trend was more prominent in HepG2 while HUVEC were resilient and neuroblastoma cells showed intermediate behavior. This could be sign of stress and formation of toxins which may

cause the cells to develop this response. This could also be attributed to formation of certain unfavorable byproducts resulting from oxidation such as nitric oxide and other plasma generated reactive species, which may in turn invoke a cell response similar to steatosis, wherein the cell may burst liberating accumulated lipids [201, 202]. However, further studies are necessary to explore these possibilities.

The sensitivity of the different cells to treatment was evident in an increasing order from HUVEC to HepG2 with neuroblastoma displaying a prominent but intermediate response. The change in cell morphology from spindle or elongated to spheroidal was similar to the results reported using melanoma [203] and epithelial cells [204], albeit with different methods of plasma exposure and different exposure times (1-2 minutes). The atmospheric pressure plasma jets used by others have a lower area application with a higher impact which resulted in cell necrosis at lower treatment times. SDBD used in our study uses lower power than typically used in cold plasma system and indirect exposure method reduces cell damage even at higher exposure times (4 minutes). This demonstrates that SDBD enables a low dose plasma exposure and offers scalability for large area exposures in cell treatment. This aspect in turn can be beneficial when inflammatory or necrotic response of tissue is undesirable during applications such as wound decontamination.

5.3.4. Changes in Viability and Attachment

Fluorescence microscopy was used to analyze cell viability and attachment. The cells pre-stained with CFDA-SE showed green fluorescence, with the brighter spots representing detached or injured cells. Fluorescence micrographs (**Figure 5**) were obtained to qualitatively assess

attached and detached cells along with visible changes in morphology as discussed in the previous section ((**Figure 4**). The brighter spots indicated cell shrinkage, and were in accordance with the change in shape from spindle or elongated to spheroidal. Also, the prominence of plasma treatment on more sensitive HepG2 cells was evident from these results. This showed that an increase in exposure time resulted in an increase in number of detached cells. Segregation was also seen at 8 minutes where the cells appeared to be more spread out and individual cells appeared to show some effects on cell-cell and cell-surface interaction molecules. These effects are evident from the images after 8 minutes of plasma exposure (**Figure 4** and **Figure 5**) and were similar to observations from other reports [205]. This may indicate impact on cell-surface interaction molecules such as integrin, as suggested by different research groups [98, 177, 182, 183, 203, 205-208].

The effects on the cells due to longer durations of exposure to the atmosphere and to lower media volumes causing desiccation was ruled out by exposing the controls to similar conditions as the samples exposed to plasma for 8 minutes without the exposure. The cells appeared to be normal without any clumping or detachment as seen in the micrographs from the inverted microscope and the fluorescence microscope. A further analysis is required through extraction, followed by transfer and culturing of detached cells to quantitatively analyze detachment and get a correlation with healthy and injured cells.

Others have demonstrated cell detachment and functionalization using non-thermal plasma, albeit with different methods of plasma generation at lower treatment times [17, 98, 182, 183, 206]. These results were focused on cell detachment and surface functionalization with little

or no emphasis on viability and cell response. In addition to qualitative analysis we also performed a quantitative study of cell viability using live/dead assay.

5.3.5. Analysis of Cell Injury and Cell Death due to Plasma Exposure

Dot plots acquired from flow cytometry using live/dead assay was used for quantitative analysis of live, injured, and dead cells (**Figure 6)**. The dot plot of SYTOX Green fluorescence versus resorufin fluorescence showed resolution of live, injured, and dead cell populations, Using flow cytometry, the stained cells were characterized as live, injure or dead by exciting at 488 nm and measuring the fluorescence emission at 530 nm and 575 nm. The population was separated into two groups: live cells with a low level of green and a high level of orange fluorescence and necrotic cells with a high level of green fluorescence and a low level of orange fluorescence (as per manufacturer's protocol). The flow cytometry results were confirmed by viewing the cells with a fluorescence microscope, using filters appropriate for fluorescein (FITC) and tetramethyl-rhodamine (TRITC). It was observed that all types of cells showed an impact of plasma exposure, although at different rates. The number of injured cells increased with variable intensity for all three different types of cells.

After 1 minute of plasma exposure, HUVEC showed a non-significant change in the percentage of live cells as compared to the control, while the neuroblastoma and HepG2 cell showed a slight reduction in the number of live cells with HepG2 showing a higher number of injured cells. After 4 minutes of plasma exposure, the impact of plasma was not prominent on HUVEC, while the neuroblastoma and HepG2 cells show a significant decrease in viability. Following 8 minutes of plasma exposure, however, all cell types showed a significant decrease in viability. The HepG2 cells showed the maximum susceptibility to plasma treatment as compared

to HUVEC and neuroblastoma cells that were comparatively more resilient even after 8 minutes of plasma treatment with more than 64% viable HUVEC as compared to HepG2 which had 37% viable cells. The response of neuroblastoma cells was intermediate when compared to the HUVEC and HepG2 cells. The cells show a variable response to plasma treatment with a change in dosage (exposure time) with a low number of cells undergoing necrosis at longer durations of plasma treatment when compared to results from Lee *et al* [203]. However, the overall performance was better than bacterial cells, that showed very low tolerance and were completely inactivated within 3-4 minutes of treatment (~3-4 log reduction) [62]. This showed that SDBD is a good alternative for wound decontamination, especially for large area applications, as it did not affect the mammalian cell viability or morphology even after 4 minutes of exposure.

The variable effects and observations of plasma treatment on different type of cells confirmed that the different cells in the human body react differently. This indicates that for *in vivo* treatments, a dose based matrix for plasma exposure durations is required to ascertain favorable effects and cell treatment without accidental cell death (necrosis) and inflammatory response by the neighboring cells. When compared to the plasma needle and other designs for plasma treatment [17, 44, 98, 143, 174, 176, 203], the plasma actuator based on SDBD design with active flow control is noninvasive and indirect, so it prevents any desiccation or media contamination. This design also helps transfer of plasma generated reactive and neutral species without added gas flow at room temperatures. This methodology enables a more controlled and precise exposure possibility as compared to other modes of plasma generation. However, SDBD may not be beneficial in cases where rapid action is required and indirect methods cannot be used.

5.3.6. Evaluation of Role of Species and pH

The spectral results observed in the previous section are in accordance with the results seen with previous air plasma studies [12, 62, 174, 209]. As there were many oxidative species generated, we investigated the change on pH of the media upon treatment. 200 µL of fresh growth media, the same as the quantity used for the cell culture studies was exposed 1, 4 and 8 minutes of plasma to check the change in pH. Measured pH values showed a decrease. This change in pH was also evident by a change in color of the phenol red in the media in the case of neuroblastoma and HepG2 that changed from pink to orange suggesting a rise in acidity (**Figure 2c**). However, after exposure to plasma, cells were incubated with addition of 2mL. With that 10 fold addition of fresh media, the change in pH was found to be negligible as the change was much less (7.4 to ~6.5). Hence, this change was not large enough to consider pH change as a factor in cell damage. Ozone alone generated during air plasma ignition was also ruled out to be the sole factor responsible for cell damage and death [177, 207]. But as the media contains buffers that may be responsible for neutralization of the ROS (reactive oxygen species) and RNS (reactive nitrogen species), further tests may be required to ascertain the mechanism of cellular damage. Tests repeated with distilled water (pH = 7) showed a greater drop in pH as compared to media (1min exposure: pH=6.5; 4 min exposure: pH =5.5; 8 min exposure: pH= 4) We hypothesize that direct effects of plasma generated species that come into contact with the cells may be responsible for the observed damage and are not observed through pH change. As the nutrients in the media may be affected, the media conditions need to be assessed in further detail. Others have also described comparable effects of plasma treated media to direct plasma exposure [177].

In applications such as wound healing and wound decontamination however, it would be advised to rinse the wound with buffers to reduce impact of pH change, which may be detrimental to the tissue. The pH was normalized back to 7.4 when excess media was added to the sample in our experiments.

5.3.7. Cell Migration Assay

To establish a better understanding of whether the plasma exposure renders cells less functional, and to understand the physical effects on the cells, a migration assay was conducted using HUVEC to observe how the cells respond to variable doses of plasma treatment. This data would be complementary to the viability analysis, as it would let us know if the cells lose their ability to form a monolayer and proliferate. The cells were exposed to plasma as described before and the images were taken at 0, 6, 12, 24 and 48 hours respectively (**Figure 7)**. The micrographs were observed for effect on cell migration. The trend in the closure of the gap between the two regions created by removal of the culture insert, as described earlier, was studied. Cells treated for 1 and 4 minutes, however, showed prominent signs of migration similar to the controls, and hence were still viable and functional. Cells treated with plasma however displayed a higher rate of migration (qualitative) to attach and form a monolayer as compared to the control, with 4 minutes being the fastest and control the slowest (**Figure 7)**. As a number of cells were detached in the case of the plasma treated samples, the density of cells seen is much lower than the control. Hence, the cells appear much more spread out as compared to the control. It can be observed from the results (**Figure 7**) that the cells treated with plasma for 8 minutes were completely detached. Due to a lower cell density, as compared to that used in viability test, suffered higher damage. Hence, no signs of migration were observed as a very small number of cells were seen in the field

of view. It should be noted that tracking of cells is required to establish whether the rate of cell migration is altered positively or negatively. Exposure to atmospheric pressure plasma jets with different gases decreased cell migration rate in HaCaT keratinocytes of epithelial origin and mouse dermal fibroblast cells [208, 210]. However, Wende *et al* [210] attributed this phenomenon to desiccation by gas flux, which is not a factor in SDBD plasma generation due to its indirect nature and self-induced flow. Further analysis of cell migration and detachment is required to assess the mechanism for increased functionality, as this assay gave a qualitative understanding of cellular response to plasma exposure.

5.4. Conclusion

Three different types of mammalian cells, namely HUVEC, neuroblastoma and HepG2, were exposed to plasma using a SDBD plasma actuator. The effects on cell morphology, viability and functionality were tested using an inverted light microscopy, fluorescence microscopy, live/dead assay and migration assay respectively. We found that an increase in the exposure time resulted in a growth in the number of detached and injured cells, with HepG2 cells displaying the highest sensitivity to plasma exposure. A higher level of clumping and a change in shape from spindle/elongated to spheroidal was observed in all cells showing a sign of oxidative stress and cells witnessing unfavorable conditions due to plasma exposure. The migration assay also confirmed that the cells maintain good functionality up to a level of 4 minutes of plasma exposure, which suggested that for applications of wound healing and cell manipulation the SDBD mode of plasma treatment is non-lethal to human cells at longer treatment durations. However, we found that different cells in the body respond to different degrees as seen from the variation in response in viability between HUVEC, neuroblastoma and HepG2 cells. Hence, there is a need to create a

matrix of nonlethal doses for possible applications such as cancer cell treatment, so as to avoid necrosis and inflammatory responses in neighboring cells. In the case of wound decontamination applications this study enables us to understand what the impact would be on exposed tissue and nerve endings and helps better design and optimizes the plasma apparatus parameters.

We also investigated the type of species generated using OES, and found the predominant species to be oxygen and nitrogen based. An analysis of the change in induced pH did not reveal a major role of pH change in cell damage, but further investigation is required to rule out involvement, as buffers in the media may act as neutralizers. We hypothesize that the exposure to ROS and RNS species may be the factors causing oxidative stress as evidenced by the change in morphology of the cells. We demonstrated that the SDBD plasma actuators provide a uniform treatment without any use of external gas flow due to the innate ability of this design to induce flow. It also has the advantage of being able to be easily scaled by changing the design of the electrodes and size of the actuator, thus making it applicable for larger surface treatment. As the treatment is indirect, a slower necrotic response is observed even with a thin layer of media (~ 0.2 mm) which makes it ideal for precision and safe surface treatments in *in vivo* as well as *ex vivo* applications. However, this method may not be ideal where rapid effects are sought and indirect treatment is not effective or convenient, such as *in vivo* with space constraints and unavailability of air or presence of fluids. This data give evidence of the selectivity of non-thermal atmospheric plasma not only between prokaryotic and eukaryotic cells but also demonstrates a variable response amongst various eukaryotic cells derived from the human body. Further analyses of the underlying mechanisms of the response observed in the data presented is needed to establish a better understanding of non-thermal plasma interaction with living cells.

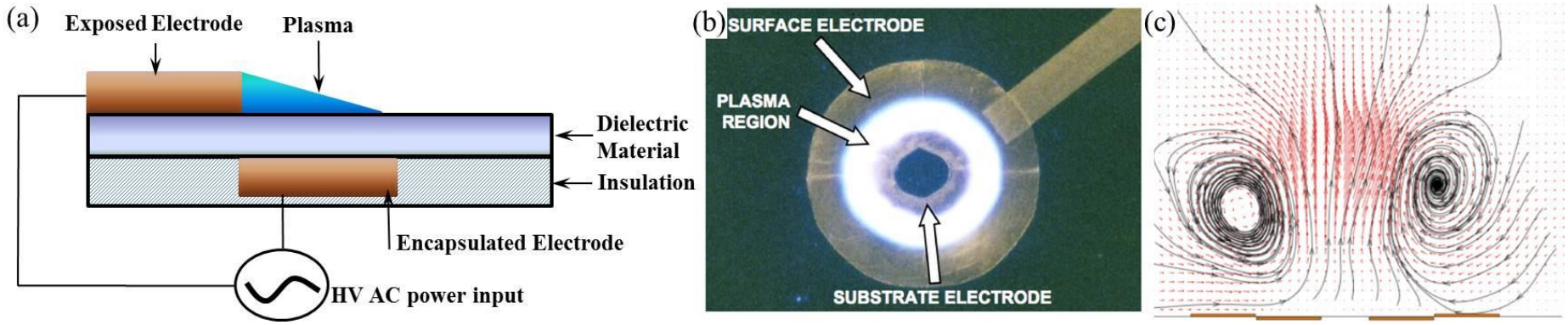

Figure 1 Plasma actuator. (a) Asymmetric arrangement of electrodes; (b) Plasma discharge for a SDBD (concentric ring arrangement).[56]; (c) Flow field for the concentric ring, annular actuator [56].

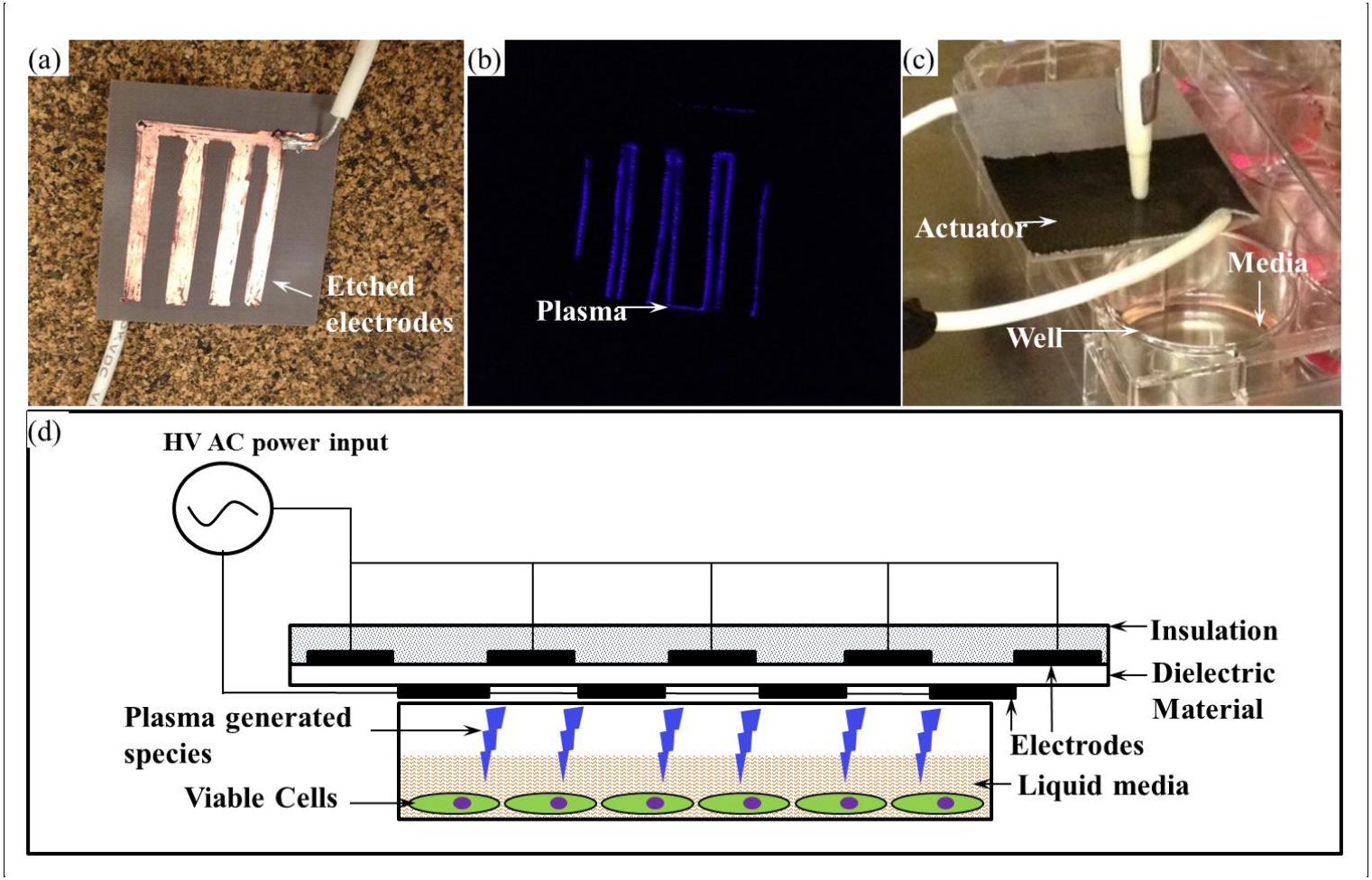

Figure 2 Experimental setup for plasma exposure: (a) Photograph of Plasma Actuator; (b) Photograph of pattern of Plasma generated; (c) Experimental setup used while exposing the cells to plasma; (d) Schematic showing various parts in the Plasma Actuator.

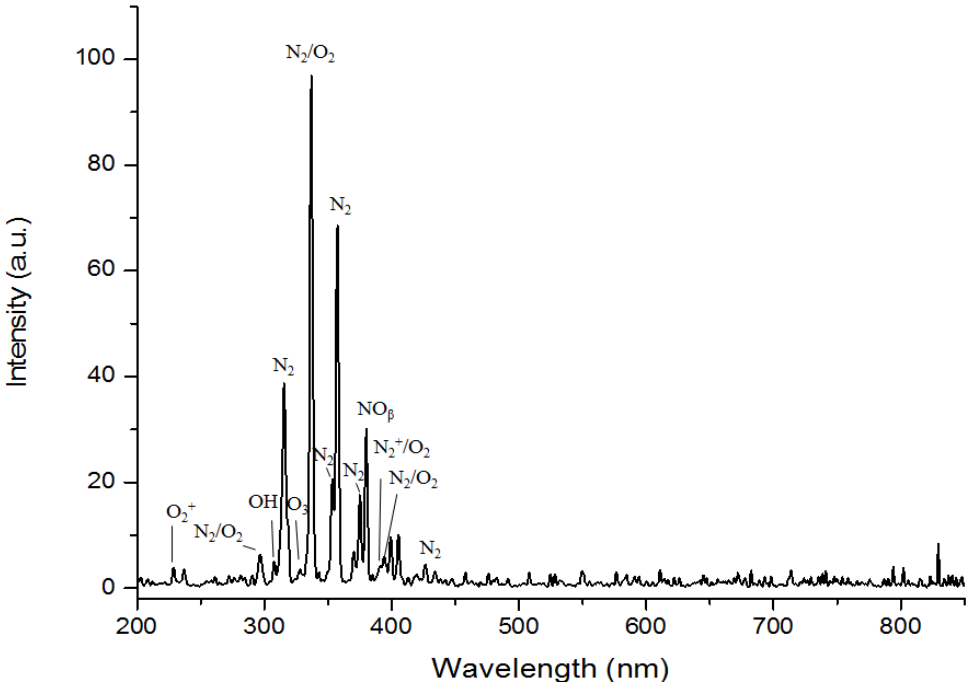

Figure 3 Optical Emission Spectroscopy (OES) results for atmospheric pressure surface dielectric barrier.

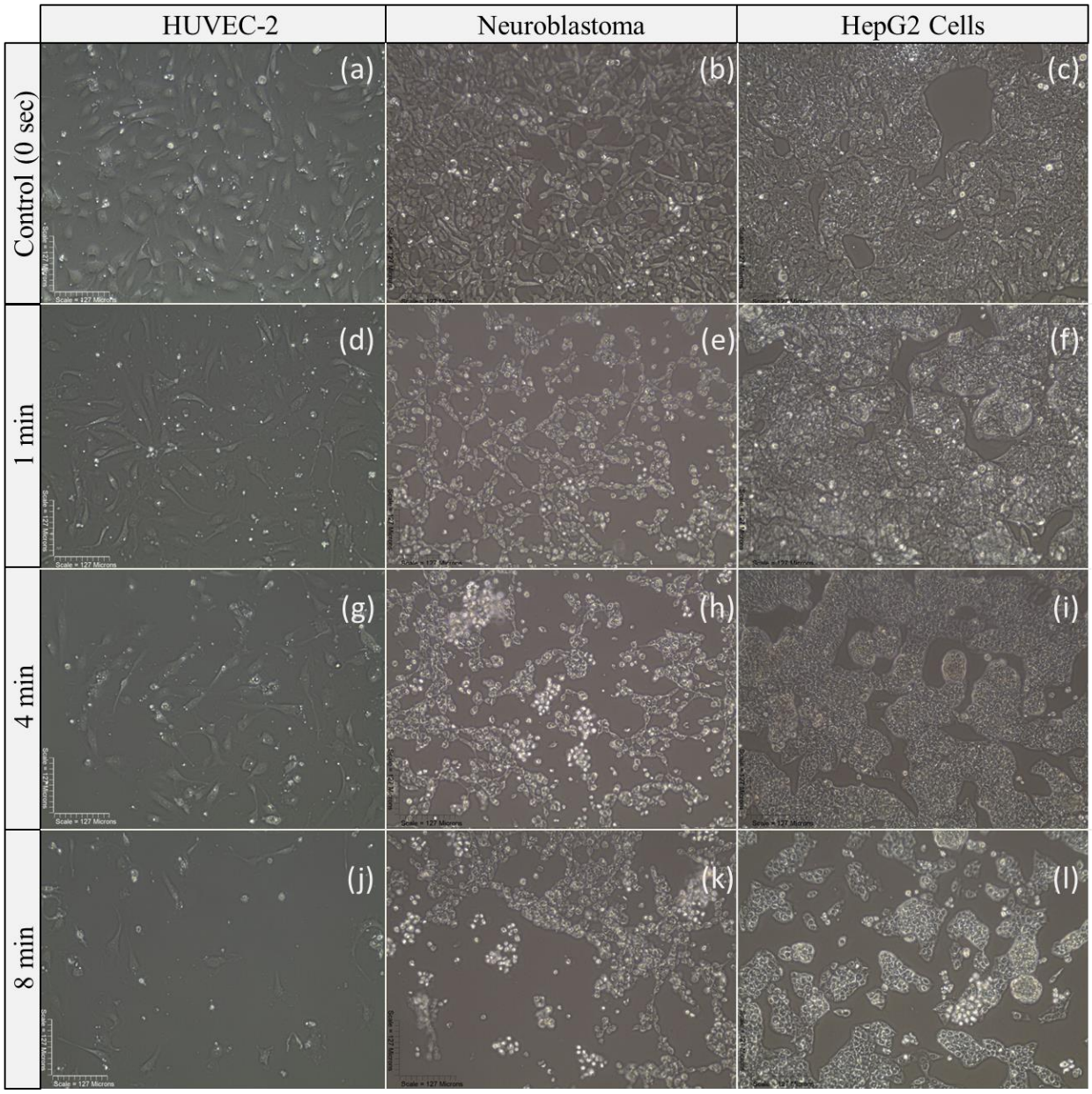

Figure 4 Micrographs showing effect of plasma treatment on HUVEC(a,d,g,j); Neuroblastoma (b,e,h,k); and HepG2 (c,f,I,l) cells with variable exposure times (0 min, 1 min, 4 min and 8 min respectively).

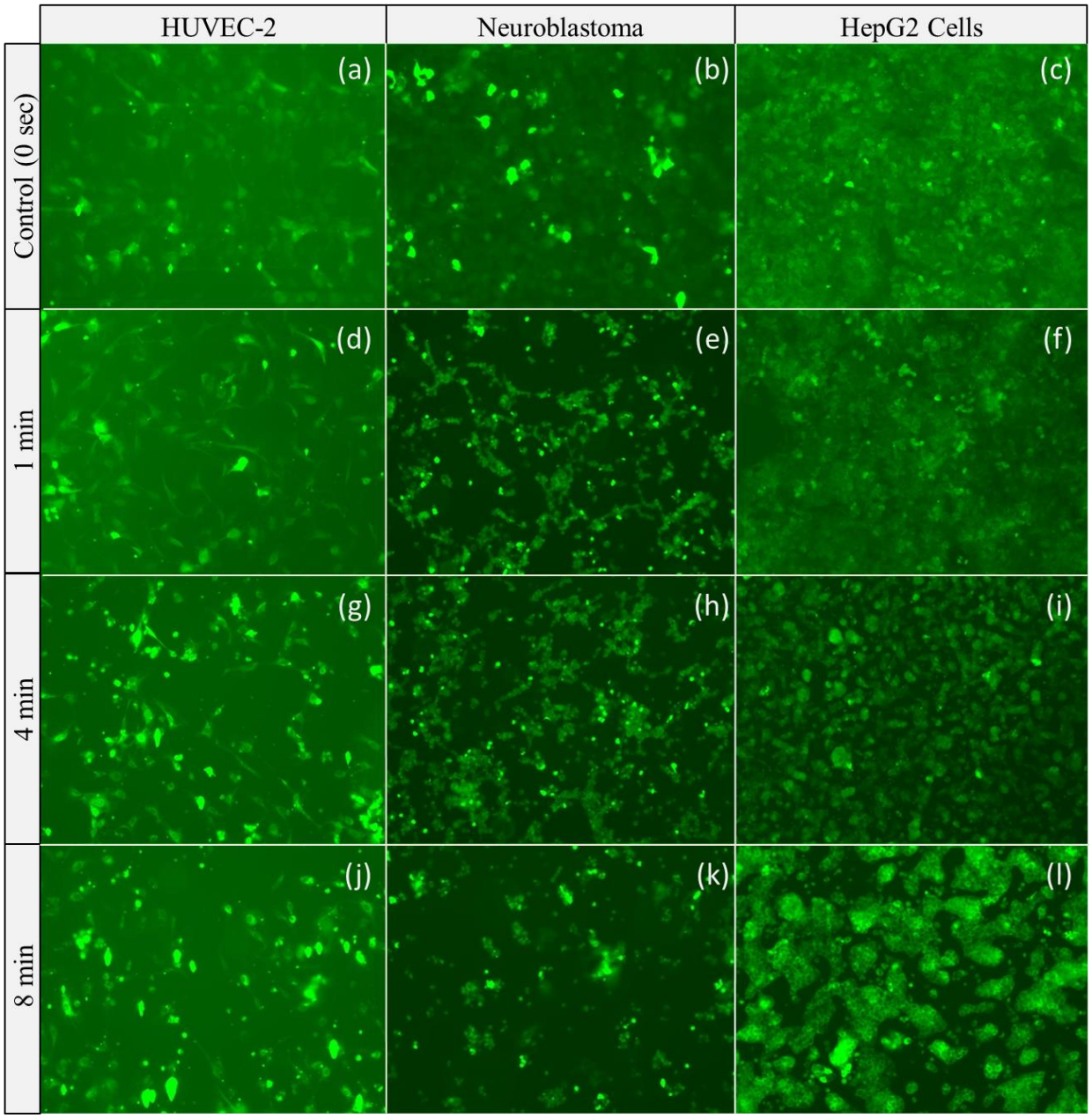

Figure 5 CFDA-SE stained fluorescent micrographs showing effect of plasma treatment on HUVEC(a,d,g,j); Neuroblastoma (b,e,h,k); and HepG2 (c,f,I,l) cells with variable exposure times (0 min, 1 min, 4 min and 8 min respectively).

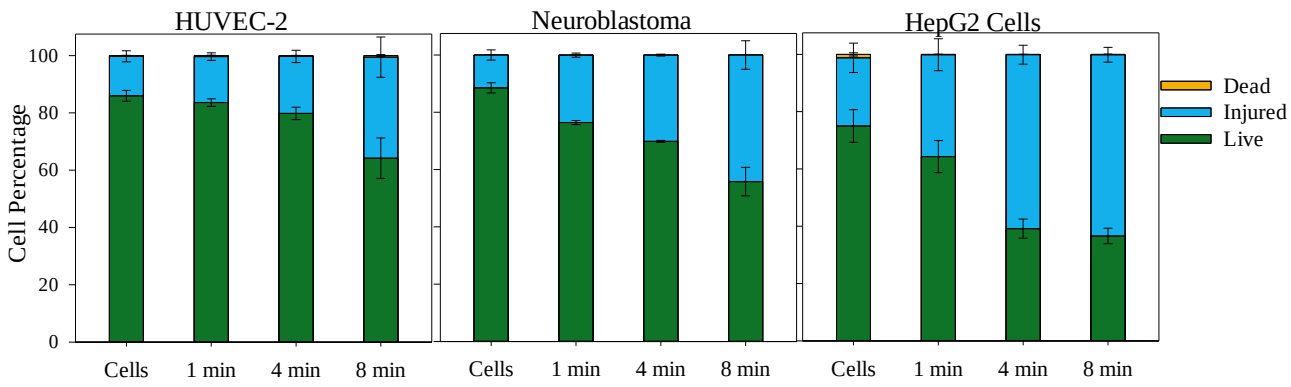

Figure 6 Plots for live, injured and dead cells via Live/Dead assay: (a) HUVEC; (b) Neuroblastoma; (c) HepG2.

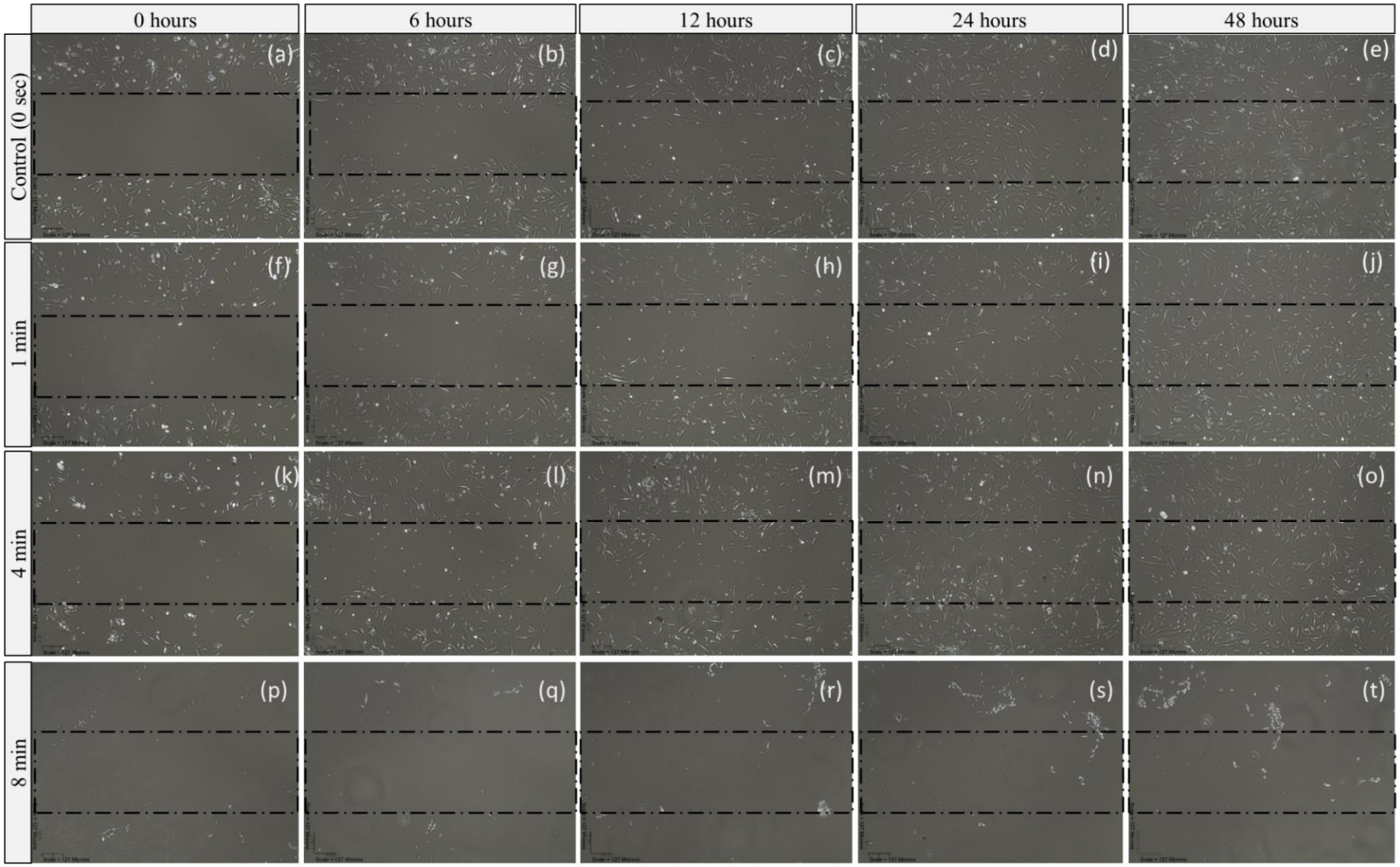

Figure 7 Micrographs showing effect of plasma treatment on migration of HUVEC at different time intervals for plasma exposure of 0 minutes (control)(a,b,c,d,e); 1 minute (f,g,h,i,j); 4 minutes (k,l,m,n,o); and 8 minutes (p,q,r,s,t) respectively. (Rectangular region indicates the gap created by removal of Culture-Insert).

Chapter 6

SDBD Generated Plasma Species responsible for Plasma-Cell Interaction

6.1. Introduction

In the past few decades, a major concern in health care is the evolution of antibiotic resistant pathogens, such as Methicillin Resistant Staphylococcus Aureus (MRSA) [211] and Carbapenem-Resistant Enterobacteriaceae (CRE) [212, 213] . Colistin, a relatively toxic drug, has become a last-resort choice in treating some strains of *Pseudomonas Aeruginosa* [214]. Currently high frequency of monitoring these infections and patient isolation are the only available approaches which do not prove very effective. Pathogen selective drugs for such bacteria are also being investigated but the strains seem to be adapting faster than the drugs can be developed and administered. New therapies also need to display selectivity in the cells. Some antibacterial antibiotic-enhancing alkaloids, which are being considered for example, are highly toxic to eukaryotic cells and may have other effects such as immunosuppression [215]. The development of novel approaches, either those that block or circumvent resistance mechanisms or those that attack new targets is essential, possibly without the aforementioned drawbacks. These methods should be able to overcome the mechanism of resistance, which can thwart the success of new, but

structurally similar antimicrobial drugs.

Cold plasmas or non-thermal plasmas have been investigated in the past few decades due to their innumerable benefits in the field of healthcare, such as disinfection and sterilization [6, 9, 62, 94, 112, 123, 169], wound decontamination and deterring nosocomial infections [101, 103, 104, 171, 181, 216], and cancer treatment [203, 217, 218]. A very good review of these application can be found in articles by Kong *et al.* [99] and Fridman *et al* [14]. Various cold plasma technologies have also shown effectiveness against Drug resistant bacteria and are currently being reviewed for clinical applications [219-221]. However, the current designs rely on close proximity [221] and needing an external gas flow for distribution of generated species. Previously, we demonstrated a novel Surface Dielectric Barrier Discharge (SDBD) method of non-thermal plasma generation which uses low power and is effective at a long range [62, 179]. The SDBD plasma generation method is a semi-direct method of exposure to plasma species. As this method is not direct, and does not use the substrate to complete the electric circuit and effects such as burning or desiccation can be mitigated. SDBD exposure showed a differential response by eukaryotic cells [179] and the lethal effects on prokaryotic cells [62]. The flow induction capabilities of SDBD plasma actuator were also demonstrated. We observed a differential response between different types of mammalian cells showing that different tissues have a dose dependent tolerance to plasma generated species. However, it was also seen that prokaryotic cells have a lower tolerance to plasma and as such a surface decontamination of different tissues can be realized without any adverse effects to the substrate. SDBD being a surface treatment can provide an alternative for precision treatments especially for surface decontamination in hospitals and medical facilities, as well as, dermatological applications.

However, the mechanism of interaction of this method of plasma generation with cells is not well understood. Hence, to get a better understanding of this mechanism, we investigate the role of different ROS and RNS along with ions on the effects observed with prokaryotic cells using *Listeria monocytogenes* and eukaryotic cells using Human Umbilical and Venous Endothelial cells (HUVECs) using SDBD plasma actuators. Using the treatment time of 4 minutes that was found to be the highest sub-lethal dose of plasma for HUVECs [179], we analyzed the effects of bacterial decontamination and oxidative stress to the mammalian cells. As a result we see that Reactive Oxygen Species (ROS) are the predominant mode of interaction of plasma with cells. We show that the optimization of the design can help lower the power requirements.

6.2. Materials and Methodology

6.2.1. Sources for Materials

Human Umbilical Vein Endothelial Cells (HUVEC-2) derived from single donors were purchased from Life Technologies (USA). Medium 200 phenol red free (PRF), low serum growth supplement (LSGS containing 2% v/v fetal bovine serum, 1 µg/mL hydrocortisone, 10 ng/mL human epidermal growth factor, 3 ng/mL basic fibroblast growth factor, and 10 µg/mL heparin), trypsin/EDTA, trypsin neutralizer solution, Image-IT LIVE Green Reactive Oxygen Species Detection Kit (Molecular Probes, USA), five strains of *Listeria monocytogenes*, F6854, 12433, G3982, J0161 and, Scott A (NIMFFAB, Oklahoma State University), tryptic soy broth (TSB, Difco, USA). Griess Reagent Kit for nitrite detection (Molecular Probes), fetal bovine serum (FBS), and a live/dead cell viability assay kit were purchased from Life Technologies (USA). The ROS and RNS scavenging agents, 2-(4-carboxyphenyl)-4,4,5,5-tetramethylimidazoline-1-oxyl-3-oxide (Carboxy-PTIO potassium salt), and N-acetyl-L-cysteine (NAC) were purchased from

Sigma- Aldrich Chemical Co. (Saint Louis, MO). 3% Hydrogen peroxide (H_2O_2) was purchased off the shelf (Vi-Jon, MO, USA). *0.254 mm thick* Teflon sheets and 0.5 cm wide copper tape were obtained from McMaster-Carr Supply Company (USA). MINIMAX70 high frequency transformer (Information Unlimited, NH, USA) was used to generate the plasma. Bovine muscle tissue was acquired from the Department of Animal Sciences at Oklahoma State University (Oklahoma, USA).

6.2.2. Plasma Actuator Arrangement

Plasma actuators were constructed using 0.0254-cm thick copper clad Teflon sheets (McMaster-Carr Supply Company, USA) as a dielectric medium, to which 0.2 cm wide copper tape (McMaster-Carr Supply Company, USA) was attached as electrodes asymmetrically on either side (Figure 1). All experiments were carried out with identical actuators operating at 13.5 W and 50% duty cycle (effective power of 6.75 W). Different configurations of electrodes were used which are described below

(i) To test the effects of power density on nitrite production, three different actuators were developed with electrodes of length 3.6 cm, 5.4 cm and 11 cm. Power per unit length of the electrode was calculated for each configuration using the equation:

$$Power\ per\ unit\ length\ \left(\frac{W}{m}\right) = \frac{Input\ Power\ (W)}{Total\ length\ of\ plasma\ (m)}$$

---------- Eq 6.1

where the total length of plasma is measured by multiplying the number of edges the plasma is generated on by the length of the electrodes. This gave power densities per unit length of 93.75 W/m, 62.5 W/m and 30.68 W/m for the three lengths.

(ii) To understand effect of number of electrodes, three actuators were prepared using 3.6 cm long electrodes on a dielectric of area 5 cm × 4 cm. The number of electrodes placed on the dielectric was 2, 4 and 7 with the same power input as above with a common encapsulated electrode on the opposite side. Samples were exposed to plasma at 1 cm distance from the sample. However, to test the effect of change in distance between the actuator and the sample, 4-electrode configuration was used. Actuator was placed at 1, 3, 5, and 7 cm from the sample.

(iii) For mammalian cell culture experiments, actuator size had to be changed to fit the culture plates, according to the description in our previous work [179]. In brief, parallel electrodes were developed on the sheets to develop 12.5 cm × 3 cm actuators with electrodes of 11 cm × 0.5 cm in dimensions on the side exposed to the sample being treated. A common ground electrode in the form of a rectangle of 11 cm × 0.5 cm was used on the opposing side (**Figure 1**). The ground electrode was covered to prevent plasma ignition of the side. The actuator was placed at ~1 cm from the surface of the cell monolayer formed on the bottom of the petri dish. Based on previous work [179], all cells were treated with plasma for 4 min.

6.2.3. Air Ion Production due to Plasma Exposure

The density of ions generated due to SDBD cold plasma exposure were measured with an air ion counter (AlphaLab, Inc., Salt Lake City, UT, model AIC), which measures separately the number of positive and negative ions per cm^3. This air ion meter is based on a Gerdien Tube (Gerdien Condenser) design and contains a fan, which pulls air through the meter at a calibrated

rate. Effect of plasma exposure was measured at 1, 3, 5, and 7 cm from the actuator surface with and without turning the fan. The air ion density was compared to the ambient air to determine the relative increase in ion density. All measurements were done in triplicates and in standby mode to prevent any bias due to induced convection by the fan of the grounded plate. Ion density was measured once a steady state reading was observed in the Air Ion Counter.

6.2.4. Microbial Inoculation and Sample Preparation

Five strains of *Listeria monocytogenes* (F6854, 12433, G3982, J0161 and, Scott A) were cultured for 24 hours at 37°C in tryptic soy broth (TSB, Difco). After 24 hours of incubation, 1 mL each of the culture was centrifuged at 12000rpm for 3 minutes to form pellets and a cocktail of each strain (1 ml each) was re-suspended in 1 mL of 0.1% (w/v) sterile peptone water (Difco) to produce the desired inoculum concentration. A cell density of 10^8-10^9 CFU/mL was obtained with a total inoculum volume of 5 mL.

The cocktail was serially diluted to get lower inoculum concentrations. The inoculum was diluted eight times to get smaller number of colonies. 100 µL of 10^6, $10^7$and 10^8 fold dilution each was plated on tryptic soy agar (TSA, Difco) for cell enumeration. 100 µL of 10 fold dilution (10^{-1}) of the original inoculum was uniformly distributed on standard glass coverslips. They were air dried for 30 minutes at room temperature in a biological safety cabinet prior to plasma treatment.

6.2.5. Electrical conductivity of plasma treated water and media

Ten mL of water and growth medium used for HUVEC culture were treated with plasma for 2 and 4 minutes. The electrical conductivity of was measured with a portable pH/EC/TDS

meter (Milwaukee Instruments, Inc., Rocky Mt, NC, model MW802) at 30 min, 1 hr, 12 hr, and 24 hr after plasma treatment.

6.2.6. Endothelial Cell Culture

HUVEC-2 was cultured in Medium 200PRF supplemented with LSGS following the vendor's protocols, as described previously [179]. In brief, the components in the supplemented medium were fetal bovine serum (FBS) 2% v/v, hydrocortisone 1 µg/mL, human epidermal growth factor 10 ng/ml, basic fibroblast growth factor (bFGF) 3 ng/mL, and heparin 10 µg/mL. HUVECs were maintained at 37°C, 5% CO_2/95% air, in a humidified cell culture incubator and fed with fresh medium every 36 hours. When confluent, cells were dissociated with 0.025% trypsin and 0.01% EDTA in PBS and neutralized with trypsin neutralizer solution (phosphate-buffered saline (PBS) containing calf serum as a trypsin inhibitor), centrifuged at 125×g for 5 minutes and resuspended in growth medium. Viable cells were counted using trypan blue and seeded into various culture plates, as required. Based on viability analysis [179], cells were exposed to plasma for 4 minutes at approximately 1 cm distance.

6.2.7. Extracellular nitrite detection

Cells were seeded into a 24 well plate at 12,000 cells per well and incubated with 500 µL media. After 24 hours, cells were pretreated with carboxy-PTIO (100 µM) that scavenges NO stoichiometrically and incubated for 45 minutes before they were exposed to plasma. The untreated samples with and without the NO scavenger were used as controls. Culture medium was retrieved at 30 min, 1 hour, 12 hours and 24 hours for nitrite analysis. Collected medium was

mixed with an equal volume of Griess Reagent Kit (for nitrite detection) as given by vendor (Molecular Probes, Life Technologies, USA), and incubated at room temperature for 20 min. The absorbance was measured at 490 nm with an Emax precision microplate reader using the software SoftMax Pro 4.3 (Molecular Devices, Sunnyvale, CA) using a calibration curve with a range of 0–100 μM concentrations of $NaNO_2$.

Fresh media was used to measure nitrite production induced by plasma to establish a baseline nitrite concentration attributed to plasma exposure to discount Nitric Oxide Synthase (NOS) activity. In the case of measuring the effect of power density and number of electrodes, tests were conducted using 1 mL of media in a 6-well plate and nitrite concentrations were measured at 1 hour after exposure.

6.2.8. Intracellular ROS detection

Cells were seeded in a 96 well plate with a density of 7,000 cells per well and incubated with 200 μL media. Caboxy- H_2DCF-DA was added to all cultures at 50μM following vendor's protocol. Five different conditions were created: (a) Control with NAC (b) Control with NAC (5mM based on ref [222]) but not exposed to plasma; (c) Plasma treated cells without NAC; (d) Plasma treated cells with NAC; (e) H_2O_2 (200μM) as a positive control. To conditions containing NAC, it was added 45 minutes prior to plasma treatment. Intracellular ROS levels were assessed using the Image-IT LIVE Green Reactive Oxygen Species Detection Kit (Molecular Probes, Life Technologies, USA) according to the manufacturer's protocol. Fluorescence intensity was measured in a microplate reader, SpectraMAX GEMINI XS using the software SoftMax Pro 4.3 (Molecular Devices, Sunnyvale, CA) at 495/529 nm. Intensity was recorded at 30 min, 1 hour 12 hours and 24 hours for the oxidative stress assay using the SpectraMAX GEMINI XS. Digital

micrographs were also acquired using an inverted microscope (Nikon Eclipse TE 2000-U, Melville, NY) at random locations.

6.2.9. Evaluation of ROS and Plasma Effects on Bovine Muscle Tissue

Two separate set of experiments were designed to evaluate the role of plasma generated ROS on muscle tissue. First, the muscle tissue was inoculated with pathogens (5 strain cocktail of *Listeria monocytogenes*) and exposed to plasma for 4 minutes with a 4 electrode configuration at 1 cm from the sample. In the second experiment The muscle tissue was coated with 1 ml of 5 mM NAC prepared in PBS to observe if the effects of plasma were dominated by ROS. Samples that did not have NAC were coated with PBS so as to prevent desiccation. Treatment conditions were the same as that for the first experiment.

6.2.10. Statistical Analysis

All the experiments were conducted in triplicates ($n = 3$) or for $n > 3$. Reported values were represented as mean ± SD. Significant difference between two groups was analyzed using a paired sample t-test with 95% confidence interval. Differences in the results were considered statistically significant when $p < 0.05$.

6.3. Results and Discussion

6.3.1. Correlation of NO_2^- Production and Power Distribution

Nitric oxide (NO) is synthesized intracellularly during the conversion of L-arginine into L-citrulline in the presence of oxygen (O_2) catalyzed by the enzyme Nitric Oxide Synthase (NOS) [223, 224]. NO is a lipophilic free radical which is chemically unstable formed when N_2 reacts with O_2 [225] with a very short half-life of approximately 3-30 seconds [223]. Endothelium-

derived NO however has an very short half-life of 3-5 seconds and quickly forms nitrates and nitrites [226, 227]. NO is an important intracellular and intercellular signaling molecule involved in regulation of cardiovascular, nervous and immunological function [228]. NO regulates vascular tone, endothelial permeability, smooth muscle cell proliferation, platelet aggregation, and other functions [228, 229]. Nitrites (NO_2^-) are generated readily in a solution of aqueous media by oxidation of NO [230] by O_3 or O_2^-. For this reason, the production of extracellular nitric oxide (NO) following exposure to cold plasma was determined by measuring the accumulation of NO_2^-, the stable metabolite of NO, secreted in the culture media to provide evidence of Reactive Nitrogen Species (RNS) being produced by the plasma source [231, 232].

The correlation of nitrite formation to power consumption we used a two electrode configuration wherein the actuator consisted two exposed electrodes with a single encapsulated electrode on the opposite side of the dielectric. The plasma was generated between the two exposed electrodes and HUVEC media (without cells) in a 6 well plate was exposed to plasma at approximately 1 cm from the actuator for a treatment time of 2 minutes. The power per unit length was varied by changng the length of the electrodes. Three different actuators, as mentioned in the previous section, with different power densities, were tested as shown in **Figure 2 (a)**. It was observed that the nitrite concentration increased with the increase in the power and was maximum for the highest power per unit length with a value of approximately 266 μM. This suggested a direct correlation of power with nitrite generation, and hence was an indicator that higher NO could be generated with a high power input. These results agree with the findings of Pavlovich *et al.* who suggested a transition to higher NOx phase with increased power density [18].

6.3.2. Correlation of NO_2^- Production and Bacterial Inactivation

The correlation of NO generation and the reduction in bacterial concentration was investigated using a five strain mixture of *Listeria monocytogenes*. As explained in the materials and methods, actuators were developed and exposure to plasma was for a period of 2 minutes and at 1 cm from the samples. It was observed that the nitrite concentration decreased with the number of electrodes, as the power per unit length decreased (**Figure 2(b)**). A slight increase was observed with the 7 electrode configuration, as compared to 4 electrode, which may be attributed to an increase in the plasma volume (albeit at lower power density).

The reduction in the bacterial load however showed an opposite trend, with an increase in logarithmic reduction with an increase in the number of electrodes (decrease in power per unit length) for the same power input. A complete inactivation of the bacterial cells was observed with the 4 and 7 electrode configurations with more than a 5 $Log_{10}(10)$ reduction. This suggested that there is no clear correlation of nitrite production, and hence NO, on the effect of bacterial reduction. A lower power density still produced a higher reduction in the *Listeria monocytogenes* which is opposed to what was seen by Pavlovich *et al.* as a transition from low power to high power regime [21]. Hence, making the results a function of design of the device as observed by other groups [18, 112, 140, 147]. The 2 electrode configuration had a power per unit length of 93.75 W/cm, as compared to the 15.63 W/cm in the 7 electrode configuration. The increase in decontamination effects with increase in the number of electrodes may be a consequence of overall increase in the relative densities of different plasma species as a result of increased plasma volume. The results do suggest that the low power, large plasma volume regime may be a better approach for sterilization and decontamination applications, thus making possible development of low power plasma devices for decontamination applications.

As all tests were carried out after sufficient drying of bacteria on glass coverslips the results observed were on a dry surface, hence, ruling out effects of moisture. However, the humidity and presence of moisture on the cellular level cannot be ruled out and further analysis is required to quantify their effect as we did observe OH radicals, through Optical Emission Spectroscopy (OES), from our previous studies [179].

6.3.3. Correlation of Ion Density and Bacterial Inactivation

The investigation of the role of ions in the plasma decontamination process a plasma actuator (four electrode configuration) was tested to observe the logarithmic reduction in the microbial load with the increase in distance from the sample (**Figure 1**). The 4 electrode configuration was used as a substantial reduction was observed with bacteria as compared to the 2 electrode configuration. It was observed that the logarithmic reduction in the bioburden decreased with the increase in distance between the sample and the actuator from 1-7 cm. This was correlated with the ion flux at these respective distances. It was observed that the ion densities decreased from approximately 2200 ions/cm^3 to 400 ions/cm^3 (negative charge). Ion density is highest in the plasma region and drops drastically beyond this region (**Figure 3**). These ions and electrons transfer energy to radicals and metastables that are responsible for microbial inactivation. The increase in metastable molecules (Ozone) was measured and was observed to increase beyond 0.14 ppm within 10 seconds. Data is shown for 4 min of exposure to plasma.

Negative ions were detected which in accord with the results demonstrated by Likhanskii *et al* [233] which may be attributed to the travel of secondary electrons and formation of the negative ion cloud near the actuator. Unlike previous work wherein a grounded, biased electrode was used [234], the steady mode of the air ion counter enabled measurement of ions convected

only by the flow induced by the plasma actuator. This prevented any biased extraction of ions from the surface of the plasma actuator.

The effects of increase in plasma volume and area was investigated by varying the number of electrodes between 2, 4 and 7. Observations were made at 1 cm for each of these actuators as it was the zone for highest ion density. It was observed that logarithmic reduction increased with the increase in electrodes for the same power input and complete inactivation was observed within 2 minutes of treatment with 7 electrode arrangement as seen in **Figure 2 (b)**. The magnitude of ions however was the same order of magnitude (~ 10^3 -10^4) for 2, 4 and 7 electrodes, which suggests that the ion density does not change enough to associate the logarithmic reduction to presence of ions. Hence, this may suggest that beyond the plasma region ions may have a synergistic effect close to the actuators but their concentration drops exponentially as distance from the plasma region increases and the plasma effects are dominated by ROS.

6.3.4. Evaluation of Conductivity for Ion Detection

Increased conductivity of plasma treated liquids corresponds with increased abundance of diffused ions in the liquid. An altered ion concentration in the media in which treated cells are suspended may contribute to the observed cellular responses, but the effect may be negligible unless a significant increase in ion concentration was observed.

The lifespan of ions were measured in Deionized (DI) water by observing the change in conductivity (**Figure 4**). The conductivity was measured in case of untreated media, and was found to be beyond the range of the instrument as compared to the readings in DI water post treatment which were nominal. The ionic perturbations were observed to be nominal in deionized media as compared to the the media because of the presence of electrolytes of sodium and potassium. Hence the effects of ions may be discounted as the conductivity observed in the DI water is very low and

may be due to the carbonic or nitric and nitrous acid species generated by presence of plasma generated reactive oxygen and nitrogen species. Another theoretical possibility is the generation of acidic H_3O^+ ions by reactions of the water molecules with H_2O_2 [235]. Untreated DI water retained a conductivity of 0 mS/cm3 even at 24 hours. The absence of change in the perturbations introduced in the conductivity of DI water post treatment for 24 hours however shows that the conductivity so created is a consequence of aforementioned oxygen and nitrogen species rather than ions which have a life span on the order of nanoseconds to milliseconds [139, 140]. Other groups have noticed the increase in acidity and have reported formation of nitrous (HNO_2) and nitric (HNO_3) acid along with H_2O_2 in unbuffered water [20, 147]. In our previous work we noticed a similar drop in pH [179] and attributed the same to formation of HNO_2 and HNO_3 along with carbonic acid (H_2CO_3) as being responsible not only for the decrease in the pH, but also the increase in conductivity due to dissociation of these acids. Antimicrobial acidified aqueous nitrate and nitrite anions have been shown to form when water is exposed to atmospheric plasmas [147, 236], which further coroborates the theory of acidification of the DI water.

We did not observe any substantial increase in ionic perturbations (conductivity) with the increase in number of electrodes. This suggests ions have little contribution to the cellular interaction and relates more to formation of nitrites and increase in oxidative species which also contribute to a decrease in pH. It was seen that the pH dropped from 7 to 3.6, 3.6 and 3.4 when exposed to plasma with the 2, 4 and 7 electrode configurations, respectively, with a 2 minute treatment at 1 cm, which remained constant over a period of 24 hours. The drop in pH suggests formation of nitrous acid [20] as evident fron the nitrite production and H_2O_2, a weak acid, which coroborates the theory as elucidated by Kono *et al*. on the synergystic antimicrobial effects of NO_2^-, H_2O_2 and low pH [236, 237]. This is another example of how device design effects device

performance evident from the difference in trends of pH change observed here and that observed by Kojtari *et al* [238]. A time course analysis is required for each of the electrode arrangements to ascertain the effect on change in pH. Hence, in an aqueous medium the ions do not contribute due to their low lifespans on the order of nanoseconds and also their inability to travel across the cell membrane due to the presence of charge, such as in the case of O_2^-.

6.3.5. Evaluation of Role of RNS and ROS in Cellular Response

The analysis of the impact of RNS and ROS without the interference of ions we used HUVEC cells to observe the effects of each of these components leveraging the use of scavengers to better investigate the role of each species (**Figure 5**). The schematic in **Figure 5** shows how the two scavengers for RNS and ROS, namely cPTIO and NAC, interact with these species respectively. First, a nitronyl nitroxide, 2-4-carboxyphenyl-4,4,5,5-tetramethylimidazoline-1-oxyl-3-oxide or cPTIO, was used as a NO scavenger. Nitronyl nitroxides such as cPTIO are generally used as spin traps in Electron Spin Resonance (ESR) [239-242]. Nitronyl nitroxides inhibit NO radical effects by oxidative transformation of NO to nitric dioxide (NO_2) and imino nitroxides [243]. Carboxy- PTIO is a water soluble NO scavenger and is known to show protective effects against NO radical in diseases such as focal cerebral ischemia [244-246]. The nitrite concentration was observed to be higher for the plasma treated samples without the scavenger (cPTIO) as compared to the other samples which is in accordance with the claims of its nature to scavenge for NO. 100 µM of carboxy-PTIO was used as it was found to be effective in mitigating the effects of both extracellular as well as intracellular NO without any effects on the cells themselves [217, 222].

In plasma, NO_2 produced by NO and ozone (O_3) reacts with H_2O to form NO_2^- and NO_3^- [19].

$NO + O_3 \rightarrow NO_2 + O_2$

$2NO_2 + H_2O \rightarrow HNO_2(aq) + HNO_3(aq)$

As nitrites are the most stable metabolite form of NO in an aqueous medium and are easily measured using the Griess assay [232, 247, 248]. One might be compelled to think that these nitrites may be the mostly a result of Nitric oxide synthase activity in the HUVEC cells, but from viability studies [179] we have seen a high viability at 4 min of plasma exposure.

The concentration of nitrite in the samples without the scavenger was found to be almost 10 fold of that with the scavenger (**Figure 6**), which indicates that the nitrite concentration is due to NO conversion to nitrites and is the concentration detected in the supernatant. The controls (no plasma exposure) with and without the scavenger had almost no signs of nitrite formation, which was constant for all the time points. Soon after the plasma exposure (30 min) the nitrite concentration was observed to be as high as 195 µM which reduced to approximately 130 µM at one hour and stabilized to approximately 100- 110 µM at the end of 24 hours.

We confirmed that the concentration of NO_2^- generated was not solely produced by HUVEC cells via NOS enzyme activity by repeating the treatment for media devoid of HUVEC cells. A similar trend in the decrease of nitrite concentration was observed as that of samples without the scavenger cPTIO. It was observed that the nitrite concentration was high soon after the plasma treatment at the 30 minute time period of around 70 µM, but, was found to reduce over time to around 18 µM over a period of 24 hours. This suggests that most of the nitrites, and hence, the NO may be synthesized due to NOS activity as the cells experience oxidative stress due to ROS.

The change in pH as seen in our previous work [179] also shows that the nitrites may not represent the complete concentration of NO generated species and some may be involved in the formation of Nitric or Nitrous acid [57, 112, 120] as mentioned earlier. In an acidic environment nitrites can also produce peroxynitrous acid (ONOOH), formed in the presence of NO_2^- and O_2^- in an acidic environment, and nitrous acid (HNO_2) [120]. The ROS can also interact with NO to produce other species responsible for the reduced pH as seen from the experiments with DI water. The media however is buffered and hence may not display a high enough pH change as seen earlier [179].

The extent of oxidative stress experienced by a cell depends on the rate at which O_2^- and H_2O_2 are made inside the cell [146] and this was explored using carboxy-H_2DCF-DA. These products are further responsible for the generation of the more potent hydroxyl radical (OH^*) through pathways such as the Fenton reaction which in turn effects the cells on various intracellular levels including damage to DNA proteins [146]. The rate of production of O_2^- and H_2O_2 depends on the frequency of the collision between the cells internal enzymes and oxygen, thus is directly dependent on the oxygen concentration experienced by the cells [146]. The intensity of fluorescence depends on the amount of oxidative stress or in this case oxidative species created in the cell and is represented by the oxidation of the dye.

NAC, being a scavenger for oxygen free radicals, interacts directly with reactive oxygen species and reactive nitrogen species [249]. Antioxidant mechanisms are based on acting as blockers for processes involving free radicals. In a normal sequence of metabolic events, the superoxide radical (O_2^-) is formed by the addition of one electron to molecular oxygen (O_2). As mentioned, O_2^- by itself cannot permeate through cell membrane, but in acidic conditions of low

pH, it forms hydroperoxyl radical (HO_2^*) which can enter cells easily. The addition of two electrons to oxygen leads to the formation of hydrogen peroxide (H_2O_2). H_2O_2 forms mostly by dismutation of superoxide radical especially in the presence of superoxide dismutase. H_2O_2 is stable and long lived and easily diffuses through the cell membrane. The addition of another electron to hydrogen peroxide forms the hydroxyl radical (OH). These radicals in turn if not reconverted to harmless metabolites, in large concentrations, result in oxidative stress.

The effect of ROS was observed through the oxidative stress response on HUVECs for various experimental conditions using the dye Carboxy-H_2DCF-DA (**Figure 7**). No significant ROS related stress was observed in any of the conditions except with plasma treatment. The positive control with 200 µM of H_2O_2 gave a response of oxidative stress in the cells similar to the plasma treated samples suggesting that over time the exposure to the ROS in the media due to plasma (or H_2O_2) results in oxidative stress, which increases over time. The fluorescence intensity recorded was highest at 24 hours after exposure, which suggests an opposite trend as compared to the results obtained through Griess assay for nitrites suggesting that ROS are responsible for the long term effects observed in the cells, and not NO. The positive control and plasma treated samples show similar trends throughout the course of observation. The samples with NAC showed a lower intensity even at 24 hours suggesting that NAC is able to neutralize the plasma generated ROS, hence, decrease the ROS accumulation and oxidative stress experienced by the cells. The plasma treated sample with NAC, however, shows a slightly higher intensity at 24 hours similar to the other samples subjected to ROS formation. This supports our hypothesis that ROS may be the key factor in plasma-cell interactions in case of SDBD. Fluorescent Micrographs (**Figure 8**) show the highest intensity for the plasma treated samples and the lowest for the controls (with NAC). Regular control without NAC (data not shown) did not show much difference from the

controls treated with NAC. The other samples showed intermediate fluorescence intensities. NAC was able to effectively able to reduce oxidative stress, and lower signal was observed from the samples treated with the same.

Antioxidants, such as NAC, intervene in these processes of ROS formation either on an intracellular or an extracellular level [250]. Since in this case the cells were pretreated with NAC which was then allowed to be retained in the media, it is assumed to act at both these levels. At the intracellular levels, NAC acts as a precursor of glutathione (GSH) synthesis by penetrating the cell where it is de-acetylated to form l-cysteine, hence aiding in the biosynthesis of glutathione peroxidase (GSH-Px) [250]. GSH-Px removes H_2O_2 by reducing GSH to glutathione disulfide (GS-SG) **(Figure 5)**. While on an extracellular level it acts as a nucleophile resulting in reduction of the oxidative species introduced by the plasma [15, 123, 217, 250]. The cyto-protective effect of NAC on renal injury has been demonstrated in various models and its ability to protect against cytotoxic injury is demonstrated by various authors [251-257]. Hence, we used NAC as a scavenger for ROS to examine the effects of ROS on HUVEC cells. The cyto-protective ability of NAC helped understand the presence of ROS and RNS, generated by reaction of ROS with NO species, through oxidative stress detection using carboxy-H_2DCF-DA. 5 mM of NAC was used as it was found to provide effective cyto-protective properties while the concentration was not cyto-toxic to the cells as seen from past literature [222, 258].

Extracellular ROS generation by SDBD plasma actuators was assessed with OES in our previous work, wherein the major oxidative species such as O_3, OH*, NO and O_2^+ were identified [179]. These species create ROS like H_2O_2 and HNO_2 in an aqueous medium [259].

$$OH + OH \rightarrow H_2O_2$$

Or

$HO_2 + HO_2 \rightarrow H_2O_2 + O_2$

Several authors have tried to validate the dominance of HNO_3 and H_2O_2 in the plasma interaction with cells especially in the generation of Plasma Activated Water (PAW) [20]. But the general observation was that these agents alone [260] or in combination did not give the same response as observed with plasma treatment [147, 238, 261], thus indicating a multicomponent chemical dynamic.

6.3.6. ROS detection and Plasma Effects on Bovine Muscle Tissue

The mechanism being dominated by ROS and oxygen based RNS, such as ONOOH, was elucidated by treating and assessing muscle tissue with plasma. It was observed that the plasma was unable to inactivate any pathogens and no logarithmic reduction was observed on the inoculated samples. However, the texture and color of the meat changed from bright red to a rustic brown demonstrating oxidation. The lack in visible reduction in the pathogen may be attributed to the surface roughness [262], porosity and presence of components like myoglobin with an affinity to be oxidized by ROS. Pavlovich *et al.* observed similar results with pig skin with a low reduction in *E. coli* concentration as compared to other substrates [18]. Further investigation of the observed phenomenon of change in the color of the meat was done by treating the samples with plasma, with and without NAC (**Figure 9)**. The controls consisted of meat samples with and without a coat of 5mM NAC which were not exposed to plasma (**Figure 9(a)**). No visual detrimental effect of NAC was observed on the tissue (**Figure 9(c)**). The other samples (with and without 5mM NAC) were exposed to plasma to observe visual change in texture and appearance. The sample exposed

to plasma showed close to no change in color while the samples exposed to plasma that did not have a coat of NAC changed quickly from a bright red to a rustic brown color (chocolate brown), with a change in texture which appeared to be wrinkled, as shown in **Figure 9 (b)**. This is also a characteristic of oxidation of oxymyoglobin (OxyMb) to form methemoglobin (MetHb) by species like NO [230], thus indicative reactive oxygen species like ozone producing oxygen stress. Hence, it can be seen that the plasma effects are dominated by ROS beyond the plasma region. This phenomenon may also be attributed to the higher concentration of iron in this tissue in the form of oxymyoglobin (or oxyhemoglobin) which when oxidized produced this color change (formation of NO_3^- from NO_2^-) [263]. Tang *et al* [264] reported a similar trend that adding glutathione to bovine muscle cytosol improved oxymyoglobin redox stability. Further analysis of the tissue sample is required for a histology all affirmation of the phenomenon.

6.4. Conclusion

Cold plasmas display a synergistic effect of a multi-component chemistry comprising of heat, charged particles (ions), reactive oxygen species (ROS), reactive nitrogen species (RNS), and UV radiation. ROS and RNS, along with other charged particles, have been implicated for the response seen with non-thermal plasmas [12, 62, 173]. However, UV radiation and heat do not play a major role in these processes. Most bacteria are very sensitive to ROS poisoning [265]. Also, the role of oxygen radicals in plasma sterilization has been justified by the rate of inactivation obtained in air or oxygen plasmas being several times faster than in noble gases [12]. A differential response has been observed by researchers between prokaryotes and eukaryotes [123, 210] as well as amongst different types of Eukaryotic cells [179]. A similar differential response has been observed between eukaryotic cells and cancer cells [266], attributed to the Warburg effect, by

which cancer cells are damaged by ROS due to their reliance on aerobic metabolism [267, 268]. Based on this benefit a selective treatment of cancer cells versus healthy mammalian cells can be achieved [182, 203, 216]. Same is the case for prokaryotic cells and their structural differences from mammalian cells[210]. RNS species such as Nitric oxide play a key (indirect or direct) role in microbial and tumor mitigation [269].

The results suggest that NO is not the primary component in the bacterial inactivation and for decontamination application a low power, higher plasma volume design would be prefered. The ion density is higher when the sample is in the plasma region and drops further away from the actuators, plasma effects are dominated by ROS rather than ions at further distance. Placing the samples closer to plasma region provides a higher synergistic effect between the ROS and ions, as compared to higher distances. ROS dominance is also demonstrated by the results observed with the scavengers and results obtained with muscle tissue. However, the effects of ions may be discounted in aqueos meduiums as seen by the effects on conductivity. Acidification plays a major role in aqueos enviroments as seen from the rapid decrease in the pH.

Other groups have reported that besides acidification and nitrate as well as nitrite generation, increase of hydrogen peroxide concentration was found as a result of plasma treatment of liquids [147]. It is postulating a central role of the O_2^- radical as antimicrobial agent. hydroperoxyl radical (HO_2) [121, 270], which is able to penetrate microorganism cell membrane and even oxidants like peroxynitrite ($ONOO^-$) as a result of NO reaction with superoxide radical (O_2^-) [271, 272]. Identifying and quantifying the ROS will help further tune the system for higher precision and effective application. As plasmas provide a surface treatment effect rather than a bulk effect, it will be beneficial to tune the system for etching like capabilities providing an exact

approach. A deeper understanding of the utilization of the flow induction capabilities of SDBD for long range applications need to be investigated, and will be looked into detail in the future.

Nitrites may be beneficial in higher concentrations for wound care applications such as acidified nitrite creams for topical NO donating wound healing agents [273] and surface disinfection for even robust strains like *C. difficile* spores [274]. Kono *et al*. elucidate the synergystic antimicrobial effects of NO_2^-, H_2O_2 and low pH [237]. Direct plasma exposure methods such as volumetric DBD may cause tissue damage, such as that seen by Pavlovich *et al.* on pig skin, along with a possibility of non- uniform treatment [18]. Hence, the semidirect method of plasma exposure used in this work is a good alternative with capabilities of flow control to push the generated plasma species to the surface being treated and also manipulate the species being generated by changing plasma parameters, thus providing the desired effect such as sterilization or wound healing. It may also be possible to create a device which can, for the same power input, generate required effects such as higher NO production for wound healing or sterilization just by changing the electrode configuration. The selectivity and tuning capabilities offered by this technology can help better tackle issues like antimicrobial resistance, chronic wounds and sterilization of other surfaces, both organic as well as inorganic. Being a multicomponent system, makes SDBD a viable candidate for innumerable applications specially sterilization and wound care.

.

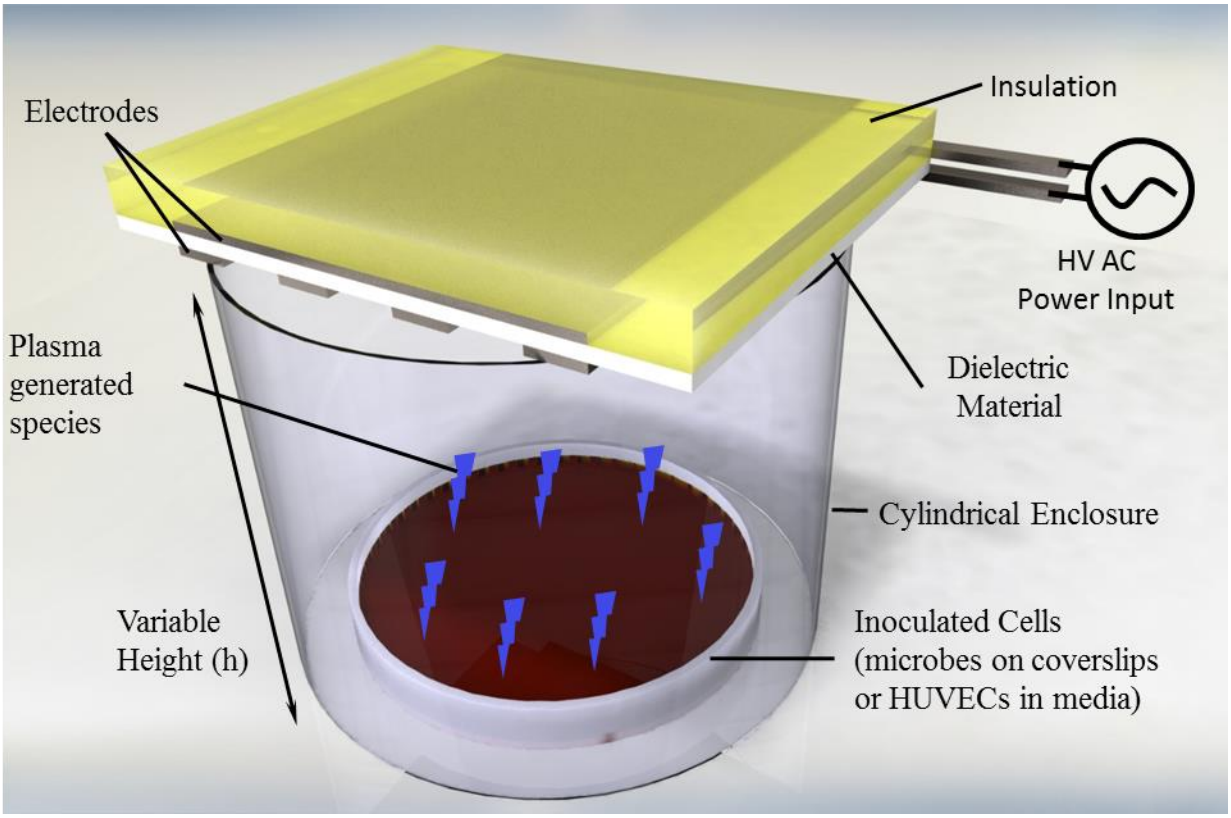

Figure 1 Schematic showing differential height treatment for the prokaryotic and Eukaryotic cells

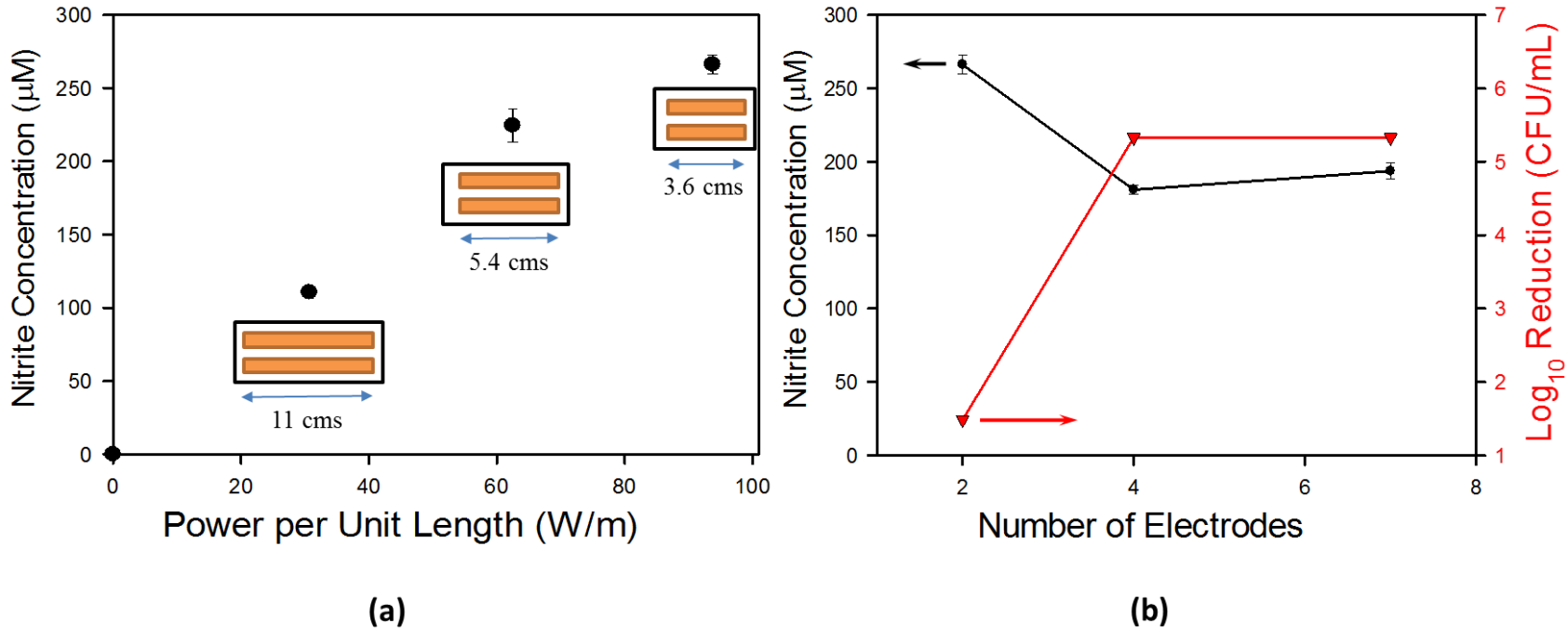

Figure 2 (a) Correlation of power density per unit length of electrode to nitrite production using two electrode configuration by changing the electrode length; (b)Correlation of reduction in Listeria monocytogenes (5 strain mixture) with increase in number of electrodes for the same power density, with production of nitrites.

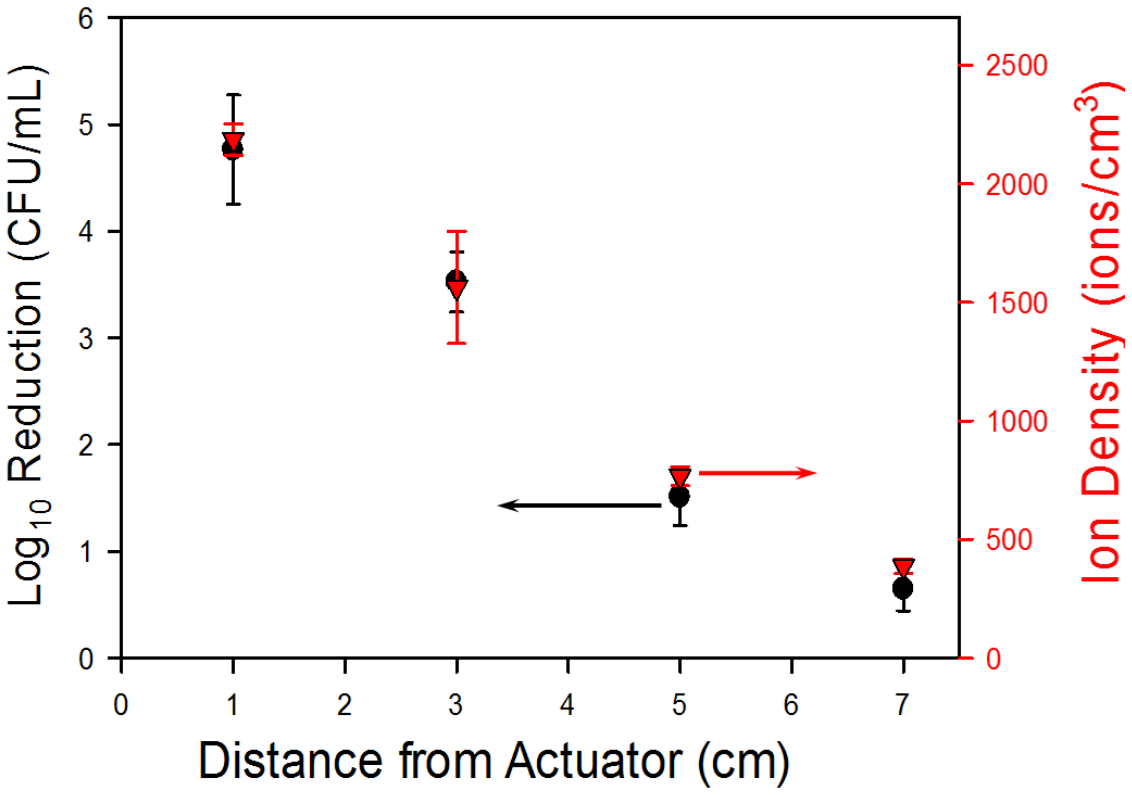

Figure 3 Correlation of change ion density and reduction in concentration of Listeria monocytogenes (5 strain mixture), with distance from plasma actuator using a four electrode configuration.

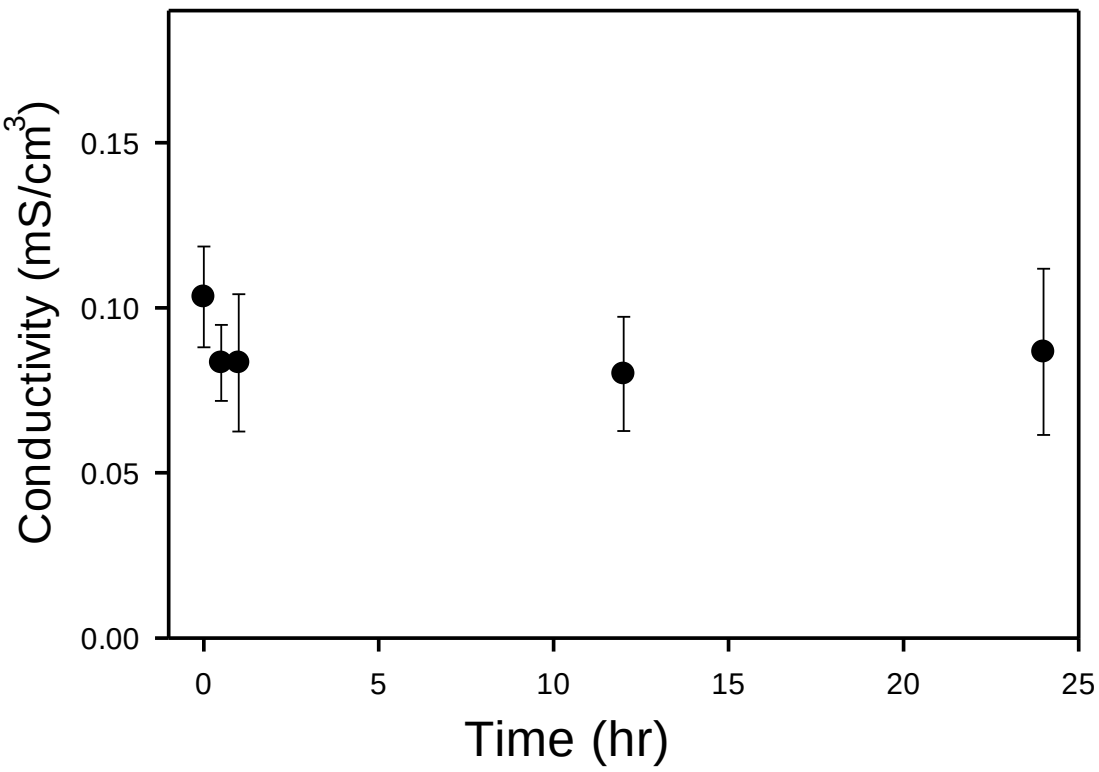

Figure 4 Change in conductivity of deionized water after a 4 minute treatment with plasma actuator using a two electrode configuration over time (24 hrs).

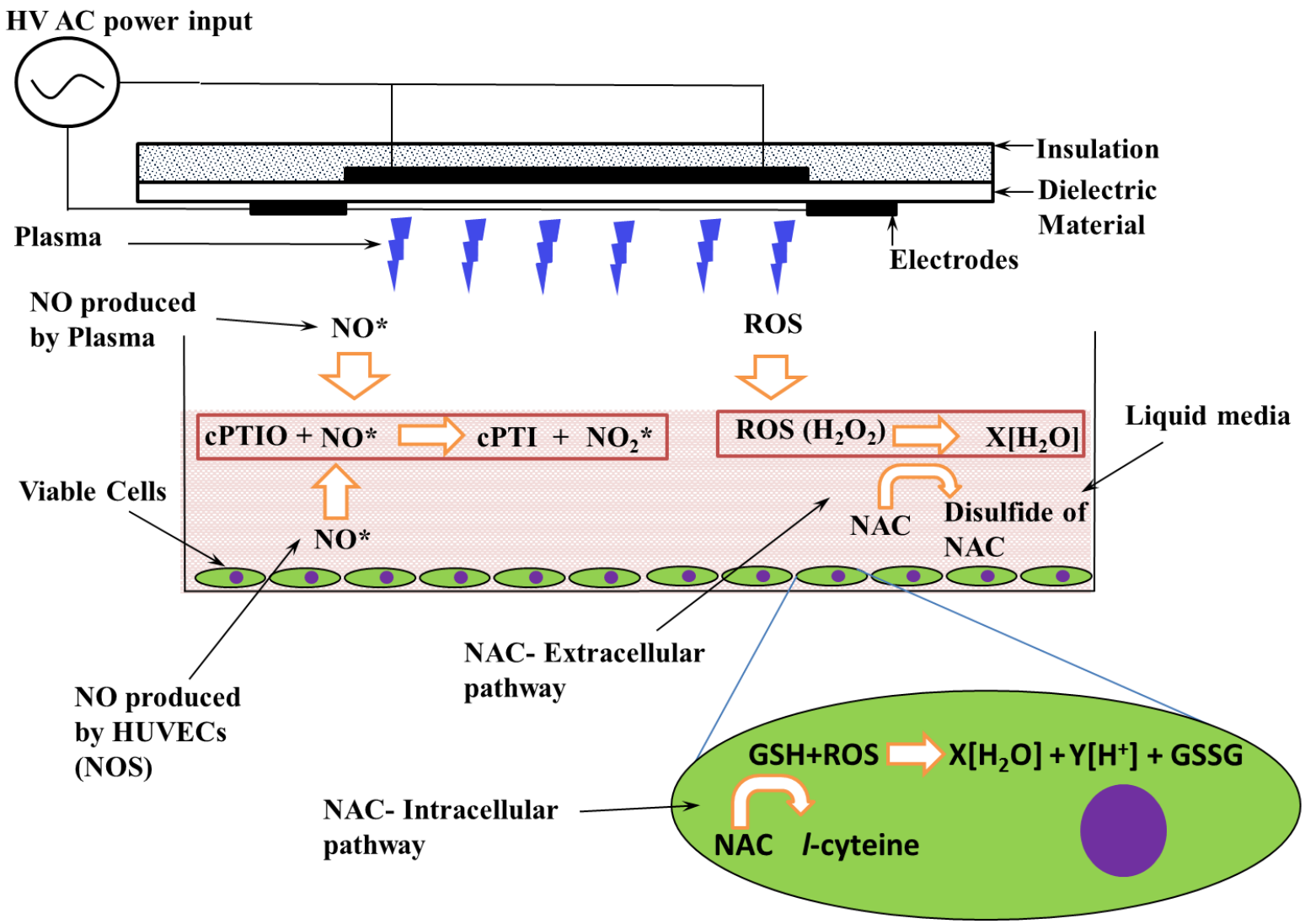

Figure 5 Schematic showing the cytoprotective interactions of ROS scavenger NAC (5mM) with different ROS species (both intracellular and extracellular mechanisms) and NO with NO scavenger cPTIO (100 µM) respectively.

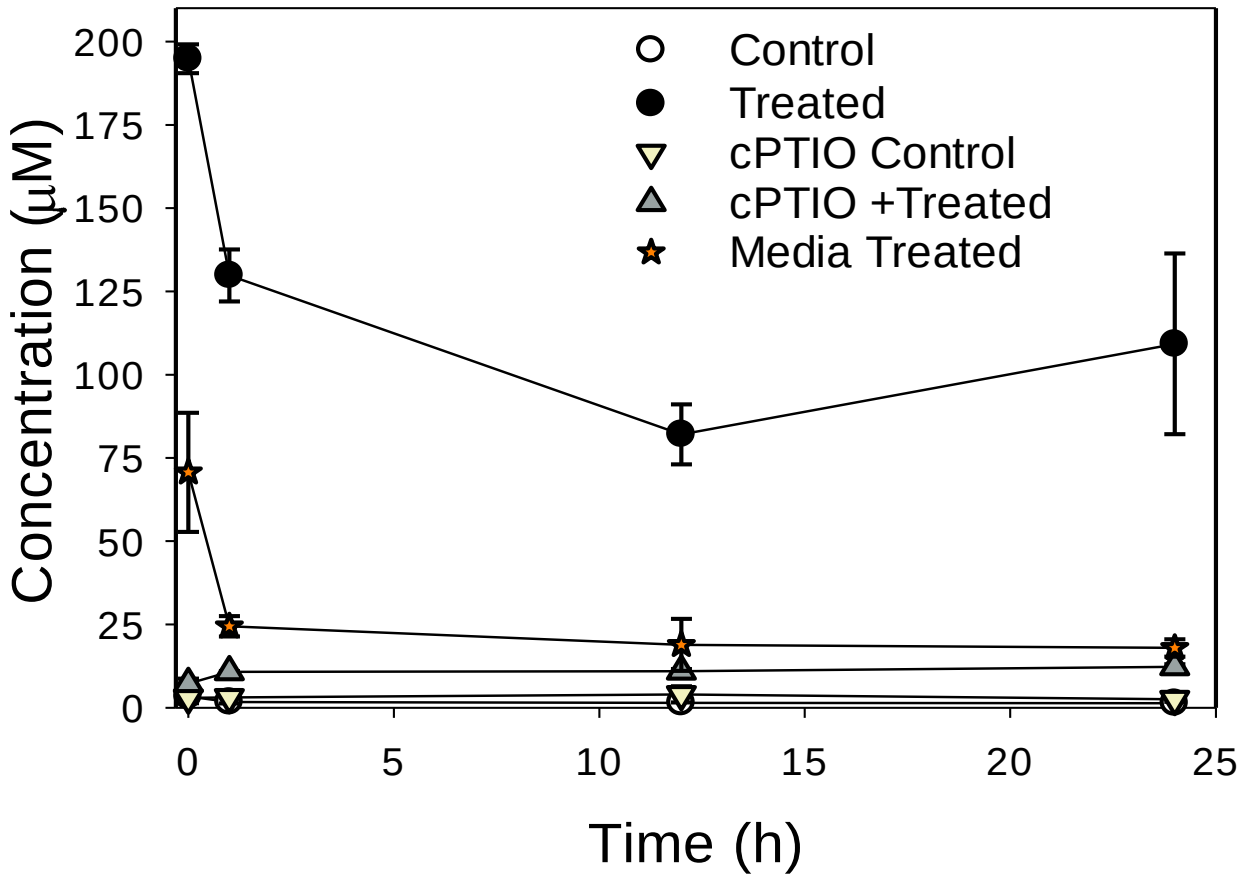

Figure 6 Analysis of plasma induced nitrite concentration as a indicator for NO generation, with and without NO scavenger cPTIO.

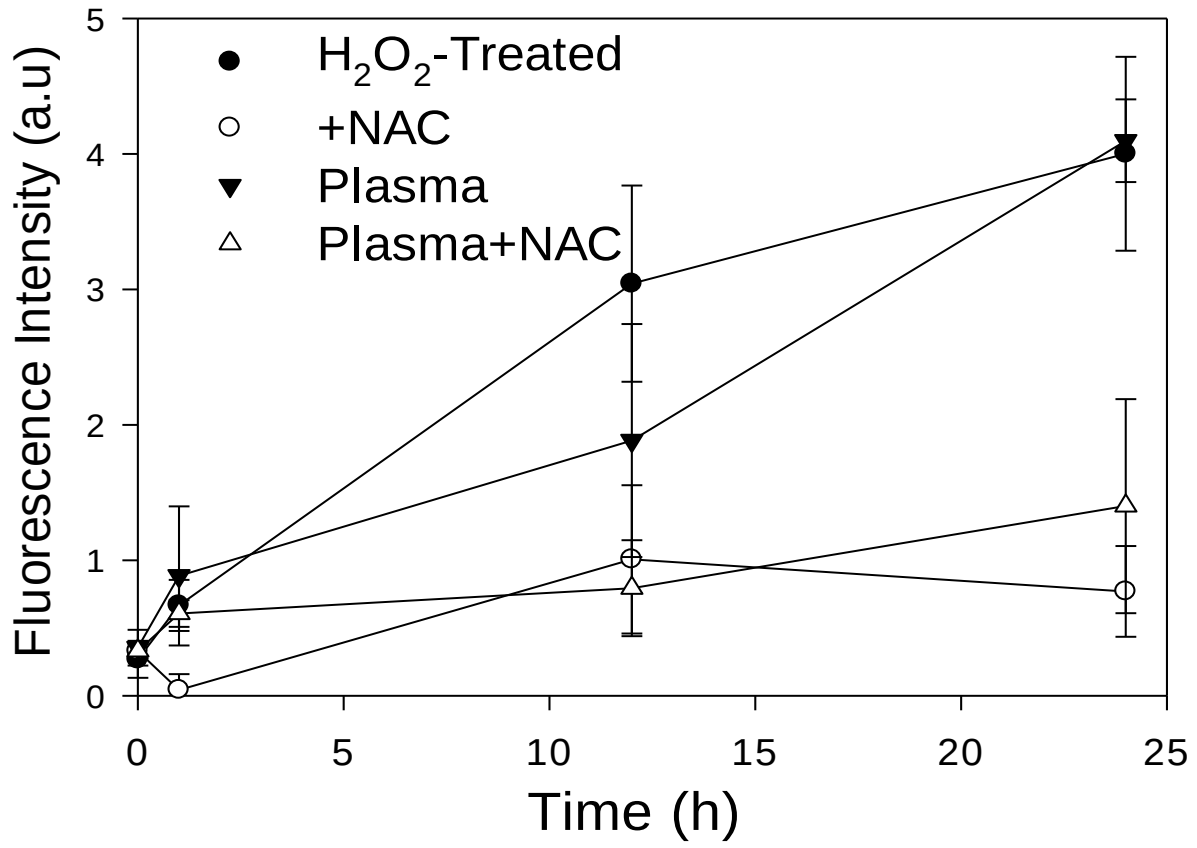

Figure 7 Analysis of plasma induced intracellular ROS (Oxidative stress response) as a indicator for ROS generation, with and without ROS scavenger NAC (5mM).

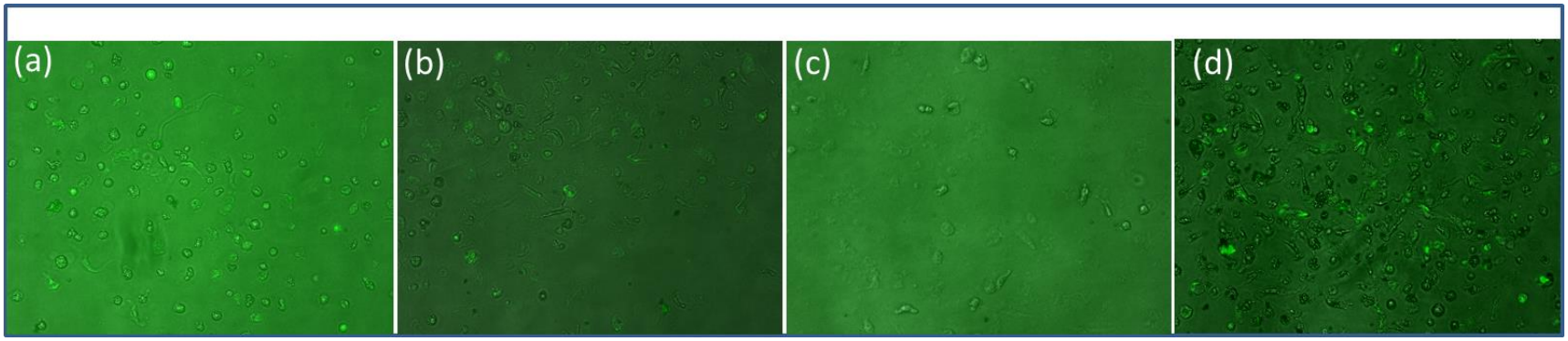

Figure 8 Fluorescent micrographs of HUVECs representing oxidative stress response to plasma with and without ROS scavenger NAC (5mM). (a) Plasma treated HUVECs; (b) Plasma treated HUVECs with NAC (5mM); (c) Positive control (200 µM H2O2); (d) untreated control with NAC (5mM).

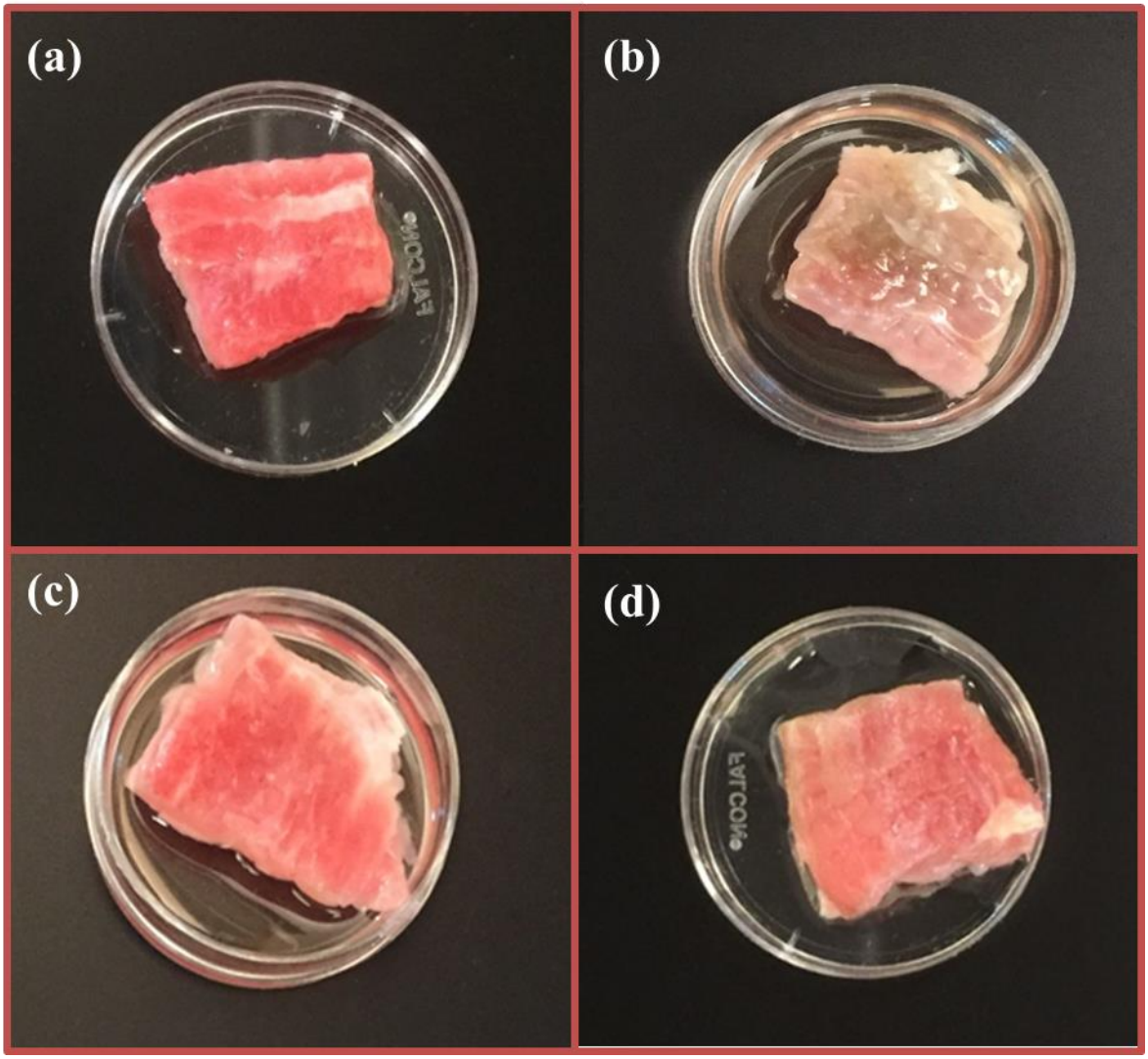

Figure 9 Effects of plasma exposure on bovine muscle tissue; (a) control (no NAC); (b) plasma treated (no NAC); (c) control (with 5mM NAC);(d) plasma treated sample (with 5mM NAC).

Chapter 7

Conclusion

7.1. Overall Conclusions

In this chapter we summarize the conclusion derived for each chapter and the future work required for implementation of SDBD technology in biological sterilization. The asymmetric arrangement of electrodes in SDBD plasma actuators was studied to understand its scaling principles and efficacy in applications of decontamination. The effect of this design was also tested against different types of Eukaryotic cells to understand the selective response based on dose. The primary plasma generated agent responsible for plasma interaction with cells for SDBD was also identified and validated.

In the chapter 2, an analysis for scaling a SDBD plasma actuator was conducted wherein investigated the impact of change in length and increase in the number of electrodes of same length on input voltage. A linear trend was observed in both the cases. An increase in width of electrode has no effect on input voltage. However, an increase in the width helped better spread of plasma over the dielectric chord-wise. It was also observed that the input voltage was a function of total length of the electrodes i.e. the sum of all the exposed or encapsulated electrodes. The voltage requirement however dropped when the total length of the encapsulated electrode was lower than the single SDBD counterpart of the multiple electrode array. This was seen to be a difference of

greater than 2.5 cm. This also showed that the change in requirement for input voltage for minor changes in length of electrode may be low and can be proven with a higher resolution input setup for voltage. Thus, we see that the design of an SDBD actuator has a specific relationship with the length of the electrodes and the power required to produce plasma. We also see that there is a specific window of voltage that can be utilized for effective use of asymmetric SDBD plasma actuators outside which there is either non-uniform plasma generation or the energy is lost as heat.

In chapter 3, two designs of SDBD plasma actuators with asymmetric and symmetric arrangement of electrodes were evaluated for their effectiveness in killing bacteria. The results indicated that an asymmetric arrangement of electrodes was around 2.5 orders of magnitude more effective in inactivation of *L. monocytogenes* and is promising for applications in the industrial environment. It was pointed out that the design of the actuator and the electrode arrangement is a key factor in low cost plasma based decontamination. The flexibility in design (planar or non-planar), and the ability to induce plasma flow gives the asymmetric arrangement an edge over other methods of plasma based decontamination. The effectiveness of the plasma actuator in inactivating bacteria related the effective log reduction of CFU/ml with the distance from the sample at a given time of exposure (4 min) and demonstrated that the potency of SDBD related reduction of bacterial load reduces with distance from the actuator. Hence, further investigation is required to determine the factors responsible for plasma based decontamination by SDBD and to design an optimized actuator for a more penetrative design for large distance (from sample) applications. A proper matrix describing the relation between bacterial load, power, distance from sample and time is required to optimize this design for large scale applications.

In Chapter 4, three different types of mammalian cells, namely HUVEC, neuroblastoma

and HepG2, were exposed to plasma using a SDBD plasma actuator. The effects on cell morphology, viability and functionality were tested using an inverted light microscopy, fluorescence microscopy, live/dead assay and migration assay respectively. It was noticed that increased exposure time resulted in detachment and clumping of cells showing signs of oxidative stress. The migration assay also confirmed that the cells maintain good functionality up to a level of 4 minutes of plasma exposure, which suggested that for applications of wound healing and cell manipulation the SDBD mode of plasma treatment is non-lethal to human cells at longer treatment durations. However, we found that different mammalian cell types respond to plasma exposure to different degrees as seen from the variation in response in viability between HUVEC, neuroblastoma and HepG2 cells. Hence, there is a need to create a matrix of nonlethal doses for possible applications such as cancer cell treatment, so as to avoid necrosis and inflammatory responses in neighboring cells. In the case of wound decontamination applications this study enables us to understand what the impact would be on exposed tissue and nerve endings and helps better design and optimizes the plasma apparatus parameters.

An investigation of the OES showed the predominant species to be oxygen and nitrogen based. An analysis of the change in induced pH did not reveal a major role of pH change in cell damage, but further investigation is required to rule out involvement, as buffers in the media may act as neutralizers. We hypothesize that the exposure to ROS and RNS species may be the factors causing oxidative stress as evidenced by the change in morphology of the cells. We demonstrated that the SDBD plasma actuators provide a uniform treatment without any use of external gas flow due to the innate ability of this design to induce flow. It also has the advantage of being able to be easily scaled by changing the design of the electrodes and size of the actuator, thus making it applicable for larger surface treatment.

In Chapter 5, we studied the role of each component involved in the interaction of SDBD plasma with the different cells. The role of ions, RNS and ROS was investigated using prokaryotic and eukaryotic cells. The ion densities were observed to be low (~ 10^3) and decreased with distance of the sample from the actuators. A similar trend was observed with the bacterial inactivation which correlated well with these findings. This suggested that ions may not be the primary components in plasma-cell interactions, however, may have a synergistic effect with other species like RNS and ROS in non-aqueous environments. In aqueous environments however, this was not the case and RNS and ROS were seen to be predominant, which was observed by monitoring the conductivity of DI water after plasma treatment. A change in pH suggested the formation of various acids. It was observed that RNS, namely NO, did not play the primary role in bacterial cell inactivation, however the NO concentration did increase with power per unit length of electrode. ROS were found to be the primary components responsible for plasma cell interaction both in prokaryotic as well as eukaryotic systems. This was established using fluorescence assays and oxidative response on muscle tissue, leveraging certain ROS and RNS scavengers. It was identified that a low power, high volume plasma regime was an optimal solution for bacterial inactivation and cell interaction, specifically for designing an efficient device for decontamination. **Figure 1** summarizes our findings based on the results of this research. The weightage of the arrows in **Figure 1** show the contribution and dominance in the process as distance between the actuator and the sample increases. The trends and responses of various cell types as observed through our experiments is also demonstrated through graphical means, to give a relative idea demonstrating our results. A similar trend with change in the number of electrodes with constant distance between the sample and the actuator is also illustrated. This figure illustrates the finding in a more visual fashion.

7.2. Significance

This research significantly advances the understanding of SDBD plasma, specifically asymmetrically arrangements of electrodes, and their interaction with various cells. The following conclusions were derived from this research:

- Scaling parameters of the SDBD plasma actuator are identified and assessed, showing that input voltage is scaled as an arithmetic progression for increase in effective electrode length and is independent of width.

- Comparison and demonstration of performance asymmetric SDBD type plasma actuator is performed with observations of superior performance of the design as compared to symmetric SDBD actuator designs.

- Multiple strains of pathogen and mammalian cell lines are tested against chosen plasma generation method demonstrating a dose dependent response of different types of cells. Mammalian cells showing more resiliency against plasma treatment with retention of functionality at higher treatment times.

- The role of different plasma generated species was identified and ROS were found to be the primary agent of plasma- cell interactions in SDBD plasma, with synergy from charged particle at close proximities.

Elaborating further on these key findings, Chapter 2 helped add information on the impact of scaling of the SDBD plasma actuator design and understand the importance of power correlation with electrode dimensions so that the optimum regime of operation may be identified. In chapter 3 the flow characteristics of plasma have been analyzed in the past and herein we saw how they

influence effective bacterial inactivation. It was shown how the characteristic of inducing a flow helps better deliver plasma generated species without an assisted flow, thus, showing the viability of using SDBD plasma actuators for non-contact decontamination applications. In chapter 4 we demonstrated the importance of cell type and the dose dependency of cell response to plasma treatment. We also identified the major plasma generated species in this mode of plasma generation. This knowledge help better understand the importance of dose dependence in application of decontamination of various tissues. Chapter 5 helped identify the primary component responsible for plasma-cell interaction and also demonstrate that the response of the cells beyond being dependent on the dose is also dependent on the device used to generate plasma. Chapters 2 and 5 also help demonstrate that various plasma related effects such as NO generation can be obtained by changing the electrode designs. An example of this is seen from the trend in chapter 2, wherein the same volume of plasma can be obtained at lower power for an electrode arrangement with parallel electrodes as compared to its single arrangement counterpart (same effective electrode length but lower encapsulated electrode length). NO generation can also be controlled by changing power per unit length of electrode by either changing the length of electrodes or increasing the number of electrodes in the array on the actuator. Thus, this research helps fill the void in understanding of how the SDBD plasma generation method defers from other methods and what is the mode of interaction of this form of plasma generation for other methods. **Figure 2** shows the evolution of the species and their lifespans as they move away from the actuator into an aqueous medium. The proximity and the input parameters coupled with the induced flow together govern the efficacy of the plasma actuator. The figure shows trends that were seen with the results from chapters 4, 5 and 6. This is very important to understand the optimal zone of operation based on the life time of a species and can help better design certain type of

plasma based actuators.

7.3. Future work and Suggestions

This research illuminates the use of SDBD in applications of decontamination through better understanding of the factors responsible for plasma-cell interaction as well as device operation. However, further understanding is required for designing a complete device for efficient decontamination.

In chapter 2, we analyzed the impact of electrode dimensions on a linear and planar geometry. A much deeper understanding is required in terms of complex geometries, so as to develop universal scaling laws. The correlation of power requirements with these geometric changes will help better design actuators for various applications. As we saw from chapter 2 and chapter 5, there is a specific regime for plasma operation so as to efficiently generate plasma for specific applications (low flow or high flow, low NO or high NO, etc.). The correlations in the form of scaling laws will help better design devices for various applications.

From chapters 3, 4 and 5, it was also understood that a geometric arrangements also influence the induced flow, and thus, influence the distribution of plasma generated species from the plasma region to the sample. Hence, the influence of factors such as shape, intra-electrode gap (spacing between the exposed electrodes), electrode arrangement (concentric, three dimensional, etc.) needs to be investigated. Apart from this, the exact ROS responsible for plasma-cell interaction also need to be identified. This will add to the knowledge based of this technology and better design devices through optimization.

Asymmetric SDBD plasma actuators investigated in this study have proven effective in decontamination and further research will help develop this technology further and move from

laboratories to field applications such as hospitals and clinics. Development of proper testing protocols and quantification of various effects such as induction of flow and generation of specific species with input parameters such as power, will help develop better devices and scale them much easily. Through focused efforts on development of this technology there is an opportunity to change the landscape of the sterilization and decontamination industry for the better.

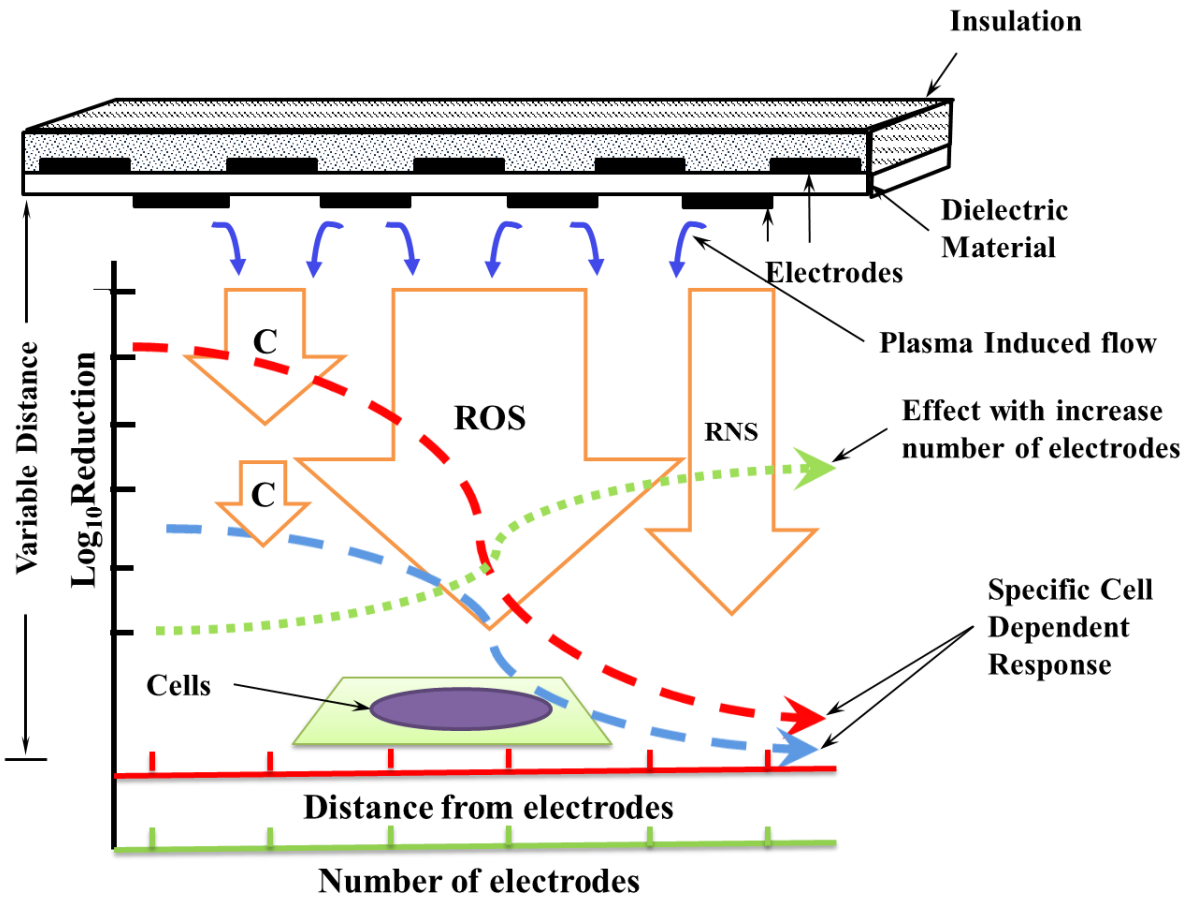

Figure 1 Schematic showing different components of plasma, their weightage (arrow width) in the decontamination process, and the cell specific response, where C= Charged ions; ROS= Reactive Oxygen Species, and RNS= Reactive Nitrogen Species.

Symbol	Species	Life span
e^-	Electron	Nanoseconds
⊕	Positive ion Eg. N^+, O^+	Microseconds to Seconds
●	Neutral species Eg. N, O, N_2^*	Microseconds to Seconds
⊖	Negative ions Eg. OH^-, O_2^-	Microseconds to Seconds
○	Reactive nitrogen species Eg. NO, NO_2	Seconds to Minutes
○	Reactive oxygen species Eg. O_3, OH	Seconds to Minutes
○	Reactive oxygen species (long lived) Eg, H_2O_2, HNO_2	Hours to Days

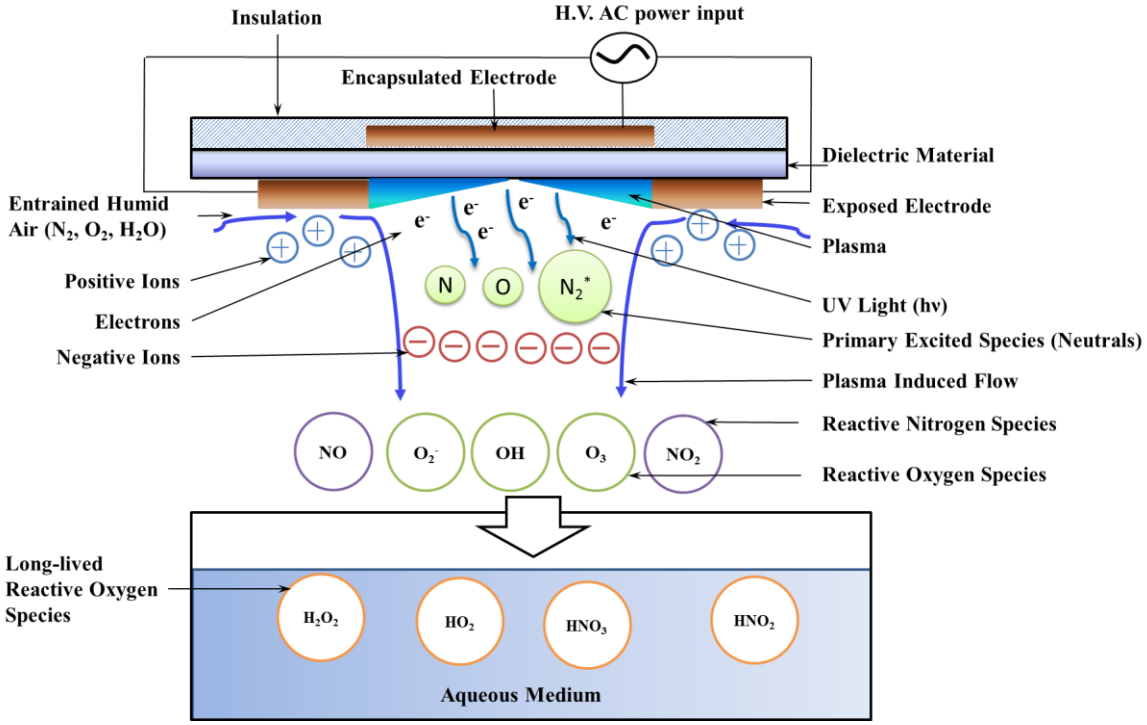

Figure 2 Schematic showing evolution of plasma species and their lifespans with an increase in distance from the actuator.

REFERENCES

1. Rutala, W.A., D.J. Weber, and C.f.D. Control, *Guideline for disinfection and sterilization in healthcare facilities, 2008*. 2008, Centers for Disease Control (US).
2. Bodenheimer, T. and H.H. Pham, *Primary care: current problems and proposed solutions.* Health Affairs, 2010. **29**(5): p. 799-805.
3. Ölmez, H. and U. Kretzschmar, *Potential alternative disinfection methods for organic fresh-cut industry for minimizing water consumption and environmental impact.* LWT-Food Science and Technology, 2009. **42**(3): p. 686-693.
4. Demirci, A. and M.O. Ngadi, *Microbial decontamination in the food industry: Novel methods and applications*. 2012: Elsevier.
5. *CDC Estimates of Foodborne Illness in the United States*. 2010.
6. Sung, S.-J., et al., *Sterilization effect of atmospheric pressure non-thermal air plasma on dental instruments.* The journal of advanced prosthodontics, 2013. **5**(1): p. 2-8.
7. Whittaker, A., et al., *Plasma cleaning of dental instruments.* Journal of Hospital Infection, 2004. **56**(1): p. 37-41.
8. Leipold, F., et al., *Decontamination of objects in a sealed container by means of atmospheric pressure plasmas.* Food Control, 2011. **22**(8): p. 1296-1301.

9. Maisch, T., et al., *Decolonisation of MRSA, S. aureus and E. coli by cold-atmospheric plasma using a porcine skin model in vitro.* PloS one, 2012. **7**(4): p. e34610.

10. Machala, Z., K. Hensel, and Y. Akishev, *Plasma for bio-decontamination, medicine and food security*. 2012: Springer Science & Business Media.

11. Becker, K.H., et al., *Non-equilibrium air plasmas at atmospheric pressure*. 2004: CRC press.

12. Laroussi, M. and F. Leipold, *Evaluation of the roles of reactive species, heat, and UV radiation in the inactivation of bacterial cells by air plasmas at atmospheric pressure.* Int. J. Mass Spectrom, 2004. **233**(1): p. 81-86.

13. Fridman, G., et al., *Comparison of direct and indirect effects of non-thermal atmospheric-pressure plasma on bacteria.* Plasma Processes and Polymers, 2007. **4**(4): p. 370-375.

14. Fridman, G., et al., *Applied plasma medicine.* Plasma Processes and Polymers, 2008. **5**(6): p. 503-533.

15. Brun, P., et al., *Helium Generated Cold Plasma Finely Regulates Activation of Human Fibroblast-Like Primary Cells.* 2014.

16. Nastuta, A.V., et al., *Stimulation of wound healing by helium atmospheric pressure plasma treatment.* Journal of Physics D: Applied Physics, 2011. **44**(10): p. 105204.

17. Kieft, I.E., et al., *Plasma treatment of mammalian vascular cells: a quantitative description.* IEEE Trans. Plasma Sci, 2005. **33**(2): p. 771-775.

18. Pavlovich, M.J., et al., *Effect of Discharge Parameters and Surface Characteristics on Ambient-Gas Plasma Disinfection.* Plasma Processes and Polymers, 2013. **10**(1): p. 69-76.

19. Arjunan, K.P., *Plasma Produced Reactive Oxygen and Nitrogen Species in Angiogenesis*. 2011, Drexel University.

20. Traylor, M.J., et al., *Long-term antibacterial efficacy of air plasma-activated water.* Journal of Physics D: Applied Physics, 2011. **44**(47): p. 472001.

21. Pavlovich, M.J., D.S. Clark, and D.B. Graves, *Quantification of air plasma chemistry for surface disinfection.* Plasma Sources Science and Technology, 2014. **23**(6): p. 065036.

22. Enloe, C., et al., *Mechanisms and responses of a single dielectric barrier plasma actuator: plasma morphology.* AIAA journal, 2004. **42**(3): p. 589-594.

23. Enloe, C.L., et al., *Mechanisms and responses of a dielectric barrier plasma actuator: Geometric effects.* AIAA journal, 2004. **42**(3): p. 595-604.

24. Font, G., C. Enloe, and T.E. McLaughlin, *Effect of volumetric momentum addition on the total force production of a plasma actuator.* AIAA paper, 2009. **4285**.

25. James, B., et al., *Momentum Transfer for an Aerodynamic Plasma Actuator with an Imposed Boundary Layer*, in *44th AIAA Aerospace Sciences Meeting and Exhibit*. 2006, American Institute of Aeronautics and Astronautics.

26. Lerouge, S., M. Wertheimer, and Y. L'H, *Plasma sterilization: a review of parameters, mechanisms, and limitations.* Plasmas and Polymers, 2001. **6**(3): p. 175-188.

27. Franklin, R. and N.S.J. Braithwaite, *80 Years of Plasma.* Plasma Sources Science and Technology, 2009. **18**(1): p. 010201.

28. Grill, A., *Cold plasma in materials fabrication*. Vol. 151. 1994: IEEE Press, New York.

29. Conrads, H. and M. Schmidt, *Plasma generation and plasma sources.* Plasma Sources Science and Technology, 2000. **9**(4): p. 441.

30. Wharmby, D. *Electrodeless lamps for lighting: a review*. in *Science, Measurement and Technology, IEE Proceedings A*. 1993. IET.

31. Mintz, D.M., et al., *Using inert gas withing plasma reactor for soft etching, cleaning*. 1997, Google Patents.

32. Eliasson, B. and U. Kogelschatz, *Nonequilibrium volume plasma chemical processing.* Plasma Science, IEEE Transactions on, 1991. **19**(6): p. 1063-1077.

33. Raizer, Y.P. and J.E. Allen, *Gas discharge physics*. Vol. 2. 1997: Springer Berlin.

34. Ehlbeck, J., et al., *Low temperature atmospheric pressure plasma sources for microbial decontamination.* Journal of Physics D: Applied Physics, 2011. **44**(1): p. 013002.

35. Eliasson, B., M. Hirth, and U. Kogelschatz, *Ozone synthesis from oxygen in dielectric barrier discharges.* Journal of Physics D: Applied Physics, 1987. **20**(11): p. 1421.

36. Eliasson, B. and U. Kogelschatz, *Modeling and applications of silent discharge plasmas.* Plasma Science, IEEE Transactions on, 1991. **19**(2): p. 309-323.

37. Gibalov, V.I. and G.J. Pietsch, *The development of dielectric barrier discharges in gas gaps and on surfaces.* J.Phys.D:Appl. Phys, 2000. **33**(20): p. 2618.

38. Lieberman, M.A. and A.J. Lichtenberg, *Principles of plasma discharges and materials processing.* MRS Bulletin, 1994. **30**: p. 899-901.

39. Kogelschatz, U., B. Eliasson, and W. Egli, *Dielectric-barrier discharges. Principle and applications.* J. Phys IV, 1997. **7**(C4).

40. Boeuf, J., et al., *Electrohydrodynamic force in dielectric barrier discharge plasma actuators.* J.Phys.D:Appl. Phys, 2007. **40**(3): p. 652.

41. Ziuzina, D., et al., *Atmospheric cold plasma inactivation of Escherichia coli in liquid media inside a sealed package.* Journal of applied microbiology, 2013. **114**(3): p. 778-787.

42. Georghiou, G.E., et al., *Numerical modelling of atmospheric pressure gas discharges leading to plasma production.* Journal of Physics D: Applied Physics, 2005. **38**(20): p. R303.

43. Ulrich, K., *Industrial innovation based on fundamental physics.* Plasma Sources Science and Technology, 2002. **11**(3A): p. A1.

44. Laroussi, M. and X. Lu, *Room-temperature atmospheric pressure plasma plume for biomedical applications.* Appl. Phys. Lett, 2005. **87**(11): p. 113902.

45. Roupassov, D., et al., *Flow separation control by plasma actuator with nanosecond pulsed-periodic discharge.* AIAA journal, 2009. **47**(1): p. 168-185.

46. Post, M.L. and T.C. Corke, *Separation control on high angle of attack airfoil using plasma actuators.* AIAA journal, 2004. **42**(11): p. 2177-2184.

47. Thomas, F.O., et al., *Optimization of dielectric barrier discharge plasma actuators for active aerodynamic flow control.* AIAA journal, 2009. **47**(9): p. 2169-2178.

48. Roth, J.R., D.M. Sherman, and S.P. Wilkinson, *Electrohydrodynamic Flow Control with a Glow-Discharge Surface Plasma.* AIAA Journal, 2000. **38**(7): p. 1166-1172.

49. Gregory, J.W., et al., *Force production mechanisms of a dielectric-barrier discharge plasma actuator.* AIAA paper, 2007. **185**: p. 2007.

50. Forte, M., et al., *Plasma actuators for airflow control: measurement of the non-stationary induced flow velocity.* Journal of Electrostatics, 2005. **63**(6–10): p. 929-936.

51. Forte, M., et al., *Optimization of a dielectric barrier discharge actuator by stationary and non-stationary measurements of the induced flow velocity: application to airflow control.* Experiments in Fluids, 2007. **43**(6): p. 917-928.

52. Font, G.I., *Boundary layer control with atmospheric plasma discharges.* AIAA journal, 2006. **44**(7): p. 1572-1578.

53. Corke, T.C., M.L. Post, and D.M. Orlov, *SDBD plasma enhanced aerodynamics: concepts, optimization and applications.* Progress in Aerospace Sciences, 2007. **43**(7): p. 193-217.

54. Corke, T.C. and M.L. Post, *Overview of plasma flow control: concepts, optimization, and applications.* AIAA paper, 2005. **563**: p. 2005.

55. Christopher, P., et al., *Boundary Layer Control Using a DBD Plasma Actuator*, in *45th AIAA Aerospace Sciences Meeting and Exhibit*. 2007, American Institute of Aeronautics and Astronautics.

56. Santhanakrishnan, A. and J.D. Jacob, *Flow control with plasma synthetic jet actuators.* J.Phys.D:Appl. Phys, 2007. **40**(3): p. 637.

57. Sakiyama, Y., et al., *Plasma chemistry model of surface microdischarge in humid air and dynamics of reactive neutral species.* Journal of Physics D: Applied Physics, 2012. **45**(42): p. 425201.

58. Capitelli, M., et al., *Plasma kinetics in atmospheric gases*. 2001, IOP Publishing.

59. Orlov, D.M., G.I. Font, and D. Edelstein, *Characterization of discharge modes of plasma actuators.* AIAA journal, 2008. **46**(12): p. 3142-3148.

60. Lagmich, Y., et al., *Model description of surface dielectric barrier discharges for flow control.* Journal of Physics D: Applied Physics, 2008. **41**(9): p. 095205.

61. Font, G.I. and W.L. Morgan, *Plasma discharges in atmospheric pressure oxygen for boundary layer separation control.* AIAA paper, 2005. **4632**: p. 2005.

62. Pai, K. and J. Jacob. *Evaluation of Dielectric Barrier Discharge Configurations for Biological Decontamination*. in *in Proc. 51st AIAA Aerosp. Sci. Meeting* 2013. Dallas, Texas: American Institute of Aeronautics and Astronautics.

63. Bolitho, M. and J. Jacob. *Thrust Vectoring Flow Control Using Plasma Synthetic Jet Actuators*. in *in Proc. 46th AIAA Aerosp. Sci. Meeting*. 2008. Reno, Nevada: American Institute of Aeronautics and Astronautics.

64. Palsule, A.S., S.J. Clarson, and C.W. Widenhouse, *Gamma irradiation of silicones.* Journal of Inorganic and Organometallic Polymers and Materials, 2008. **18**(2): p. 207-221.

65. Kurtz, S.M., *UHMWPE biomaterials handbook: ultra high molecular weight polyethylene in total joint replacement and medical devices*. 2009: Academic Press.

66. Anderson, J.M. and R.E. Marchant, *Biomaterials: factors favoring colonization and infection.* 2000.

67. Flanagan, M.E., et al., *A national collaborative for reducing health care–associated infections: Current initiatives, challenges, and opportunities.* American Journal of Infection Control, 2011. **39**(8): p. 685-689.

68. O'Connor, N., et al., *Cold atmospheric pressure plasma and decontamination. Can it contribute to preventing hospital-acquired infections?* Journal of Hospital Infection, 2014. **88**(2): p. 59-65.

69. Edwards, J.R., et al., *National Healthcare Safety Network (NHSN) Report, data summary for 2006, issued June 2007.* American Journal of Infection Control, 2007. **35**(5): p. 290-301.

70. *National Nosocomial Infections Surveillance (NNIS) System Report, data summary from January 1992 through June 2004, issued October 2004*, in *American Journal of Infection Control*. 2004. p. 470-485.

71. Burke, J.P., *Infection Control — A Problem for Patient Safety.* New England Journal of Medicine, 2003. **348**(7): p. 651-656.

72. Mahieu, L.M., et al., *Additional hospital stay and charges due to hospital-acquired infections in a neonatal intensive care unit.* Journal of Hospital Infection, 2001. **47**(3): p. 223-229.

73. Sheng, W.H., et al., *Comparative impact of hospital-acquired infections on medical costs, length of hospital stay and outcome between community hospitals and medical centres.* Journal of Hospital Infection, 2005. **59**(3): p. 205-214.

74. Wenzel, R.P., *The economics of nosocomial infections.* Journal of Hospital Infection, 1995. **31**(2): p. 79-87.

75. Stone, P.W., E. Larson, and L.N. Kawar, *A systematic audit of economic evidence linking nosocomial infections and infection control interventions: 1990-2000.* American Journal of Infection Control, 2002. **30**(3): p. 145-152.

76. Magill, S.S., et al., *Multistate Point-Prevalence Survey of Health Care–Associated Infections.* New England Journal of Medicine, 2014. **370**(13): p. 1198-1208.

77. *Antibiotic resistance threats in the United States*. 2013, Centers for Disease Control and Prevention (CDC): Atlanta: CDC.

78. Noronha, A.M. and S. Brozak, *A 21st century nosocomial issue with endoscopes*. Vol. 348. 2014.

79. Rutala, W.A. and D.J. Weber, *Gastrointestinal endoscopes: A need to shift from disinfection to sterilization?* JAMA, 2014. **312**(14): p. 1405-1406.

80. Silverstone, S.E. and D.E. Hill, *Evaluation of sterilization of dental handpieces by heating in synthetic compressor lubricant.* General dentistry, 1999. **47**(2): p. 158-160.

81. Spotts Whitney, E.A., et al., *Inactivation of Bacillus anthracis spores.* Emerging infectious diseases, 2003. **9**(6): p. 623-627.

82. Gerhardt, P. and E. Ribi, *Ultrastructure of the exosporium enveloping spores of Bacillus cereus.* Journal of bacteriology, 1964. **88**(6): p. 1774.

83. Setlow, P., *Mechanisms which contribute to the long-term survival of spores of Bacillus species.* Journal of Applied Bacteriology, 1994. **76**(S23): p. 49S-60S.

84. Setlow, P., *Mechanisms for the prevention of damage to DNA in spores of Bacillus species.* Annual Reviews in Microbiology, 1995. **49**(1): p. 29-54.

85. Farkas, J., *Irradiation as a method for decontaminating food: a review.* International journal of food microbiology, 1998. **44**(3): p. 189-204.

86. Aymerich, T., P. Picouet, and J. Monfort, *Decontamination technologies for meat products.* Meat Science, 2008. **78**(1): p. 114-129.

87. Khadre, M.A., A.E. Yousef, and J.G. Kim, *Microbiological Aspects of Ozone Applications in Food: A Review.* Journal of Food Science, 2001. **66**(9): p. 1242-1252.

88. Kim, J.-G., A.E. Yousef, and G.W. Chism, *USE OF OZONE TO INACTIVATE MICROORGANISMS ON LETTUCE.* Journal of Food Safety, 1999. **19**(1): p. 17-34.

89. Brown, B., H. Lu, and D. Duquette, *Effect of Flow Rates on Localized Corrosion Behavior of 304 Stainless Steel in Ozonated 0.5 N NaCl.* Corrosion, 1992. **48**(12): p. 970-975.

90. Pascual, A., I. Llorca, and A. Canut, *Use of ozone in food industries for reducing the environmental impact of cleaning and disinfection activities.* Trends in Food Science & Technology, 2007. **18, Supplement 1**: p. S29-S35.

91. Guzel-Seydim, Z.B., A.K. Greene, and A.C. Seydim, *Use of ozone in the food industry.* LWT - Food Science and Technology, 2004. **37**(4): p. 453-460.

92. Seymour, I. and H. Appleton, *Foodborne viruses and fresh produce.* Journal of Applied Microbiology, 2001. **91**(5): p. 759-773.

93. Dietz, P., R. Bohm, and D. Strauch, *[Investigations on disinfection and sterilization of surfaces by ultraviolet radiation (author's transl)].* Zentralbl Bakteriol Mikrobiol Hyg B, 1980. **171**(2-3): p. 158-67.

94. Kuo, S.P., *Plasma assisted decontamination of bacterial spores.* Open Biomed Eng J, 2008. **2**: p. 36-42.

95. Migdal, W. and A. Chmielewski, *Radiation decontamination of herbs and spices.* 2005.

96. Tendero, C., et al., *Atmospheric pressure plasmas: A review.* Spectrochimica Acta Part B: Atomic Spectroscopy, 2006. **61**(1): p. 2-30.

97. Schütze, A., et al., *The atmospheric-pressure plasma jet: a review and comparison to other plasma sources.* Plasma Science, IEEE Transactions on, 1998. **26**(6): p. 1685-1694.

98. Yonson, S., et al., *Cell treatment and surface functionalization using a miniature atmospheric pressure glow discharge plasma torch.* J.Phys.D:Appl. Phys, 2006. **39**(16): p. 3508.

99. Kong, M.G., et al., *Plasma medicine: an introductory review.* New Journal of Physics, 2009. **11**(11): p. 115012.

100. Kalghatgi, S.U., et al., *Mechanism of blood coagulation by nonthermal atmospheric pressure dielectric barrier discharge plasma.* IEEE Trans. Plasma Sci, 2007. **35**(5): p. 1559-1566.

101. Julák, J. and V. Scholtz, *Decontamination of human skin by low-temperature plasma produced by cometary discharge.* Clinical Plasma Medicine, 2013. **1**(2): p. 31-34.

102. Isbary, G., et al., *Cold atmospheric argon plasma treatment may accelerate wound healing in chronic wounds: Results of an open retrospective randomized controlled study in vivo.* Clinical Plasma Medicine, 2013. **1**(2): p. 25-30.

103. Isbary, G., et al., *A first prospective randomized controlled trial to decrease bacterial load using cold atmospheric argon plasma on chronic wounds in patients.* British Journal of Dermatology, 2010. **163**(1): p. 78-82.

104. Isbary, G., et al., *Successful and safe use of 2 min cold atmospheric argon plasma in chronic wounds: results of a randomized controlled trial.* British Journal of Dermatology, 2012. **167**(2): p. 404-410.

105. Sladek, R.E., et al., *Plasma treatment of dental cavities: a feasibility study.* Plasma Science, IEEE Transactions on, 2004. **32**(4): p. 1540-1543.

106. Goree, J., et al., *Killing of S. mutans bacteria using a plasma needle at atmospheric pressure.* Plasma Science, IEEE Transactions on, 2006. **34**(4): p. 1317-1324.

107. Cha, S. and Y.-S. Park, *Plasma in dentistry.* Clinical Plasma Medicine, 2014. **2**(1): p. 4-10.

108. Stoffels, E., et al., *Plasma needle: a non-destructive atmospheric plasma source for fine surface treatment of (bio) materials.* Plasma Sources Science and Technology, 2002. **11**(4): p. 383.

109. Yong, H.I., et al., *Evaluation of pathogen inactivation on sliced cheese induced by encapsulated atmospheric pressure dielectric barrier discharge plasma.* Food Microbiology, (0).

110. Song, H.P., et al., *Evaluation of atmospheric pressure plasma to improve the safety of sliced cheese and ham inoculated by 3-strain cocktail Listeria monocytogenes.* Food Microbiology, 2009. **26**(4): p. 432-436.

111. SHINTANI, H., et al., *Inactivation of microorganisms and endotoxins by low temperature nitrogen gas plasma exposure.* Biocontrol science, 2007. **12**(4): p. 131-143.

112. Schwabedissen, A., et al., *PlasmaLabel–a new method to disinfect goods inside a closed package using dielectric barrier discharges.* Contributions to Plasma Physics, 2007. **47**(7): p. 551-558.

113. Moisan, M., et al., *Low-temperature sterilization using gas plasmas: a review of the experiments and an analysis of the inactivation mechanisms.* Int. J. Pharma, 2001. **226**(1): p. 1-21.

114. Laroussi, M., I. Alexeff, and W.L. Kang, *Biological decontamination by nonthermal plasmas.* IEEE Trans. Plasma Sci, 2000. **28**(1): p. 184-188.

115. Laroussi, M., *Nonthermal decontamination of biological media by atmospheric-pressure plasmas: Review, analysis, and prospects.* IEEE Trans. Plasma Sci, 2002. **30**(4): p. 1409-1415.

116. Laroussi, M., *Sterilization of contaminated matter with an atmospheric pressure plasma.* IEEE Trans. Plasma Sci, 1996. **24**(3): p. 1188-1191.

117. Klämpfl, T.G., et al., *Cold atmospheric air plasma sterilization against spores and other microorganisms of clinical interest.* Applied and environmental microbiology, 2012. **78**(15): p. 5077-5082.

118. Kelly-Wintenberg, K., et al., *Room temperature sterilization of surfaces and fabrics with a one atmosphere uniform glow discharge plasma.* J. Ind. Microbio. Biot, 1998. **20**(1): p. 69-74.

119. Kelly-Wintenberg, K., et al., *Use of a one atmosphere uniform glow discharge plasma to kill a broad spectrum of microorganisms.* Journal of Vacuum Science & Technology A, 1999. **17**(4): p. 1539-1544.

120. Graves, D.B., *The emerging role of reactive oxygen and nitrogen species in redox biology and some implications for plasma applications to medicine and biology.* Journal of Physics D: Applied Physics, 2012. **45**(26): p. 263001.

121. Gaunt, L.F., C.B. Beggs, and G.E. Georghiou, *Bactericidal Action of the Reactive Species Produced by Gas-Discharge Nonthermal Plasma at Atmospheric Pressure: A Review.* Plasma Science, IEEE Transactions on, 2006. **34**(4): p. 1257-1269.

122. Fröhling, A., et al., *Indirect plasma treatment of fresh pork: Decontamination efficiency and effects on quality attributes.* Innovative Food Science & Emerging Technologies, 2012. **16**: p. 381-390.

123. Brun, P., et al., *Disinfection of ocular cells and tissues by atmospheric-pressure cold plasma.* PloS one, 2012. **7**(3): p. e33245.

124. Misra, N.N., et al., *In-package atmospheric pressure cold plasma treatment of strawberries.* Journal of Food Engineering, 2014. **125**: p. 131-138.

125. Ziuzina, D., et al., *Atmospheric cold plasma inactivation of Escherichia coli, Salmonella enterica serovar Typhimurium and Listeria monocytogenes inoculated on fresh produce.* Food microbiology, 2014. **42**: p. 109-116.

126. Misra, N.N., et al., *In-package atmospheric pressure cold plasma treatment of cherry tomatoes.* Journal of bioscience and bioengineering, 2014. **118**(2): p. 177-182.

127. Rød, S.K., et al., *Cold atmospheric pressure plasma treatment of ready-to-eat meat: Inactivation of< i> Listeria innocua</i> and changes in product quality.* Food microbiology, 2012. **30**(1): p. 233-238.

128. Niemira, B.A., *Cold plasma decontamination of foods*.* Annual review of food science and technology, 2012. **3**: p. 125-142.

129. Selcuk, M., L. Oksuz, and P. Basaran, *Decontamination of grains and legumes infected with Aspergillus spp. and Penicillum spp. by cold plasma treatment.* Bioresource technology, 2008. **99**(11): p. 5104-5109.

130. Laroussi, M., et al., *Inactivation of bacteria by the plasma pencil.* Plasma Processes and Polymers, 2006. **3**(6-7): p. 470-473.

131. Laroussi, M., et al., *The plasma pencil: a source of hypersonic cold plasma bullets for biomedical applications.* Plasma Science, IEEE Transactions on, 2008. **36**(4): p. 1298-1299.

132. Vleugels, M., et al., *Atmospheric plasma inactivation of biofilm-forming bacteria for food safety control.* Plasma Science, IEEE Transactions on, 2005. **33**(2): p. 824-828.

133. Shimizu, T., et al., *Characterization of microwave plasma torch for decontamination.* Plasma Processes and Polymers, 2008. **5**(6): p. 577-582.

134. Shimizu, T., et al., *Characterization of Low-Temperature Microwave Plasma Treatment With and Without UV Light for Disinfection.* Plasma Processes and Polymers, 2010. **7**(3-4): p. 288-293.

135. Ermolaeva, S.A., et al., *Bactericidal effects of non-thermal argon plasma in vitro, in biofilms and in the animal model of infected wounds.* Journal of medical microbiology, 2011. **60**(1): p. 75-83.

136. Boudam, M., et al., *Bacterial spore inactivation by atmospheric-pressure plasmas in the presence or absence of UV photons as obtained with the same gas mixture.* J.Phys.D:Appl. Phys, 2006. **39**(16): p. 3494.

137. Lawrence, C.A. and S.S. Block, *Disinfection, sterilization, and preservation.* Disinfection, sterilization, and preservation., 1968.

138. Beggs, C.B., *A quantitative method for evaluating the photoreactivation of ultraviolet damaged microorganisms.* Photochemical & Photobiological Sciences, 2002. **1**(6): p. 431-437.

139. Sysolyatina, E.V., et al., *Experimental Evidences on Synergy of Gas Discharge Agents in Bactericidal Activity of Nonthermal Plasma.* 2013. **3**(1-2): p. 137-152.

140. Sysolyatina, E., et al., *Role of the charged particles in bacteria inactivation by plasma of a positive and negative corona in ambient air.* Plasma Processes and Polymers, 2014. **11**(4): p. 315-334.

141. Yamamoto, M., M. Nishioka, and M. Sadakata. *Sterilization using a corona discharge with H2O2 droplets and examination of effective species*. in *in Proc. 15th Int. Symp. Plasma Chemistry*. 2001.

142. Kuzmichev, A., et al. *Features of sterilization by different types of atmospheric pressure discharges*. in *in Proc. 7th Int. Symp. High Press. Low Temp. Plasma Chem., Hakone VII, Greifswald, Germany*. 2000.

143. Herrmann, H.W., et al., *Decontamination of chemical and biological warfare, (CBW) agents using an atmospheric pressure plasma jet (APPJ).* Phys. of Plasmas, 1999. **6**(5): p. 2284-2289.

144. Halliwell, B. and J.M. Gutteridge, *Free radicals in biology and medicine*. Vol. 3. 1999: Oxford university press Oxford.

145. Farr, S.B. and T. Kogoma, *Oxidative stress responses in Escherichia coli and Salmonella typhimurium.* Microbiological reviews, 1991. **55**(4): p. 561-585.

146. Imlay, J.A., *Pathways of oxidative damage.* Annual Reviews in Microbiology, 2003. **57**(1): p. 395-418.

147. Oehmigen, K., et al., *The role of acidification for antimicrobial activity of atmospheric pressure plasma in liquids.* Plasma Processes and Polymers, 2010. **7**(3-4): p. 250-257.

148. Schutze, A., et al., *The atmospheric-pressure plasma jet: a review and comparison to other plasma sources.* Plasma Science, IEEE Transactions on, 1998. **26**(6): p. 1685-1694.

149. Shibata, M., N. Nakano, and T. Makabe, *Effect of O2(a1Δg) on plasma structures in oxygen radio frequency discharges.* Journal of Applied Physics, 1996. **80**(11): p. 6142-6147.

150. Gadri, R.B., et al., *Sterilization and plasma processing of room temperature surfaces with a one atmosphere uniform glow discharge plasma (OAUGDP).* Surface and Coatings Technology, 2000. **131**(1–3): p. 528-541.

151. Montie, T.C., K. Kelly-Wintenberg, and J. Reece Roth, *An overview of research using the one atmosphere uniform glow discharge plasma (OAUGDP) for sterilization of surfaces and materials.* IEEE Trans. Plasma Sci, 2000. **28**(1): p. 41-50.

152. Zoran, F. and J.C. John, *Microdischarge behaviour in the silent discharge of nitrogen - oxygen and water - air mixtures.* Journal of Physics D: Applied Physics, 1997. **30**(5): p. 817.

153. Kondrashove, M.N., et al., *The primary physico-chemical mechanism for the beneficial biological/medical effects of negative air ions.* Plasma Science, IEEE Transactions on, 2000. **28**(1): p. 230-237.

154. Goldstein, N., R. Goldstein, and M. Merzlyak, *Negative air ions as a source of superoxide.* International Journal of Biometeorology, 1992. **36**(2): p. 118-122.

155. Challenger, O., et al., *Negative air ionisation and the generation of hydrogen peroxide.* Science of The Total Environment, 1996. **177**(1–3): p. 215-219.

156. Cabiscol, E., J. Tamarit, and J. Ros, *Oxidative stress in bacteria and protein damage by reactive oxygen species.* International Microbiology, 2010. **3**(1): p. 3-8.

157. Broadwater, W.T., R. Hoehn, and P. King, *Sensitivity of three selected bacterial species to ozone.* Applied Microbiology, 1973. **26**(3): p. 391-393.

158. Hamelin, C., F. Sarhan, and Y.S. Chung, *Induction of deoxyribonucleic acid degradation inEscherichia coli by ozone.* Experientia, 1978. **34**(12): p. 1578-1579.

159. Ishizaki, K., et al., *Effect of ozone on plasmid DNA of Escherichia coli in situ.* Water Research, 1987. **21**(7): p. 823-827.

160. Hunt, N.K. and B.J. Mariñas, *Inactivation of Escherichia coli with ozone: chemical and inactivation kinetics.* Water Research, 1999. **33**(11): p. 2633-2641.

161. Pratt, R. and R.W. Barnard, *Some effects of ionized air on Penicillium notatum.* Journal of the American Pharmaceutical Association, 1960. **49**(10): p. 643-646.

162. Phillips, G., G.J. Harris, and M.W. Jones, *Effect of air ions on bacterial aerosols.* International journal of biometeorology, 1964. **8**(1): p. 27-37.

163. Kellogg, E., et al., *Superoxide involvement in the bactericidal effects of negative air ions on Staphylococcus albus.* 1979.

164. Shargawi, J., et al., *Sensitivity of Candida albicans to negative air ion streams.* Journal of applied microbiology, 1999. **87**(6): p. 889-897.

165. Noyce, J. and J. Hughes, *Bactericidal effects of negative and positive ions generated in nitrogen on starved Pseudomonas veronii.* Journal of electrostatics, 2003. **57**(1): p. 49-58.

166. Noyce, J. and J. Hughes, *Bactericidal effects of negative and positive ions generated in nitrogen on Escherichia coli.* Journal of electrostatics, 2002. **54**(2): p. 179-187.

167. Mendis, D., M. Rosenberg, and F. Azam, *A note on the possible electrostatic disruption of bacteria.* IEEE Trans. Plasma Sci, 2000. **28**(4): p. 1304-1306.

168. Laroussi, M., D. Mendis, and M. Rosenberg, *Plasma interaction with microbes.* New Journal of Physics, 2003. **5**(1): p. 41.

169. Machala, Z., L. Chládeková, and M. Pelach, *Plasma agents in bio-decontamination by dc discharges in atmospheric air.* Journal of Physics D: Applied Physics, 2010. **43**(22): p. 222001.

170. Schoenbach, K.H., et al., *The effect of pulsed electric fields on biological cells: experiments and applications.* Plasma Science, IEEE Transactions on, 1997. **25**(2): p. 284-292.

171. Ermolaeva, S.A., et al., *Comparative Study of Three Nonthermal Plasma Sources against Causative Agents of Nosocomial Infections.* Plasma Medicine, 2012. **2**(1-3).

172. Alkawareek, M.Y., et al., *Eradication of Pseudomonas aeruginosa biofilms by atmospheric pressure non-thermal plasma.* PloS one, 2012. **7**(8): p. e44289.

173. Sosnin, E.A., et al., *The effects of UV irradiation and gas plasma treatment on living mammalian cells and bacteria: a comparative approach.* IEEE Trans. on Plasma Sci, 2004. **32**(4): p. 1544-1550.

174. Mastanaiah, N., J.A. Johnson, and S. Roy, *Effect of Dielectric and Liquid on Plasma Sterilization Using Dielectric Barrier Discharge Plasma.* PloS one, 2013. **8**(8): p. e70840.

175. Laroussi, M., J.P. Richardson, and F.C. Dobbs. *Biochemical pathways in the interaction of non-equilibrium plasmas with bacteria*. in *in Proc. Electromed. ,Portsmouth, VA*. 2001.

176. Kalghatgi, S.U., et al. *Non-thermal dielectric barrier discharge plasma treatment of endothelial cells*. in *in Proc. EMBS 2008. 30th Annu. Int. Conf. of the IEEE*. 2008. IEEE.

177. Kalghatgi, S., et al., *DNA Damage in Mammalian Cells by Non-thermal Atmospheric Pressure Microsecond Pulsed Dielectric Barrier Discharge Plasma is not Mediated by Ozone.* Plasma Process. Poly, 2012. **9**(7): p. 726-732.

178. Kalghatgi, S., et al., *Effects of non-thermal plasma on mammalian cells.* PloS one, 2011. **6**(1): p. e16270.

179. Pai, K.K., et al., *Dose Dependent Selectivity and Response of Different Types of Mammalian Cells to Surface Dielectric Barrier Discharge (SDBD) Plasma.* Plasma Processes and Polymers, 2015: p. DOI:10.1002/ppap.201400134.

180. Chen, C.-Y., et al., *Blood clotting by low-temperature air plasma.* IEEE Trans. Plasma Sci, 2009. **37**(6): p. 993-999.

181. Fridman, G., et al., *Blood coagulation and living tissue sterilization by floating-electrode dielectric barrier discharge in air.* Plasma Chem. Plasma Process, 2006. **26**(4): p. 425-442.

182. Stoffels, E., I. Kieft, and R. Sladek, *Superficial treatment of mammalian cells using plasma needle.* J.Phys.D:Appl. Phys, 2003. **36**(23): p. 2908.

183. Stoffels, E., R. Sladek, and I. Kieft, *Gas plasma effects on living cells.* Phys. Scripta, 2004. **2004**(T107): p. 79.

184. Laroussi, M., *Cold Plasma.* AccessScience, McGraw Hill, 2002.

185. Huang, J., T.C. Corke, and F.O. Thomas, *Plasma actuators for separation control of low-pressure turbine blades.* AIAA journal, 2006. **44**(1): p. 51-57.

186. Roth, J.R. and D. Xin, *Optimization of the Aerodynamic Plasma Actuator as an Electrohydrodynamic (EHD) Electrical Device*, in *44th AIAA Aerospace Sciences Meeting and Exhibit*. 2006, American Institute of Aeronautics and Astronautics.

187. Dmitriy, O., et al., *Modeling and Experiment of Leading Edge Separation Control Using SDBD Plasma Actuators*, in *45th AIAA Aerospace Sciences Meeting and Exhibit*. 2007, American Institute of Aeronautics and Astronautics.

188. Dmitri, O., F. Gabriel, and E. Damiel, *Characterization of Discharge Modes of Plasma Actuator*, in *46th AIAA Aerospace Sciences Meeting and Exhibit*. 2008, American Institute of Aeronautics and Astronautics.

189. Jérôme, P., M. Eric, and T. Gérard, *Asymmetric surface dielectric barrier discharge in air at atmospheric pressure: electrical properties and induced airflow characteristics.* Journal of Physics D: Applied Physics, 2005. **38**(19): p. 3635.

190. Hoskinson, A.R., N. Hershkowitz, and D.E. Ashpis, *Force measurements of single and double barrier DBD plasma actuators in quiescent air.* Journal of Physics D: Applied Physics, 2008. **41**(24): p. 245209.

191. Hoskinson, A.R. and N. Hershkowitz, *Modelling of dielectric barrier discharge plasma actuators with thick electrodes.* Journal of Physics D: Applied Physics, 2011. **44**(8): p. 085202.

192. Hoskinson, A.R. and N. Hershkowitz, *Differences between dielectric barrier discharge plasma actuators with cylindrical and rectangular exposed electrodes.* Journal of Physics D: Applied Physics, 2010. **43**(6): p. 065205.

193. Hoskinson, A.R., L. Oksuz, and N. Hershkowitz, *Microdischarge propagation and expansion in a surface dielectric barrier discharge.* Applied Physics Letters, 2008. **93**(22): p. -.

194. Sladek, R.E., T.A. Baede, and E. Stoffels, *Plasma-needle treatment of substrates with respect to wettability and growth of Escherichia coli and Streptococcus mutans.* Plasma Science, IEEE Transactions on, 2006. **34**(4): p. 1325-1330.

195. Scallan, E., et al., *Foodborne illness acquired in the United States—major pathogens.* Emerg Infect Dis, 2011. **17**(1).

196. Ferreira, V., et al., *Listeria monocytogenes Persistence in Food-Associated Environments: Epidemiology, Strain Characteristics, and Implications for Public Health.* Journal of Food Protection®, 2014. **77**(1): p. 150-170.

197. Valderrama, W.B. and C.N. Cutter, *An ecological perspective of Listeria monocytogenes biofilms in food processing facilities.* Critical reviews in food science and nutrition, 2013. **53**(8): p. 801-817.

198. Iyer, P., K.J. Walker, and S.V. Madihally, *Increased matrix synthesis by fibroblasts with decreased proliferation on synthetic chitosan-gelatin porous structures.* Biotechnol Bioeng, 2012. **109**(5): p. 1314-25.

199. Djafarzadeh, R., et al., *Recombinant GPI-anchored TIMP-1 stimulates growth and migration of peritoneal mesothelial cells.* PloS one, 2012. **7**(4): p. e33963.

200. Pearse, R.W.B., et al., *The identification of molecular spectra*. Vol. 297. 1976, London: Chapman and Hall

201. Lerner, L.H., et al., *Nitric oxide synthase in toxic epidermal necrolysis and Stevens–Johnson syndrome.* J. Invest. Dermatol., 2000. **114**(1): p. 196-199.

202. Leduc, M., et al., *Effects of Non-thermal Plasmas on DNA and Mammalian Cells.* Plasma Process. Polym, 2010. **7**(11): p. 899-909.

203. Lee, H., et al., *Degradation of adhesion molecules of G361 melanoma cells by a non-thermal atmospheric pressure microplasma.* New J. Phys, 2009. **11**(11): p. 115026.

204. Hoentsch, M., et al., *Time-dependent effects of low-temperature atmospheric-pressure argon plasma on epithelial cell attachment, viability and tight junction formation in vitro.* J.Phys.D:Appl. Phys, 2012. **45**(2): p. 025206.

205. Haertel, B., et al., *Surface molecules on HaCaT keratinocytes after interaction with non-thermal atmospheric pressure plasma.* Cell Biol. Int, 2012. **36**(12): p. 1217-1222.

206. Kieft, I., et al., *Electric discharge plasmas influence attachment of cultured CHO K1 cells.* Bioelectromagnetics, 2004. **25**(5): p. 362-368.

207. Haertel, B., et al., *Differential Influence of Components Resulting from Atmospheric-Pressure Plasma on Integrin Expression of Human HaCaT Keratinocytes.* BioMed Res. Int, 2013. **2013**.

208. Shashurin, A., et al., *Living tissue under treatment of cold plasma atmospheric jet.* Appl. Phys. Lett, 2008. **93**(18): p. 181501.

209. Ying-Hong, L., et al., *Optical emission spectroscopy investigation of a surface dielectric barrier discharge plasma aerodynamic actuator.* Chinese Phys. Lett, 2008. **25**(11): p. 4068.

210. Wende, K., et al., *Distinctive activity of a nonthermal atmospheric-pressure plasma jet on eukaryotic and prokaryotic cells in a cocultivation approach of keratinocytes and microorganisms.* IEEE Trans. Plasma Sci, 2010. **38**(9): p. 2479-2485.

211. Grundmann, H., et al., *Emergence and resurgence of meticillin-resistant Staphylococcus aureus as a public-health threat.* The Lancet, 2006. **368**(9538): p. 874-885.

212. Carbapenemases, C.A., *Global spread of carbapenemase-producing Enterobacteriaceae.* 2011.

213. Levy, S.B. and B. Marshall, *Antibacterial resistance worldwide: causes, challenges and responses.* Nature medicine, 2004. **10**: p. S122-S129.

214. Markou, N., et al., *Intravenous colistin in the treatment of sepsis from multiresistant Gram-negative bacilli in critically ill patients.* Critical Care, 2003. **7**(5): p. R78.

215. Cushnie, T.P.T., B. Cushnie, and A.J. Lamb, *Alkaloids: An overview of their antibacterial, antibiotic-enhancing and antivirulence activities.* International Journal of Antimicrobial Agents, 2014. **44**(5): p. 377-386.

216. Heinlin, J., et al., *Plasma applications in medicine with a special focus on dermatology.* Journal of the European Academy of Dermatology and Venereology, 2011. **25**(1): p. 1-11.

217. Ahn, H.J., et al., *Targeting cancer cells with reactive oxygen and nitrogen species generated by atmospheric-pressure air plasma.* PloS one, 2014. **9**(1).

218. Volotskova, O., et al., *Targeting the cancer cell cycle by cold atmospheric plasma.* Scientific Reports, 2012. **2**: p. 636.

219. Daeschlein, G., et al., *Cold plasma–a new antimicrobial treatment tool against multidrug resistant pathogens.* Worldwide Research Efforts in the Fighting Against Microbial Pathogens–From Basic Research to Technological Developments. Ed. Mendez-Vilas. Brown Walker Press Boca Raton, Florida, USA, 2013: p. 110-113.

220. Kvam, E., et al., *Nonthermal atmospheric plasma rapidly disinfects multidrug-resistant microbes by inducing cell surface damage.* Antimicrobial agents and chemotherapy, 2012. **56**(4): p. 2028-2036.

221. Isbary, G., et al., *Non-thermal plasma—More than five years of clinical experience.* Clinical Plasma Medicine, 2013. **1**(1): p. 19-23.

222. Ma, Y., et al., *Non-thermal atmospheric pressure plasma preferentially induces apoptosis in p53-mutated cancer cells by activating ROS stress-response pathways.* PloS one, 2014. **9**(4): p. e91947.

223. Arjunan, K.P. and A.M. Clyne, *A nitric oxide producing pin-to-hole spark discharge plasma enhances endothelial cell proliferation and migration.* Plasma Medicine, 2011. **1**(3-4).

224. Umar, S. and A. van der Laarse, *Nitric oxide and nitric oxide synthase isoforms in the normal, hypertrophic, and failing heart.* Molecular and cellular biochemistry, 2010. **333**(1-2): p. 191-201.

225. Brisset, J.-L. and E. Hnatiuc, *Peroxynitrite: a re-examination of the chemical properties of non-thermal discharges burning in air over aqueous solutions.* Plasma Chemistry and Plasma Processing, 2012. **32**(4): p. 655-674.

226. Ignarro, L.J., *Endothelium-derived nitric oxide: actions and properties.* The FASEB Journal, 1989. **3**(1): p. 31-36.

227. Marletta, M.A., et al., *Macrophage oxidation of L-arginine to nitrite and nitrate: nitric oxide is an intermediate.* Biochemistry, 1988. **27**(24): p. 8706-8711.

228. Aktan, F., *iNOS-mediated nitric oxide production and its regulation.* Life sciences, 2004. **75**(6): p. 639-653.

229. Kojda, G. and D. Harrison, *Interactions between NO and reactive oxygen species: pathophysiological importance in atherosclerosis, hypertension, diabetes and heart failure.* Cardiovascular research, 1999. **43**(3): p. 652-671.

230. Ignarro, L.J., *Biosynthesis and metabolism of endothelium-derived nitric oxide.* Annual review of pharmacology and toxicology, 1990. **30**(1): p. 535-560.

231. Amano, F. and T. Noda, *Improved detection of nitric oxide radical (NO•) production in an activated macrophage culture with a radical scavenger, car□y PTIO, and Griess reagent.* FEBS Letters, 1995. **368**(3): p. 425-428.

232. Sherman, M.P., et al., *Pyrrolidine Dithiocarbamate Inhibits Induction of Nitric Oxide Synthase Activity in Rat Alveolar Macrophages.* Biochemical and Biophysical Research Communications, 1993. **191**(3): p. 1301-1308.

233. Likhanskii, A., et al., *Modeling of interaction between weakly ionized near-surface plasmas and gas flow.* AIAA Paper, 2006. **1204**: p. 2006.

234. Müller, S., R.-J. Zahn, and J. Grundmann, *Extraction of Ions from Dielectric Barrier Discharge Configurations.* Plasma Processes and Polymers, 2007. **4**(S1): p. S1004-S1008.

235. Chih Wei, C., L. How-Ming, and C. Moo Been, *Inactivation of Aquatic Microorganisms by Low-Frequency AC Discharges.* Plasma Science, IEEE Transactions on, 2008. **36**(1): p. 215-219.

236. Naïtali, M., et al., *Combined effects of long-living chemical species during microbial inactivation using atmospheric plasma-treated water.* Applied and environmental microbiology, 2010. **76**(22): p. 7662-7664.

237. Kono, Y., et al., *Lactate-dependent killing of Escherichia coli by nitrite plus hydrogen-peroxide: A possible role of nitrogen dioxide.* Archives of biochemistry and biophysics, 1994. **311**(1): p. 153-159.

238. Kojtari, A., et al., *Chemistry for antimicrobial properties of water treated with non-equilibrium plasma.* J. Nanomed. Biotherapeutic Discovery, 2013. **4**: p. 120.

239. Akaike, T., et al., *Antagonistic action of imidazolineoxyl N-oxides against endothelium-derived relaxing factor/. bul. NO (nitric oxide) through a radical reaction.* Biochemistry, 1993. **32**(3): p. 827-832.

240. Az-ma, T., K. Fujii, and O. Yuge, *Reaction between imidazolineoxil N-oxide (carboxy-PTIO) and nitric oxide released from cultured endothelial cells: quantitative measurement of nitric oxide by ESR spectrometry.* Life sciences, 1994. **54**(11): p. PL185-PL190.

241. Hogg, N., et al., *Reactions of nitric oxide with nitronyl nitroxides and oxygen: prediction of nitrite and nitrate formation by kinetic simulation.* Free radical research, 1995. **22**(1): p. 47-56.

242. Konorev, E.A., et al., *Nitronyl nitroxides as probes to study the mechanism of vasodilatory action of nitrovasodilators, nitrone spin traps, and nitroxides: role of nitric oxide.* Free Radical Biology and Medicine, 1995. **18**(2): p. 169-177.

243. Cao, B.-J. and M.E.A. Reith, *Nitric oxide scavenger carboxy-PTIO potentiates the inhibition of dopamine uptake by nitric oxide donors.* European Journal of Pharmacology, 2002. **448**(1): p. 27-30.

244. Fang, S.-Y., et al., *Nitric oxide scavenger carboxy-PTIO reduces infarct volume following permanent focal ischemia.* Acta anaesthesiologica Taiwanica: official journal of the Taiwan Society of Anesthesiologists, 2006. **44**(3): p. 141-146.

245. Onitsuka, M., et al., *Nitric oxide contributes to irreversible membrane dysfunction caused by experimental ischemia in rat hippocampal CA1 neurons.* Neuroscience research, 1998. **30**(1): p. 7-12.

246. Yoshida, M., et al., *Therapeutic effects of imidazolineoxyl N-oxide against endotoxin shock through its direct nitric oxide-scavenging activity.* Biochemical and biophysical research communications, 1994. **202**(2): p. 923-930.

247. Sun, J., et al., *Measurement of nitric oxide production in biological systems by using Griess reaction assay.* Sensors, 2003. **3**(8): p. 276-284.

248. Wimalawansa, S.J., *Nitric oxide and bone.* Annals of the New York Academy of Sciences, 2010. **1192**(1): p. 391-403.

249. Zafarullah, M., et al., *Molecular mechanisms of N-acetylcysteine actions.* Cellular and Molecular Life Sciences CMLS, 2003. **60**(1): p. 6-20.

250. De Vries, N. and S. De Flora, *N-acetyl-l-cysteine.* Journal of Cellular Biochemistry, 1993. **53**(S17F): p. 270-277.

251. Nitescu, N., et al., *N-acetylcysteine attenuates kidney injury in rats subjected to renal ischaemia-reperfusion.* Nephrology Dialysis Transplantation, 2006. **21**(5): p. 1240-1247.

252. Shimizu, M., et al., *N-acetylcysteine attenuates the progression of chronic renal failure (vol 68, pg 2208, 2005).* KIDNEY INTERNATIONAL, 2006. **70**(12): p. 2156-2156.

253. Zhang, F., S.S. Lau, and T.J. Monks, *The Cytoprotective Effect of N-acetyl-L-cysteine against ROS-Induced Cytotoxicity Is Independent of Its Ability to Enhance Glutathione Synthesis.* Toxicological Sciences, 2011. **120**(1): p. 87-97.

254. Luo, J., et al., *The molecular mechanisms of the attenuation of cisplatin-induced acute renal failure by N-acetylcysteine in rats.* Nephrology Dialysis Transplantation, 2008. **23**(7): p. 2198-2205.

255. Kim, J.H., et al., *N-acetylcysteine attenuates glycerol-induced acute kidney injury by regulating MAPKs and Bcl-2 family proteins.* Nephrology Dialysis Transplantation, 2010. **25**(5): p. 1435-1443.

256. Roederer, M., et al., *Cytokine-stimulated human immunodeficiency virus replication is inhibited by N-acetyl-L-cysteine.* Proceedings of the National Academy of Sciences, 1990. **87**(12): p. 4884-4888.

257. Zhang, H., et al., *Protective effects of N-acetyl-L-cysteine in endotoxemia.* American Journal of Physiology-Heart and Circulatory Physiology, 1994. **266**(5): p. H1746-H1754.

258. Lunov, O., et al., *Cell death induced by ozone and various non-thermal plasmas: therapeutic perspectives and limitations.* Scientific reports, 2014. **4**.

259. Lukes, P., et al., *Aqueous-phase chemistry and bactericidal effects from an air discharge plasma in contact with water: evidence for the formation of peroxynitrite through a pseudo-second-order post-discharge reaction of H2O2 and HNO2.* Plasma Sources Science and Technology, 2014. **23**(1): p. 015019.

260. Vandamme, M., et al., *ROS implication in a new antitumor strategy based on non-thermal plasma.* International Journal of Cancer, 2012. **130**(9): p. 2185-2194.

261. Ercan, U.K., et al., *Nonequilibrium Plasma-Activated Antimicrobial Solutions are Broad-Spectrum and Retain their Efficacies for Extended Period of Time.* Plasma Processes and Polymers, 2013. **10**(6): p. 544-555.

262. Kholodnykh, A.I., et al., *Precision of measurement of tissue optical properties with optical coherence tomography.* Applied Optics, 2003. **42**(16): p. 3027-3037.

263. Ignarro, L.J., et al., *Oxidation of Nitric Oxide in Aqueous Solution to Nitrite but not Nitrate: Comparison with Enzymatically Formed Nitric Oxide From L-Arginine.* Proceedings of the National Academy of Sciences of the United States of America, 1993. **90**(17): p. 8103-8107.

264. Tang, J., et al., *Effect of Glutathione on Oxymyoglobin Oxidation.* Journal of Agricultural and Food Chemistry, 2003. **51**(6): p. 1691-1695.

265. Stoffels, E., Y. Sakiyama, and D.B. Graves, *Cold Atmospheric Plasma: Charged Species and Their Interactions With Cells and Tissues.* Plasma Science, IEEE Transactions on, 2008. **36**(4): p. 1441-1457.

266. Siu, A., et al., *Differential effects of cold atmospheric plasma in the treatment of malignant glioma.* PloS one, 2015. **10**(6).

267. Vander Heiden, M.G., L.C. Cantley, and C.B. Thompson, *Understanding the Warburg effect: the metabolic requirements of cell proliferation.* science, 2009. **324**(5930): p. 1029-1033.

268. Engel, R.H. and A.M. Evens, *Oxidative stress and apoptosis: a new treatment paradigm in cancer.* Frontiers in bioscience: a journal and virtual library, 2005. **11**: p. 300-312.

269. Stuehr, D.J. and C.F. Nathan, *Nitric oxide. A macrophage product responsible for cytostasis and respiratory inhibition in tumor target cells.* The Journal of Experimental Medicine, 1989. **169**(5): p. 1543-1555.

270. Ikawa, S., K. Kitano, and S. Hamaguchi, *Effects of pH on Bacterial Inactivation in Aqueous Solutions due to Low-Temperature Atmospheric Pressure Plasma Application.* Plasma Processes and Polymers, 2010. **7**(1): p. 33-42.

271. Kröncke, K.-D., K. Fehsel, and V. Kolb-Bachofen, *Nitric Oxide: Cytotoxicity versus Cytoprotection— How, Why, When, and Where?* Nitric Oxide, 1997. **1**(2): p. 107-120.

272. Wink, D.A. and J.B. Mitchell, *Chemical biology of nitric oxide: insights into regulatory, cytotoxic, and cytoprotective mechanisms of nitric oxide.* Free Radical Biology and Medicine, 1998. **25**(4–5): p. 434-456.

273. Weller, R. and M.J. Finnen, *The effects of topical treatment with acidified nitrite on wound healing in normal and diabetic mice.* Nitric Oxide, 2006. **15**(4): p. 395-399.

274. Wullt, M., I. Odenholt, and M. Walder, *Activity of three disinfectants and acidified nitrite against Clostridium difficile spores.* Infection Control, 2003. **24**(10): p. 765-768.

APPENDICES

Supplemental Material

*** This data is part of a manuscript in preparation in collaboration with Chris Timmons, a Ph.D candidate in Plant Pathology.**

Materials and Methods

Bacterial strains and culture conditions. Multiple-strain mixtures of *Salmonella enterica* subspecies *enterica* (serovars Enteritidis, Typhimurium, Javiana, Seftenburg, and Poona), Shiga toxin-producing *Escherichia coli* (serotypes O157:H7, O111:H2, O26:H11, O103:H2, O121:H19, O145:H28, and O45:NM), or *Listeria monocytogenes* (strains F6854, 12433, G3982, J0161, and Scott A) were used for inoculation of sterile glass coverslips, cherry tomatoes, and pecans. Multiple-strain mixtures were used to more accurately represent environmental contamination of inoculated surfaces. Each bacterial strain was separately grown aerobically overnight with shaking (250 rpm) at 37°C in 5 mL tryptic soy broth (TSB, Difco, Sparks, MD). The bacterial concentration of each overnight liquid culture was determined by serially diluting the culture in 0.1% (w/v) sterile peptone (Difco, Sparks, MD) and plating in duplicate on tryptic soy agar (TSA, Difco, Sparks, MD), incubated overnight at 37°C.

Preparation of inoculum. To prepare the inocula, 1 mL of each liquid culture was centrifuged at 12,000 rpm for 3 minutes and re-suspended in 1 mL of 0.1% (w/v) sterile peptone before being combined with all other strains of the same species. The multiple-strain bacterial mixtures were then diluted to approximately 10^8 CFU/mL and 100 µL of the bacterial suspensions were used as inocula (approximately 10^7 CFU/inoculated surface), spotted in 20-25 spots (between 10^5 and 10^6 CFU/spot) onto single sterile 22 x 22 mm glass coverslips, whole unshelled pecans, or cherry tomatoes. Pecans and cherry tomatoes were obtained from a local native pecan orchard and local grocery store, respectively, and stored at 4°C until inoculated. Glass coverslips were inoculated with *Se,* STEC, and *Lm* whereas pecans and cherry tomatoes were only inoculated with *Se*. Inocula spots were evenly spaced over the entire surface of the coverslips or within a 2 cm^2 region on the upper surface of pecans and cherry tomatoes. Inoculation spots were dried in a biosafety cabinet for 60 minutes prior to cold plasma treatment.

Cold plasma treatment by SDBD. SDBD actuators were constructed using 3.6 cm x 0.5 cm x 0.5 mm (*l* x *w* x *h*) copper electrodes (McMaster-Carr Supply Company, GA, USA) placed asymmetrically on both sides of 5 cm^2 x 0.127 mm Teflon dielectric barrier sheets (McMaster-Carr Supply Company, GA). The grounded electrodes were insulated to prevent plasma ignition. SDBD actuators were operated with an input power of 13.5 V with a 50% duty cycle using a high voltage transformer (Information Unlimited, NH). Pulse width modulation (PWM) with an Arduino Uno microcontroller setup (Arduino LLC, Italy) was used to allow actuators to be on for 800 ms and off for 300 ms. Pulsed power was used since it was found to reduce heating, extending actuator lifespans.

Inoculated coverslips were placed in sterile 35 mm petri dishes and treated with open-air SDBD actuators for 2 and 4 min from a distance of 1, 3, 5, and 7 cm. 10 individual actuators were tested at 3cm from the sample at treatment time of 2 min for repeatability and consistency in decontamination, with two technical replicates for each actuator. For all other consequent tests, two technical replicates were treated for each of 3 biological replicates at each distance and time at room temperature (~25°C) and atmospheric pressure. Inoculated pecans and cherry tomatoes were also placed in sterile 35 mm petri dishes but were treated for 4 and 10 min at 1cm.

Assessment of bacterial inactivation. Treated and untreated control inoculated coverslips, pecans, and cherry tomatoes were washed by vortexing for 30 s in 10 mL 0.1% (w/v) sterile peptone in 50 mL conical tubes. The wash fluid was 10-fold serially diluted in 0.1% peptone for enumeration, for which 100 µL of each dilution was plated in duplicate on TSA and incubated overnight at 37 °C. Pecans and cherry tomatoes, which were inoculated with *Se*, were plated on TSA with a xylose lysine deoxycholate (XLD, Difco, Sparks, MD) agar overlay. XLD agar is a selective medium for *Salmonella* and was used to differentiate inoculated bacteria from background bacteria already present on the produce surfaces. Bacterial inactivation was assessed by comparing plate counts of each treatment and untreated controls.

Statistical analysis. Three biological repeats containing 2 replicates of each treatment were conducted. The plate counts of recovered cells from wash fluids for each replicate were transformed to log CFU/mL. Analysis of variance (ANOVA) was calculated from plate counts using SAS (Statistical Analysis System. Inst. Inc., Cary, NC, USA). Significant difference was

defined at $P < 0.05$ or $P < 0.01$. Decimal reduction time (D-value) in minutes was calculated for the inoculated coverslips at each treatment distance according to the equation $D = t/(\log N_0 - \log N_u)$.

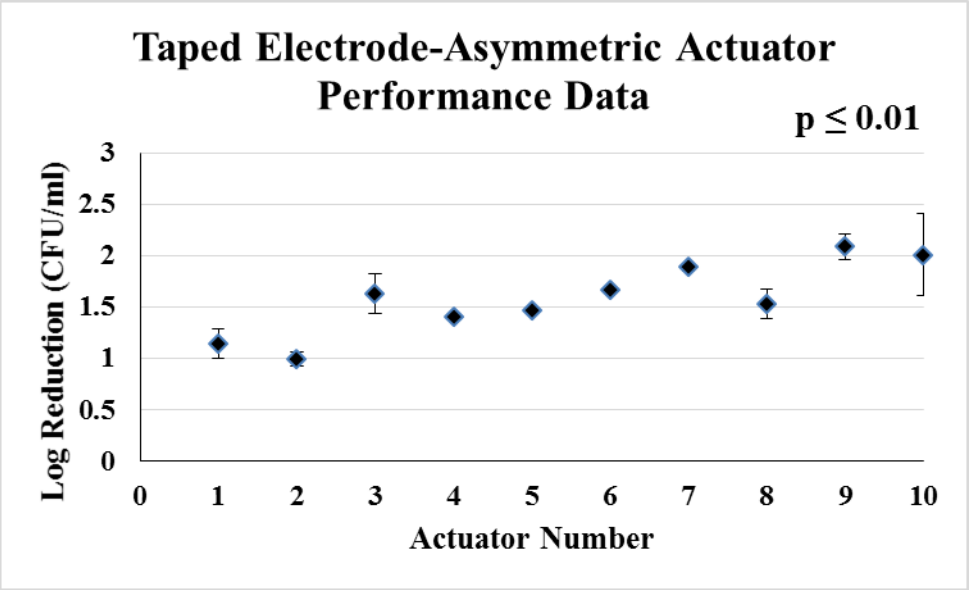

Figure S-1. Performance data for asymmetric SDBD plasma actuator with 4 electrodes placed at 3 cm from sample (5 strain mixture of L. monocytogenes).

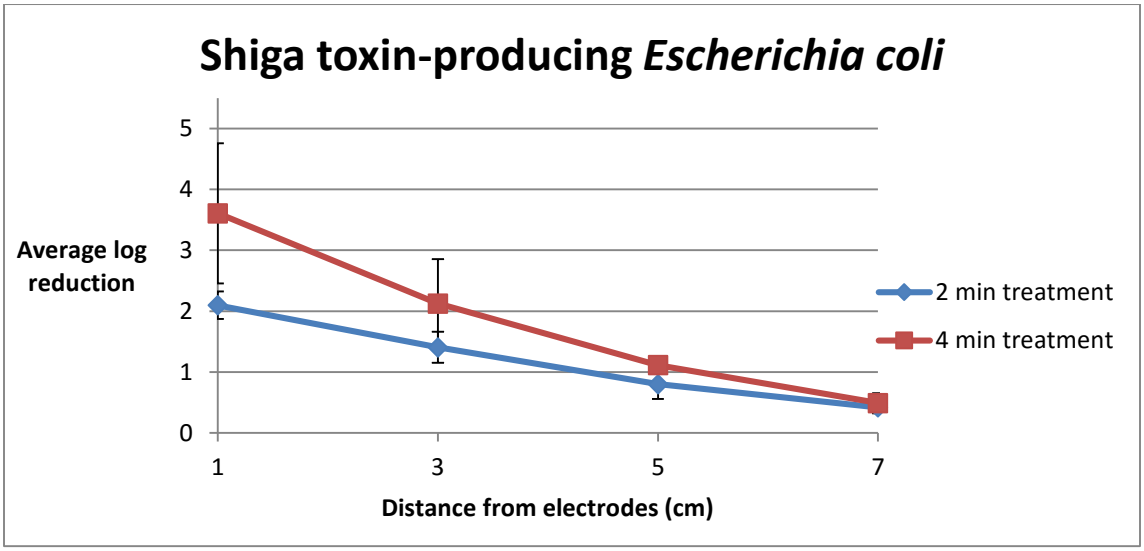

Figure S-2. Average log_{10} reductions in Shiga toxin-producing Escherichia coli bacterial populations after 2 and 4 min treatments with cold plasma at 1, 3, 5, and 7 cm.

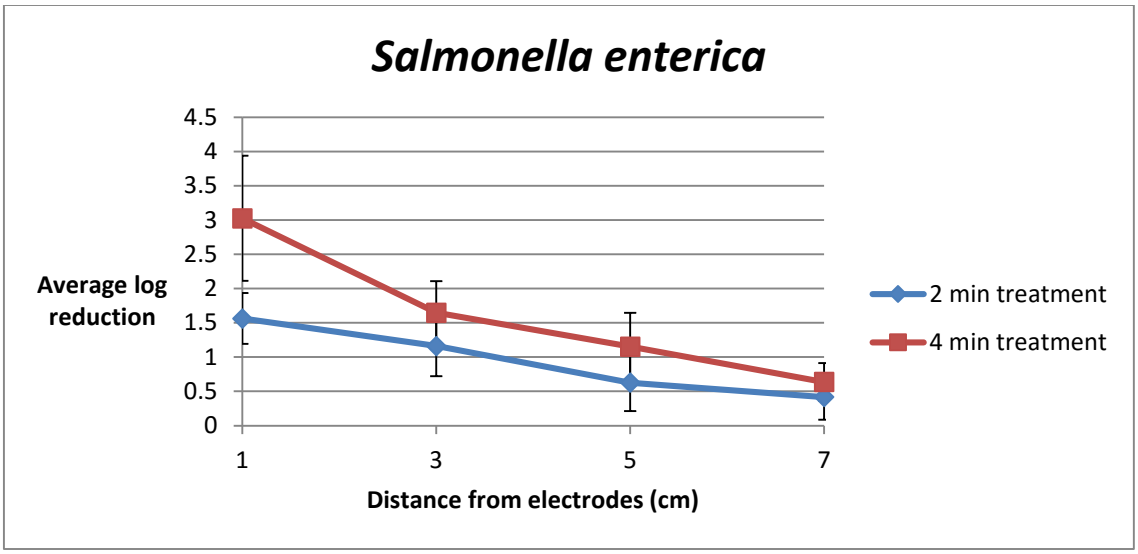

Figure S-3. Average log_{10} reductions in Salmonella enterica bacterial populations after 2 and 4 min treatments with cold plasma at 1, 3, 5, and 7 cm.

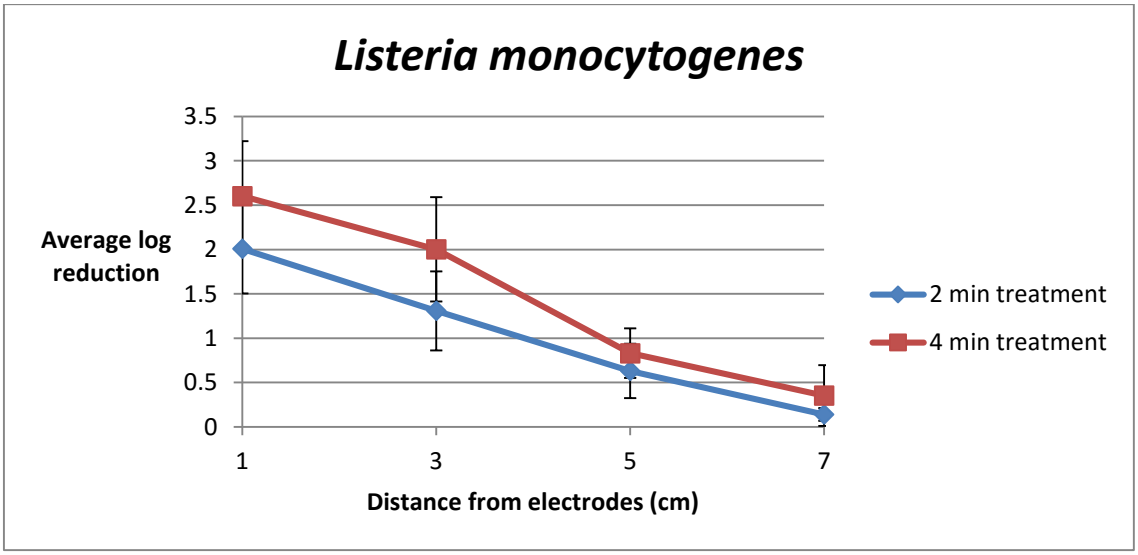

Figure S-4. Average log_{10} reductions in Listeria monocytogenes bacterial populations after 2 and 4 min treatments with cold plasma at 1, 3, 5, and 7 cm.

Table S-1. Average D-values in minutes for Salmonella, STEC, and Listeria inoculated on glass coverslips after 2 min of cold plasma treatment at 1, 3, 5, and 7 cm.

Treatment distance	***Salmonella*** **D-value (min) ± SD**	**STEC D-value (min) ± SD**	***Listeria*** **D-value (min) ± SD**
1 cm	1.324 ± 0.277	0.961 ± 0.1	1.035 ± 0.239
3 cm	1.878 ± 0.618	1.451 ± 0.239	1.649 ± 0.537
5 cm	5.376 ± 5.14	2.641 ± 0.704	4.061 ± 2.742
7 cm	8.537 ± 7.962	4.970 ± 1.339	16.586 ± 6.714

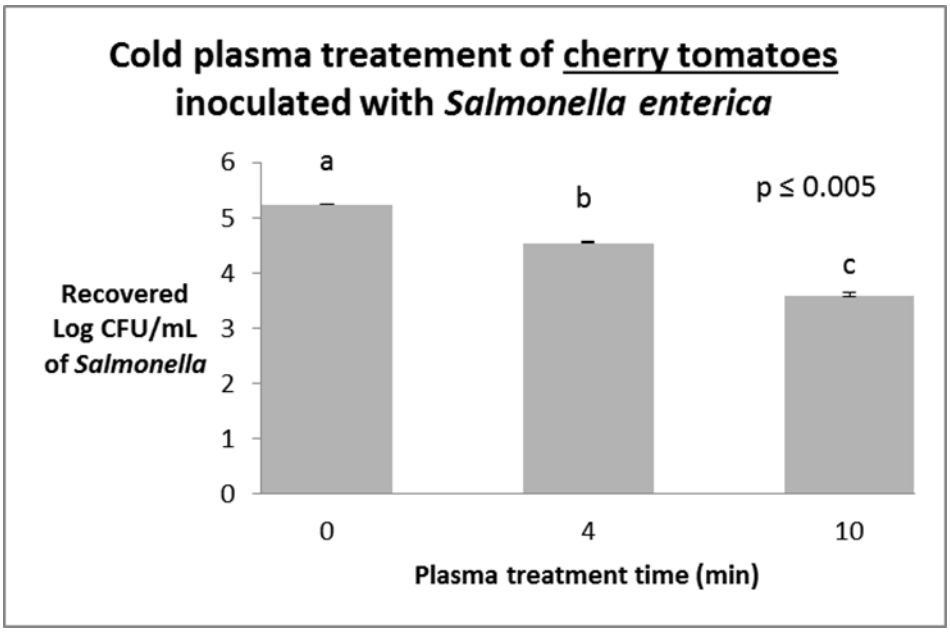

Figure S-5. Recovered log10 CFU/mL of Salmonella enterica inoculated on cherry tomatoes after 4 and 10 min of cold plasma treatment at 1 cm.

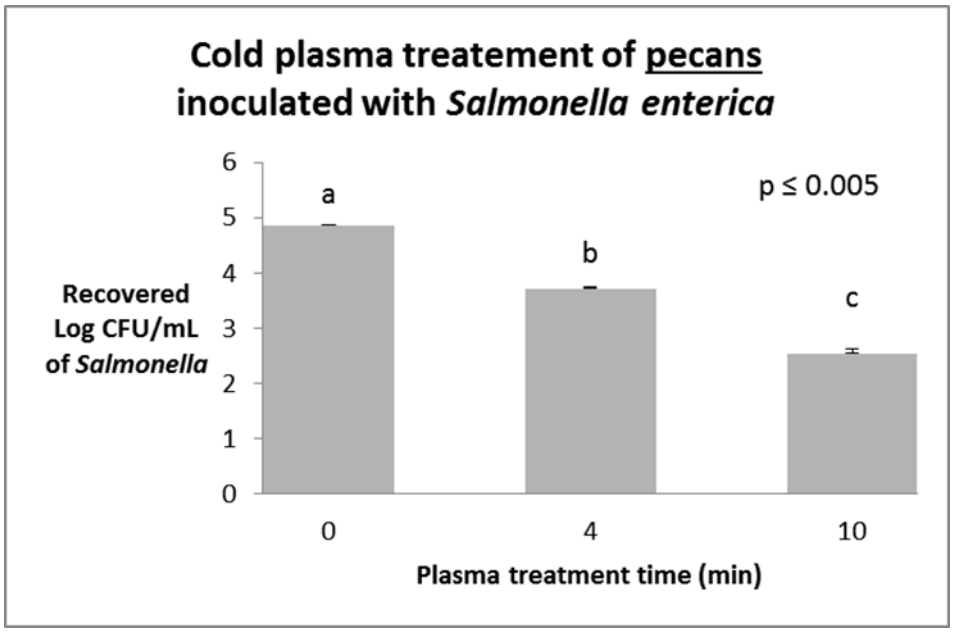

Figure S-6. Recovered log10 CFU/mL of Salmonella enterica inoculated on cherry tomatoes after 4 and 10 min of cold plasma treatment at 1 cm.

VITA

Kedar Kamlakant Pai

Candidate for the Degree of

Doctor of Philosophy

Thesis: ASYMMETRIC SURFACE DIELECTRIC BARRIER DISCHARGE AS A NOVEL METHOD FOR BIOLOGICAL DECONTAMINATION

Major Field: Mechanical and Aerospace Engineering

Biographical:

Education:

Completed the requirements for the Doctor of Philosophy in Mechanical and Aerospace Engineering at Oklahoma State University, Stillwater, Oklahoma in December, 2015.

Completed the requirements for the Master of Science in Mechanical and Aerospace Engineering at Oklahoma State University, Stillwater, Oklahoma in 2012.

Completed the requirements for the Bachelor of Technology in Mechanical Engineering at National Institute of Technology Raipur, Raipur, India in 2010.

Experience:

2010- 2015 Teaching Associate/Assistant, Oklahoma State University, Stillwater, OK

- Lead undergraduate level class lectures on Fluid Mechanics, Experimental Fluid mechanics, Thermodynamics II and Measurements and Instrumentation

2010- 2015 Research Associate/Assistant, Oklahoma State University, Stillwater, OK

- Lead Collaborations between Mechanical and Aerospace Engineering, Chemical Engineering and Plant Pathology and Entomology for development of cold plasma technology for various applications

Professional Memberships:

- American Society of Mechanical Engineers (2011-present)